

OPEN ACCESS

African Journal of
**Environmental Science and
Technology**



June 2020
ISSN 1996-0786
DOI: 10.5897/AJEST
www.academicjournals.org



**ACADEMIC
JOURNALS**
expand your knowledge

About AJEST

African Journal of Environmental Science and Technology (AJEST) provides rapid publication (monthly) of articles in all areas of the subject such as Biocidal activity of selected plant powders, evaluation of biomass gasifier, green energy, Food technology etc. The Journal welcomes the submission of manuscripts that meet the general criteria of significance and scientific excellence. Papers will be published shortly after acceptance. All articles are peer-reviewed

Indexing

The African Journal of Environmental Science and Technology is indexed in:

[CAB Abstracts](#), [CABI's Global Health Database](#), [Chemical Abstracts \(CAS Source Index\)](#), [China National Knowledge Infrastructure \(CNKI\)](#), [Dimensions Database](#), [Google Scholar](#), [Matrix of Information for The Analysis of Journals \(MIAR\)](#), [Microsoft Academic](#)

AJEST has an [h5-index of 14](#) on Google Scholar Metrics

Open Access Policy

Open Access is a publication model that enables the dissemination of research articles to the global community without restriction through the internet. All articles published under open access can be accessed by anyone with internet connection.

The African Journal of Environmental Science and Technology is an Open Access journal. Abstracts and full texts of all articles published in this journal are freely accessible to everyone immediately after publication without any form of restriction.

Article License

All articles published by African Journal of Environmental Science and Technology are licensed under the [Creative Commons Attribution 4.0 International License](#). This permits anyone to copy, redistribute, remix, transmit and adapt the work provided the original work and source is appropriately cited. Citation should include the article DOI. The article license is displayed on the abstract page the following statement:

This article is published under the terms of the [Creative Commons Attribution License 4.0](#)

Please refer to <https://creativecommons.org/licenses/by/4.0/legalcode> for details about [Creative Commons Attribution License 4.0](#)

Article Copyright

When an article is published by in the African Journal of Environmental Science and Technology, the author(s) of the article retain the copyright of article. Author(s) may republish the article as part of a book or other materials. When reusing a published article, author(s) should; Cite the original source of the publication when reusing the article. i.e. cite that the article was originally published in the African Journal of Environmental Science and Technology. Include the article DOI Accept that the article remains published by the African Journal of Environmental Science and Technology (except in occasion of a retraction of the article) The article is licensed under the Creative Commons Attribution 4.0 International License.

A copyright statement is stated in the abstract page of each article. The following statement is an example of a copyright statement on an abstract page.

Copyright ©2016 Author(s) retains the copyright of this article.

Self-Archiving Policy

The African Journal of Environmental Science and Technology is a RoMEO green journal. This permits authors to archive any version of their article they find most suitable, including the published version on their institutional repository and any other suitable website.

Please see <http://www.sherpa.ac.uk/romeo/search.php?issn=1684-5315>

Digital Archiving Policy

The African Journal of Environmental Science and Technology is committed to the long-term preservation of its content. All articles published by the journal are preserved by [Portico](#). In addition, the journal encourages authors to archive the published version of their articles on their institutional repositories and as well as other appropriate websites.

<https://www.portico.org/publishers/ajournals/>

Metadata Harvesting

The African Journal of Environmental Science and Technology encourages metadata harvesting of all its content. The journal fully supports and implement the OAI version 2.0, which comes in a standard XML format. [See Harvesting Parameter](#)

Memberships and Standards



Academic Journals strongly supports the Open Access initiative. Abstracts and full texts of all articles published by Academic Journals are freely accessible to everyone immediately after publication.



All articles published by Academic Journals are licensed under the [Creative Commons Attribution 4.0 International License \(CC BY 4.0\)](#). This permits anyone to copy, redistribute, remix, transmit and adapt the work provided the original work and source is appropriately cited.



[Crossref](#) is an association of scholarly publishers that developed Digital Object Identification (DOI) system for the unique identification published materials. Academic Journals is a member of Crossref and uses the DOI system. All articles published by Academic Journals are issued DOI.

[Similarity Check](#) powered by iThenticate is an initiative started by CrossRef to help its members actively engage in efforts to prevent scholarly and professional plagiarism. Academic Journals is a member of Similarity Check.

[CrossRef Cited-by](#) Linking (formerly Forward Linking) is a service that allows you to discover how your publications are being cited and to incorporate that information into your online publication platform. Academic Journals is a member of [CrossRef Cited-by](#).



Academic Journals is a member of the [International Digital Publishing Forum \(IDPF\)](#). The IDPF is the global trade and standards organization dedicated to the development and promotion of electronic publishing and content consumption.

Contact

Editorial Office: ajest@academicjournals.org

Help Desk: helpdesk@academicjournals.org

Website: <http://www.academicjournals.org/journal/AJEST>

Submit manuscript online <http://ms.academicjournals.org>

Academic Journals
73023 Victoria Island, Lagos, Nigeria
ICEA Building, 17th Floor,
Kenyatta Avenue, Nairobi, Kenya.

Editors

Prof. Sulejman Redzic

Faculty of Science
University of Sarajevo
Bosnia and Herzegovina.

Dr. Guoxiang Liu

Energy & Environmental Research Center
(EERC)
University of North Dakota (UND)
North Dakota 58202-9018
USA

Prof. Okan Külköylüoğlu

Faculty of Arts and Science
Department of Biology
Abant İzzet Baysal University
Turkey.

Dr. Abel Ramoelo

Conservation services,
South African National Parks,
South Africa.

Editorial Board Members

Dr. Manoj Kumar Yadav

Department of Horticulture and Food
Processing
Ministry of Horticulture and Farm Forestry
India.

Dr. Baybars Ali Fil

Environmental Engineering
Balıkesir University
Turkey.

Dr. Antonio Gagliano

Department of Electrical, Electronics and
Computer Engineering
University of Catania
Italy.

Dr. Yogesh B. Patil

Symbiosis Centre for Research & Innovation
Symbiosis International University
Pune,
India.

Prof. Andrew S Hursthouse

University of the West of Scotland
United Kingdom.

Dr. Hai-Linh Tran

National Marine Bioenergy R&D Consortium
Department of Biological Engineering
College of Engineering
Inha University
Korea.

Dr. Prasun Kumar

Chungbuk National University,
South Korea.

Dr. Daniela Giannetto

Department of Biology
Faculty of Sciences
Mugla Sıtkı Koçman University
Turkey.

Dr. Reem Farag

Application department,
Egyptian Petroleum Research Institute,
Egypt.

Table of Content

Molecular characterisation of bacteria strains of septic tank sewage samples from related sites in Delta and Edo States of Nigeria using 16S rRNA denaturing gradient gel electrophoresis (DGGE)	132
Oyem, I. M., and Oyem, H. H. and Atuanya E. I.	
Physicochemical influence on the spatial distribution of faecal bacteria and polychaetes in the Densu Estuary, Ghana	139
Akita L. G., Laudien J., Akrong M., Biney C., Nyarko E. and Addo S.	
Quantifying forest cover at Mount Kenya: Use of Sentinel-2 for a discrimination of tropical tree composites	159
Jonas Fierke, Martin Kappas and Daniel Wyss	

Full Length Research Paper

Molecular characterisation of bacteria strains of septic tank sewage samples from related sites in Delta and Edo States of Nigeria using 16S rRNA denaturing gradient gel electrophoresis (DGGE)

Oyem, I. M.^{1*} and Oyem, H. H.¹ and Atuanya, E. I.²

¹Department of Integrated Science College of Education Agbor, P. M. B. 2090, Agbor, Delta State, Nigeria.

²Department of Microbiology, University of Benin, P. M. B 1154, Benin City, Edo State, Nigeria.

Received 30 April, 2020, Accepted 4 June, 2020

The molecular characterization of raw septic tank sewage in the region under study was evaluated using 16S rRNA denaturing gradient gel electrophoresis (DGGE). Raw effluent samples from three septic tanks in the Delta and Edo States region of Nigeria was collected between November 2018 and January 2019 for testing. A composite sample was formed from the three samples collected. The raw sewage sample was sequenced for genomic DNA using *Norgen* DNA extraction kit to determine the microorganisms present in raw sewage sample. Gene sequence analysis revealed the presence of *Methanococcus methanococcus* 288171278, *Deferribacteres bacterium* 291088137, *Flavobacteria bacterium* 308271278, *Bacteroides dorei* 671713918, *Clostridium difficile* 115249003, *Kuenenia stuttgartiensis* 91203347, *Methanosarcina bankerii* 827396966, *Methanococcus maripaludis* 4505076 and *Methanobacterium formicicum* 693274837, and *Desulfitobacterium dichloroeliminans* 430782295. The *phylogram* of the different isolates shows that methane producing bacteria were 7 out of the 13 bacteria isolated; representing 53.8% of the total species occurrence in the sample.

Key words: Gene sequence, bacteria, raw sewage, septic tank.

INTRODUCTION

Sewage, which is liquid waste, is the waste water of a community. It is a combination of water borne wastes from homes, business, health institutions and industries. It may also contain groundwater, surface water and storm water (APHA, 1992). Waste water emanating from sundry human activities may carry pathogenic organisms that can transmit diseases to humans and other animals and

contain organic matter that can cause odour and nuisance problems, hold nutrients that may cause eutrophication of receiving water bodies and can lead to ecotoxicology (Doelle, 2001). For reasons of public health and of conservation, man has been forced to develop methods of waste-water storage and treatment which result in the mineralization of the organic components of

*Corresponding author. E-mail: ifyoyem2011@yahoo.com. Tel: +2347034717335.

waste water prior to its discharge into the natural environment. This is usually achieved by an adequate public or community sewerage system. However, such a system is not quite feasible in developing and under developed nations of the world (Rojer, 2002). Hence, individual household sewage disposal system often referred to as septic tank system is the most commonly used domestic waste water disposal method currently being used (Whithers et al., 2014; Schaidler et al., 2017; Connelly et al., 2019).

A septic system is an enclosed receptacle designed to collect waste water, segregate settle-able and floatable solids, accumulate and digest organic matter and discharge partially treated effluent. The most widely accepted type is the gravity fed (made of sandcrete block) used by over 40% of the people in Nigeria (Fidelia, 2004). This consists of a septic tank where approximately 54% of the ultimate sewage treatment is accomplished (Robert and Terry, 2004; Schaidler et al., 2017). The septic tank act largely as a settling tank, within which the organic components of the waste water undergo limited aerobic digestion. Effluent from septic tank is as dangerous as raw sewage as it contains effluent concentrations higher than both locally and internationally acceptable limits (Burubai, 2005).

Consequently, attention is being focused on the fermentation of human waste for the production of methane (Zinder, 1993). Methanogenesis is a naturally occurring process that takes place in rice fields and animal digestive tracts, as well as one that can be induced under the right conditions in an artificially constructed anaerobic environment (Lowe et al., 1993; Richards et al., 1994). Both situations utilize the power of methanogens, a bacterial type that can transform organic material into methane through cyclical pathway of production in which intermediate products like acetic acid are formed. Acetate is the ultimate end product of many fermentative pathways and the source of most methane from the anaerobic food chain (Zinder, 1984).

A better understanding of the microbial diversity in septic tank system can improve the stability of the anaerobic process (Bitton, 1999; Connelly et al., 2019). Yet understanding the workings of the process is hampered by the paucity of research papers in the literature (Marti et al., 2013; Ye and Zhang, 2013; Cai et al., 2014; Logares et al., 2015; Newton et al., 2015; Connelly et al., 2019; Numberger et al., 2019). The microbes responsible for the metabolic reactions in the system are the crucial factor in the anaerobic process (Bitton, 1999; Schaidler et al., 2017). Understanding and being able to improve our knowledge of the biology of the process as well as the identity of the organisms which promote or inhibit the efficiency of the system is essential to effectively control the start-up and operation of septic tank systems (Schink, 1997; Connelly et al., 2019). Molecular methods like, the PCR-based DGGE technique and sequence analysis have been successfully used to

monitor and identify microorganisms within the system (Boon et al., 2002; Odeyemi et al., 2018; Abada et al., 2019; Numberger et al., 2019). The PCR-based DGGE marker construct can effectively be used to study the inherent changes in the microbial population present in the system (Muyzer et al., 1993).

In this work, the diversity, dynamics and degradation potentials of microbial community of the septic tank system was studied using the PCR-based DGGE molecular characterisation technique with the view to further understand and engineer the system in order to optimize its function and utilization.

MATERIALS AND METHODS

Study area

It is a descriptive study carried out in Edo and Delta State, Nigeria in the months of November 2018 and January 2019 with samples analysed at BioSolutions Technologies Laboratory, Akure, Ondo State, Nigeria. The sampling was done in three different locations within Edo and Delta regions of Nigeria (Figure 1); Agbor (A) located 6° 15' 93" N and 6° 11' 59" E with a population of 222,400 and a land mass of 436 km², Benin (B) located 6° 20' N and 5° 38' E with a population of 1,471,188 and land mass of 1204 km² and Sapele (C) located 5° 54' N and 5° 40' E with a population of 232,000 and a land mass of 394 km² (NPC, 2006). The major occupation of the people is farming and trading.

Molecular analysis

Methodology was based on PCR and Sanger sequencing analysis (Sanger and Coulson, 1975).

DNA extraction

Ten millilitre of the sewage sample was filtered through 0.22 µm filter pore and then was thawed in a minus 86°C freezer in three consecutive times to release DNA. Further DNA purification was done with Norgen DNA extraction kit. Analysis was done at BioSolutions Technologies Laboratory Akure.

Polymerase chain reaction procedures

Sample was gently vortexed and all solutions after thawing were briefly centrifuged using Eppendorf centrifuge model 5402-Germany. A reaction master mix was prepared by adding the following components (except template DNA) for each 25 µL reaction to a tube at room temperature. The master mix was thoroughly mixed and appropriate volumes were dispensed into PCR tubes or plates. Template DNA (≤500ng/reaction) was added to the individual PCR tubes or wells containing the master mix. Sequence for primers used were PfastBact (Forward): 5' (GGA TTA TTC ATA CCG TCC CA) 3' PfastBact (Reverse): 5' (CAA ATG TGG TAT GGC TGA TT) 3' EUB (Forward): 5' (GCA CAA GCG GTG GAG CAT GTGG); 3'EUB (Reverse): 5' (GCC CGG GAA CGT ATT CAC CG) 3'. The PCR cycle started with an initial denaturation step at 94°C for 5 min. This was followed by 30 cycles of denaturation at 94°C for 30 s, annealing at 55°C for 30 s, extension at 72°C for 30 s, and a final extension at 72°C for 5

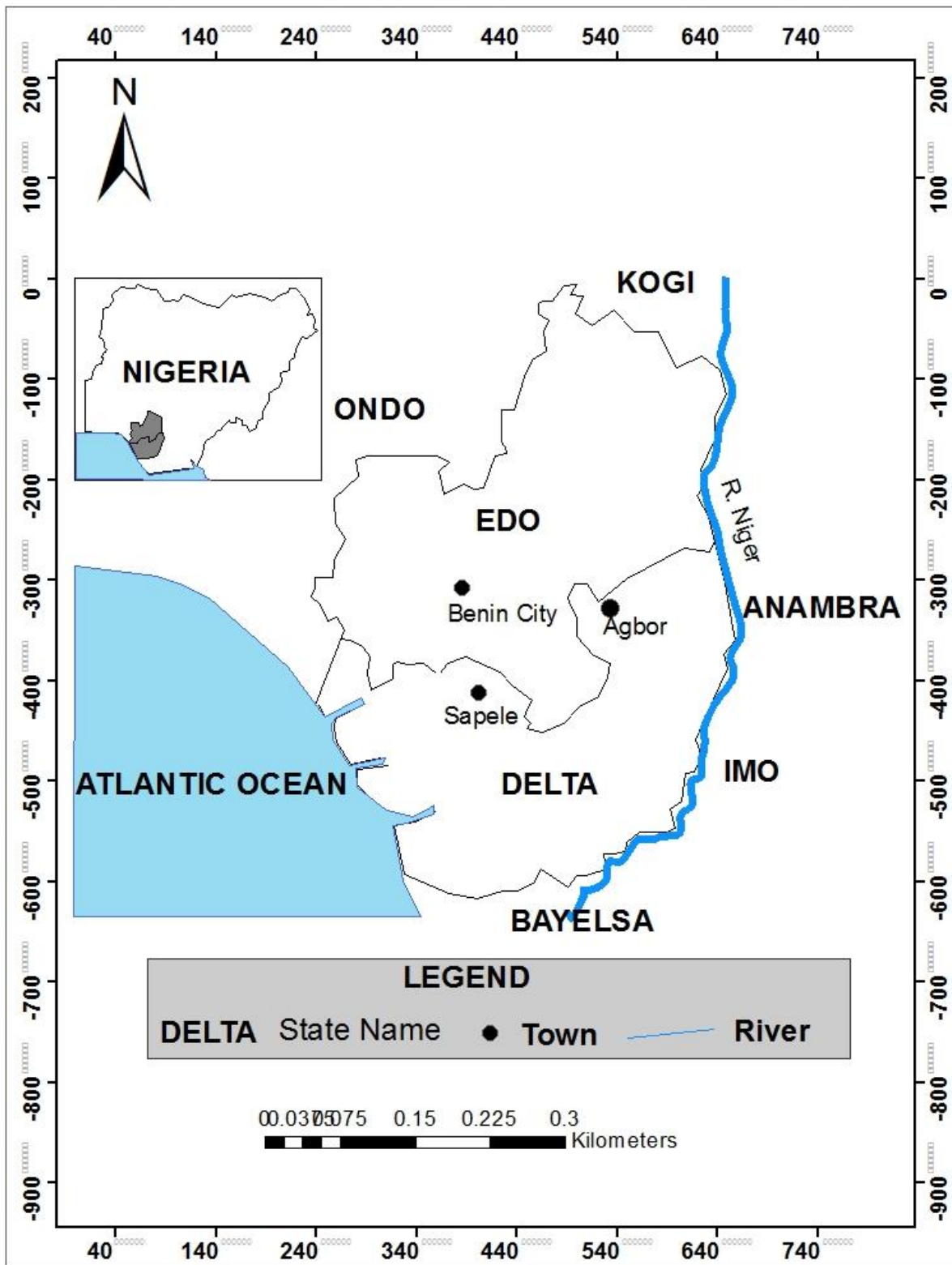


Figure 1. Study area.

min that was followed by cooling to 4°C. Few microliters of the samples were run on a 1% agarose gel at 90 V for 30 min in order

to verify amplification. The entire PCR reaction was loaded onto a 1% agarose gel and the correct band size (approximately

1500 bp) was excised. Data acquisition was performed during the annealing/extension step.

Acrylamide gel procedure

After determining the percentage gel to be poured, the separation gel layer was used after adding the necessary volumes of reagents to a 100 ml flask (gel will begin polymerizing after adding per sulfate and TEMED; these were added just before pouring the gel). Solution was mixed well by gently swirling the flask. The solution was then quickly poured (or pipetted) into the gel casting apparatus and allowed to polymerize. A flat interface between the separating and stacking layers was ensured. The separation layer was gently overlaid with water or n-butanol after pouring the separation layer. The stacking layer was poured on top of the solution gel, after the separating gel layer has been polymerized; the water or butanol overlay was then decanted. The stacking layer was prepared as prescribed. Necessary volumes of reagents were sequentially added to a flask. Solution was mixed well by gently swirling the flask then quickly pouring (or pipetting) the solution on top of the separation layer. Comb was inserted and layer allowed to polymerize completely before removing comb. Gel was then placed in the electrophoresis apparatus at 75 V.

Preparation of samples

Sixty microlitre of 30, 60, 90, and 100% urea and NaOH (denaturants) was dispensed into Eppendoff tube then 4 microlitre of amplicons was pipetted into them and homogenized thoroughly. Samples were incubated at room temperature for 30 min. PCR was then redone. Pipetted amplicons were put into acrylamide gel and the electrophoresis procedures ran for at least an hour.

Running the gel

The 10x buffer concentrate was diluted (1:9) to make a 1X solution of the buffer. To make 1 L of 1X electrophoresis buffer, 100 mL of the buffer concentrate was added to 900 mL of distilled water. The appropriate volume was then added to the electrophoresis apparatus and ran according to the manufacturer's instructions.

DNA sequencing

Sequence analysis from resultant nucleotides base pairs was performed using BLAST analysis by direct blasting on American data base <http://blast.ncbi.nlm.nih.gov>. For every set of isolate, a read was Basic Local Alignment Search Tool (BLAST) and the resultant top hits with minimum E-score for every BLAST result showing species name was used to name the specific organism. Sequencing result in FASTA format and corresponding ID after BLAST analysis on NCBI website. BLAST is a computer algorithm program used for comparing nucleotide or amino acid sequences of DNA and/or RNA with available sequences of online database of the National Center of Biotechnology Information (NCBI) and calculates statistical significance (Donkor et al., 2014; NCBI, 2017, 2020).

RESULTS

The result of the molecular characterisation of the raw sewage sample obtained from septic tank using 16S rRNA DGGE (Figure 2) show distinct bands on sodium

dodecyl sulphate (SDS) ranging from 18.5 to 100 kDa. Two primers were used representing the two lanes of bands. Each band on the lanes represents a gene from a bacterium.

Result from the PCR analysis of raw domestic sewage sample obtained from the various locations sampled and the subsequent blasting of the sequences using NCBI Blast Online shows the presence of mainly anaerobic and facultative anaerobic methanogens. *Methanococcus methanococcus*, *Deferribacteres bacterium* (partial genome 291088137), *Flavobacteria bacteria*, *Bacteroides dorei* (CP 008741) *Clostridium difficile* (AM180355), *Kuenenia stuttgartiensis*, (CT573073), *Zymonas mobilis* (AE008692), *Methanosarcina bankerii* (CP00746), *Methanococcus maripaludis* (BX950229), *Bacteroides metaiotamicron* (CAE015928), *Methanobacterium formicicum* (CP006933), *Desulfitobacterium dichloroeliminans* (CP003344) and *Desulfobacterium* sp. (FR695868) are the different species identified from the study. The phylogram of the different isolates (Figure 3) shows that methane producing bacteria were 7 out of the 13 bacteria isolated representing 53.8% of the total species occurrence in the sample.

DISCUSSION

The result from the PCR analysis of raw domestic sewage sampled in this study and the subsequent blasting of the sequences using NCBI Blast Online shows the presence of mainly anaerobic and facultative anaerobic organisms especially of the methanogen group. *Methanococcus methanococcus*, *Deferribacteres bacterium* (partial genome 291088137), *Flavobacteria bacteria*, *Bacteroides dorei* (CP 008741), *Clostridium difficile* (AM180355), *Kuenenia stuttgartiensis* (CT573073), *Zymonas mobilis* (AE008692), *Methanosarcina bankerii* (CP00746), *Methanococcus maripaludis* (BX950229), *Bacteroides metaiotamicron* (CAE015928), *Methanobacterium formicicum* (CP006933) *Desulfitobacterium dichloroeliminans* (CP003344) and *Desulfobacterium* sp. (FR695868) are the different species identified from the analysis. Zabranska and Pokorna (2018), as well as Connelly et al. (2019) reported a microbial community underpinned by anaerobic degrading methanogens. The phylogram of the different isolates shows that methane producing bacteria were 7 out of the 13 bacteria isolated (53.8%) of the total species occurrence in the sample. This provided an overall picture of the microbial community present the septic tank. This result is in consonance with the work of Connelly et al. (2019) who stated that the septic system appeared to be underpinned by microbial communities that had the potential to support complete degradation of organics by methanogenic anaerobic digestion. Sequence analysis of the 16S rRNA gene has been

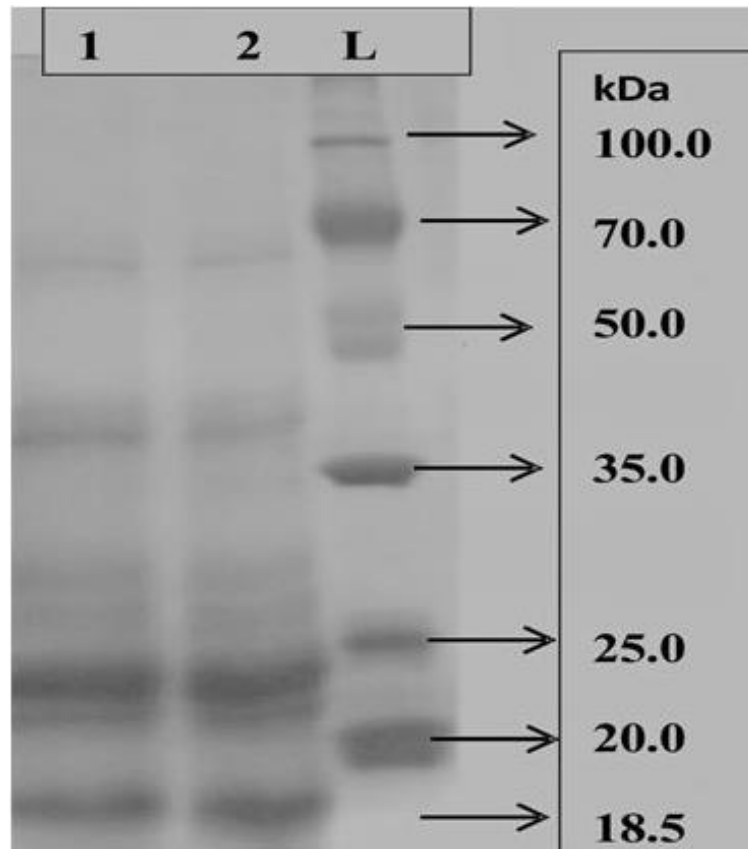


Figure 2. Molecular characteristics of the sewage sample obtained directly from septic tank using 16SrRNA DGGE show distinct bands on SDS ranging from 18.5 to 100 kDa.

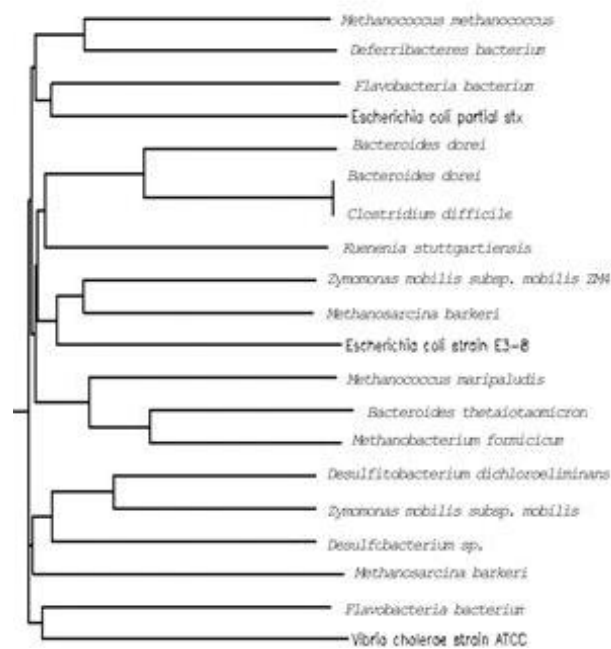


Figure 3. Phylogram of micro-organisms isolated from raw sewage sample using 16SrRNA DGGE.

widely used to identify bacterial species and perform taxonomic studies (Petti, 2007; Odeyemi et al., 2018; Abada et al., 2019; Numberger et al., 2019). Unfortunately, 16S rRNA hyper variable regions exhibit different degrees of sequence diversity, and no single hyper variable region is able to distinguish among all bacteria. Bacterial activity can be divided into two major distinct phases in the anaerobic digestion; namely acidogenesis (during which acid forming bacteria reduce complex organic matter to organic acids) and methanogenesis (during which specific methanogens may convert the acetate into methane and carbon (IV) oxide). As methane production is an end product, it can also be used to predict septic tank efficiency. Thus, it is important to be able to define the methanogenic species present in these reactors (Smith et al., 1989). Similar organisms were obtained in a study carried out by Garrity and Holt (2001) where they found methanogens in anaerobic sediments and anaerobic sewage sludge bioreactors. Species within this family use acetate as their sole energy source, which is metabolised into methane and carbon IV oxide. The diversity of the methanogenic population depends mainly on the composition of the substrate (Levesque and Guiot, 2004), changes in temperature, pH stability (Odeyemi et al., 2018) and indicators as well as the solids retention time (Cassery and Erijman, 2003; Schaidler et al., 2017). Clay soils are known to have higher retention time with a hydraulic conductivity ratio of 1×10^{-11} to 4.7×10^{-9} mm.

PCR analysis also confirms the presence of *Desulfobacterium dichloroeliminans* (CP003344) and *Desulfobacterium* sp. (FR695868) which are sulphate-reducing bacteria in this study. This aligned to the hybridization analysis of 16S rDNA DGGE to investigate the diurnal behaviour of sulphate reducing bacteria in biofilms from an activated sludge basin of a wastewater treatment plant by Teske et al. (1998) were profiles showed that *Desulfobulbus* and *Desulfovibrio* populations came up at the onset of the sulphate reduction.

The use of traditional microbiological techniques in determining population structures and characteristics is limited as it has been shown that many organisms are not readily cultured on selective media (Briones and Raskin, 2003). A better understanding of the diversity of the methanogenic bacteria in bioreactors can improve the anaerobic process stability (Bitton, 1999). The methanogens are responsible for the terminal metabolic reactions in a bioreactor and are considered to be the key players in the anaerobic process. The ability to monitor methanogens and understand their ecology is essential to effectively control the start-up and operation of anaerobic digesters in general and the septic tank specifically (Schink, 1997). Finally, certain phylogenetic groups like the methanogens or the methanotrophs exhibit a restricted metabolic potential, which is determined by characteristic functional genes. The detection of these specific genes for example methanol dehydrogenase structural genes of methanotrophs has

been used to verify results obtained by the 16S rRNA sequence analysis (Holmes et al., 1995).

Conclusion

The use of septic tank sewage system is an age long practice that is gaining more and more relevance in recent years due to its ease of use, affordability and efficiency. For the system to perform optimally, its operation and utilization techniques must be well studied. Microorganisms particularly bacteria play an important role in the digestion of septic tank constituents into less toxic compounds which the soil can receive and further act upon. The use of traditional microbiological techniques in determining population structures and characteristics is limited as it has been shown that many organisms are not readily cultured on selective media, hence, the need to utilize molecular techniques in identifying and characterizing microbial species.

The phylogram of the different isolates from this study shows that methane producing bacteria were 7 out of the 13 bacteria isolated (53.8%) of the total species occurrence in the sample, while sulphate-reducing and ammonium-oxidizing bacteria accounted for the remaining 6 isolates representing 46.2% of the total bacteria population. This provided an overall picture of the microbial community present the septic tank. A better understanding of the diversity of the methanogenic bacteria in bioreactors can improve the anaerobic process stability; since methanogens are the most occurring species in many anaerobic digesters.

The methanogens are responsible for the terminal metabolic reactions in a bioreactor and are considered to be the key players in the anaerobic process. The ability to monitor methanogens and understand their ecology is essential to effectively control the start-up and operation of anaerobic digesters in general and the septic tank specifically. Lastly, the introduction of noxious chemicals in the form of disinfectant and cleaning agents by humans, may have significantly affected the microbial community and dynamics of the septic tank, this is considered to be a crucial factor in the low biodegradation efficiency of the septic system.

ACKNOWLEDGEMENTS

The author wish to thank Dr. Emmanuel Imariagbe of the Department of Environmental Toxicology University of Benin, Benin City Edo State who made meaningful contributions to this work and Prof. Lawrence Okoror of Biosolutions Technologies Akure, Ondo State Nigeria for running the molecular aspect of this work.

REFERENCES

Abada E, Al-Fifi Z, Al-rajab AJ, Mahdi M, Sharma M (2019). Molecular

- identification of biological contaminants in different drinking water resources of Jazan region, Saudi Arabia. (2019). *Journal of Water and Health* 17(4):622–632.
- American Public Health Association (APHA) (1992). Standard methods for the examination of water and waste water. American Public Health Association 18th edition Washington D.C.
- Bitton G (1999). *Waste water Microbiology*, Second Edition, Wineglass, NY. p. 139.
- Boon N, De Windt W, Verstracte W, Top EM (2002). Evaluation of nested PCR-DDE with group specific 16S rRNA primers for the analysis of bacterial communities from different waste water treatment plants microbes. *Ecology* 39:101-112.
- Briones A, Raskin L (2003). Diversity and dynamic of microbial communities in engineered environments and their implications for process stability *Current Opinion in Biotechnology* 14:270-276.
- Burubai W (2005). Source water pollution abatement and best management practices. In *Proceedings of 7th African USA International Conference on Manufacturing Technology* pp. 277-282. Port Harcourt, Nigeria (12-14 July).
- Cai L, Ju F, Zhang T (2014). Tacking human sewage microbiome in a municipal wastewater treatment plant. *Applied Microbiology and Biotechnology* 98:3317-3326.
- Cassery C, Erijman L (2003). Molecular monitoring of microbial diversity in an UASB REACTOR *International Biodeterioration and Biodegradation* 52:7-12.
- Connolly S, Pussayanavin T, Randle-Boggis RJ, Wicheansan A, Jampathong S, Keating C, Ijaz UZ, Sloan WT, Kootatet T (2019). Solar septic tank: Next Generation sequencing reveal a effluent microbial community composition as a useful index of system performance. *Water* 1:2660.
- Doelle HW (2001) *Biotechnology and Human Development in developing countries* www. Ejbotechnology. Info.
- Donkor ES, Dayie NT KD, Adiku TK (2014). Basic local alignment search tool (BLAST) and fast alignment (FASTA). *Journal of Bioinformatics and Sequence Analysis* 6(1):1-6.
- Fidelia N (2004). Source water pollution abatement and best management practices. In *Proceedings of 7th Africa-USA international Conference on Manufacturing Technology*, pp. 277-282. Port Harcourt, Nigeria (12-14 July).
- Garrity GM, Holt JG (2001). Phylum All., Euryarchaeota phy. Nov., In: D.R. Boone, R.W. Castenholz (Eds), *Bergey's Manuel of Systemic Bacteriology* second ed., Springer, New York, pp. 211-294.
- Holmes AJ, Owens NJP, Murrell JC (1995). Defection of novel marine methanotrophs using phylogenetic and functional gene probes after methane enrichment. *Microbiology* 141:1947-1955.
- Levesque MJ, Guiot SR (2004). Positioning of *Methanosaeta* and *Methanosarcina* sp. within the microstructure of carbohydrate-fed anaerobic granules, In: *Proceedings of the 10th Anaerobic Digestion Conference*, Montreal Canada pp. 1934-1937.
- Logares R, Mangot J-F, Massana R (2015). Rarity in aquatic microbes: Placing protists on the map. *Research in Microbiology* 166:831–841.
- Lowe SE, Jain MK, Zeikus JG (1993). Biology, ecology and biotechnological applications of anaerobic bacteria adapted to environmental stress in temperature, pH, salinity or substrates. *Microbiological Reviews* 57:451-509.
- Marti E, Jofre J, Balcazar JL (2013). Prevalence of antibiotic resistance genes and bacterial community composition in a river influenced by a wastewater treatment plant. *PLoS ONE* 8:e78906
- Muyzer G, Waal EC de, Uitterlinden AG (1993). Profiling of complex microbial populations by denaturing gradient gel electrophoresis analysis of polymerase chain reaction-amplified genes coding for 16S rRNA *Applied and Environmental Microbiology* 59:695-700.
- National Centre for Biotechnology Information (NCBI) (2017). Pubchem Compound Database (ID) Sept 16, 2017.
- National Centre for Biotechnology Information (NCBI) (2020). Pubchem Compound Database (ID) May 27, 2020.
- Newton RJ, McLellan SL, Dila DK, Vineis JH, Morrison HG, Murat Eren A (2015). Sewage reflects the microbiomes of human population. *mBio* 6(2):e02574-14.
- Numberger D, Ganzert L, Zoccarato L, Muhldorfer K, Sauer S, Grossart H-P, Greenwood AD (2019). Characterization of bacterial communities in wastewater with enhanced taxonomic resolution by full-length 16S rRNA sequencing. *Nature* 9:9673.
- Odeyemi AT, Ayantola KJ, Peter S (2018). Molecular characterization of bacterial isolates and physicochemical assessment of well water samples from hostels at Osekita, Iworoko-Ekiti, Ekiti State. *American Journal of Microbiology Research* 6(1):22–32.
- Petti CA (2007). Detection and Identification of microorganisms by gene amplification and sequencing. *Clinical Infectious Diseases* 44:1108-1114.
- Richards BK, Herndon HG, Jewell WJ, Cummings RJ, White TE (1994). In situ methane enrichment in methanogenic energy crop digesters. *Biomass and Bioenergy* 6(4):275-282.
- Robert W, Terry B (2004). *Septic tank operations*. USDA-104. GPO Washington DC., p. 76
- Rojer RN (2002). *Introduction to Environmental analysis*. New York: John Wiley and Sons Ltd. pp 313.
- Schaider LA, Rodgers KM, Rudel RA (2017). Review of organic wastewater compounds concentrations and removal in onsite wastewater treatment systems. *Environmental Science Technology* 51:7304–7317.
- Schink B (1997). Energetics of syntrophic cooperation in methanogenic degradation. *Microbiological and Molecular Biology Review* 94:262-280.
- Smith T, Ince M (1989). *Septic System Density and Ground Water Contamination in Illinois: A survey of state and local regulation*. NTIS Report PB. 89-178545.
- Sanger F, Coulson AR (1975). A rapid method for determining sequence in DNA by primed synthesis with DNA polymerase. *Journal of Molecular Biology* 25:(3) 441-448.
- Teske A Ramsing NB, Habicht K, Fukui MK, Uver J, Jergensen BB, Cohen Y (1998). Sulphate –reducing bacteria and their activities in cyanobacteria mats of solar lake (Sinai Egypt). *Applied and Environmental Microbiology* 64:2943-2951.
- Whithers PJA, Jordan P, May L, Jarvie HP, Deal NE (2014). Do septic tank systems pose a hidden threat to water quality? *Frontiers in Ecology and the Environment* 12:123–130.
- Ye L, Zhang T (2013). Bacterial communities in different sections of a wastewater treatment plant revealed by 16S rDNA 454 pyrosequencing. *Applied Microbiology and Biotechnology* 97:2681–2690.
- Zabraska J, Pokorna D (2018). Bioconversion of carbon dioxide to methane using hydrogen and hydrogenotrophic methanogens. *Biotechnology Advances* 36:707-720.
- Zinder SH (1984). Microbiology of anaerobic conversion of organic wastes to methane: Recent developments. *News* 50:294-298.
- Zinder SH (1993). Physiological ecology of methanogens. In Ferry, J.G (ed) *Methanogenesis: Ecology, Physiology, Biochemistry and Genetics*. New York: Chapman and Hall. pp. 128-206.

Full Length Research Paper

Physicochemical influence on the spatial distribution of faecal bacteria and polychaetes in the Densu Estuary, Ghana

Akita L. G.^{1*}, Laudien J.², Akrong M.³, Biney C.⁴, Nyarko E¹. and Addo S.¹

¹Department of Marine and Fisheries, University of Ghana, P. O. Box LG 99, Legon-Accra, Ghana.

²Alfred Wegner Institute Helmholtz Centre of Polar and Marine Research, Am Alten Hafen 26, 27568 Bremerhaven, Germany.

³CSIR-Water Research Institute, P. O. Box M 32, GP-018-964, Accra, Ghana.

⁴Ecosystem Environmental Solutions Limited, GD-213-5404, Accra, Ghana.

Received 28 February, 2020; Accepted 2 April, 2020

Coastal ecosystems are increasingly impacted by man-made disturbances including pollution from agriculture, aquaculture and municipal waste. This study employed multiple ecological indicators to assess environmental quality of the Densu Estuary and understanding of environmental controls on the spatial distribution of organisms. Physicochemical parameters were measured *in situ*. Water and sediment samples were collected from ten stations and analysed for nutrients, total suspended solids and organisms using standard methods. The water quality index for the Densu Estuary ranged from 359.5 to 484.4, suggesting an unhealthy ecosystem. The abundance of indicator species, e.g. faecal bacteria (*Escherichia coli*, *Enterococcus* species) and polychaetes (*Capitella* and *Nereis* species) varied significantly ($p < 0.05$) among stations. Contaminated sites are located landwards with high human impacts. Faecal bacteria and polychaete abundance correlated significantly ($p < 0.05$) with the respective physicochemical parameters. Canonical analysis (74.11%) showed the physicochemical influence on the spatial distribution of species. The pH significantly ($p < 0.05$) controlled the spatial distribution of faecal bacteria and polychaetes in the Densu Estuary. The results suggest environmental pollution in the Densu Estuary, useful baseline information for effective legislation towards its sustainable management.

Key words: Biological indicators, water quality index, pollution, estuarine ecology, Densu Estuary.

INTRODUCTION

Estuaries contain mixed fresh and marine water which include productive wetlands and most productive biogenic zones of nearshore waters (Twilley et al., 1992; Armah, 1993; McLusky and Elliot, 2010; Mahu et al.,

2016). They are habitats for benthic invertebrates, feeding ground for nektonic, migratory birds and nursing grounds of fishes (Lamptey and Armah, 2008; Aggrey-Fynn et al., 2011; Greene et al., 2015). Growing human

*Corresponding author. E-mail: lailah.akita@gmail.com.

populations, urbanization and industrial activities increasingly affect coastal ecosystems (Monney et al., 2013; Nyarko et al., 2015; Yeleliere et al., 2018). The management of solid and liquid waste is a major problem in Ghana, especially in urban areas and cities due to inadequate waste treatment facilities and management (Aglanu and Appiah, 2017). The waste is mostly transported by rivers and streams into estuaries and eventually into the sea (Mahu et al., 2015; Klubi et al., 2018). Access to clean and safe drinking water in cities is inadequate in supply and many people die of water-borne diseases (Shuval, 2003; Cabral, 2010; Odonkor and Ampofo, 2013).

The coastal environments are mostly impacted through pollution, land use and hydrological changes (Shuval, 2005; Stewart et al., 2008; Lamptey et al., 2013; Klubi et al., 2019). Estuaries are complex dynamic environments that are susceptible to anthropogenic alterations (Bucci et al., 2012; Greene et al., 2015; Klubi et al., 2018). Intensive industrialization and population growth exists around urban coastal areas of Ghana. The human activities (e.g., agrochemical inland runoff, mining, industrial and domestic waste discharges) can alter the environmental characteristics of the coastal water bodies including estuaries, lagoons, rivers among others (Lamptey and Armah, 2008; Okyere et al., 2011; Nyarko et al., 2015; Yeleliere et al., 2018).

The Densu Estuary is located in the dry equatorial climate region of Ghana with the climate governed by the monsoon, the harmattan and the equatorial air masses (Armah and Amalalo, 1998; Teley, 2001; Karikari and Ansa-Asare, 2006). The primary aim of this study was to assess the human impacts on the environmental quality of the Densu Estuary through multiple ecological indicators. The specific objective was to gain knowledge on how physicochemical factors influence the spatial distribution of organisms in the Densu Estuary. We hypothesize that (i) physicochemical parameters vary in the estuarine system and (ii) physicochemical parameters are drivers for the spatial distribution of organisms within the system. The preliminary results established hydrochemical dynamic coupled with the ecological conditions of the Densu Estuary. The spatial pattern of organism reflects not only physicochemical characteristics of the water body, but also the state of sediment quality and further insight into estuarine ecology.

MATERIALS AND METHODS

Study site

The Densu Estuary is located between 5°30'N and 5°31'N and 0°17'W and 0°18'W (Figure 1). The river basin has a catchment area of 2,565 km² and is 116 km long (Debrah, 1999). The Densu River has its source in the Atewa-Atwiredu mountain range near Kibi in the East Akyem District of the Eastern Region of Ghana (Hagan et al., 2011). The Densu River Basin is one of the most important river basins of Ghana. It encompasses the northwestern

suburbs of Accra, the capital of Ghana and is densely populated. The basin is endowed with rivers and streams, mostly ephemeral, but few perennial known to be polluted (WRI, 2003; Fianko et al., 2009). The major tributaries include Adeiso (Adaíso), Nsaki (Nsaki), Dobro, Mame and Kuia. The Densu River enters the Weija Reservoir and discharges into the Densu Estuary, which drains into the Gulf of Guinea, Ghana.

The Densu Estuary is surrounded by a wetland (also known as "Densu Delta", "Densu Wetland", "Densu Ramsar"), recognized as the Ramsar site due to its ecological biodiversity. It is surrounded by mangroves (e.g., *Avicennia africana*), which serve as nursery grounds for migratory fish species (Koranteng, 1995), habitat for birds (especially long-distance migratory birds along the East Atlantic Flyway); it supports approximately 57 species of seashore birds (population ~35,000 specimens). The estuarine waters support about 15 species of finfish (14 genera and 9 families, most common of which are *Sarotherodon melanotheron* and *Tilapia zilli*). The beachfront is also a nursing ground for marine turtles (e.g., *Lepidohelys olivacea*, *Chelonia mydas* and *Dermodochelys coriacea*). The estuary is also used for crab fisheries and oyster farming. Furthermore, the wetland serves as floodplain. The availability and quality of water in the estuary and wetland play an important role in defining not only where people can live, but also their quality of life (Solley et al., 1998).

Field sampling

At ten stations (S1 to S10) water and sediment samples were taken to assess the ecological integrity of the Densu Estuary (Figure 1 and Table 1). Sampling line transects started landwards and ended seawards (Figure 1). Sampling was carried out on the 19th of May 2017 during mid-tide (11:15 to 13:30). Samples were taken from water depths ranging from 0.10 to 0.70 m. Coordinates for each station are recorded using the Global Position System (GPS), Garmin etreX Model (www.garmin.com).

Physicochemical parameters such as temperature, salinity, specific electrical conductivity, redox potential, dissolved oxygen concentration and saturation were measured *in situ* using a Horiba Digital Water Quality Multi-parameter instrument (Horiba Probe, Model U-52G 30M, Horiba Company Limited, Japan). Sample bottles were washed three times with estuary water before filling. Water samples (N = 10) were collected from 10 cm depth in 500 ml bottles for phosphate and nitrates and suspended particles analyses. Additionally, water samples (N = 10) were collected in 500 ml plastic bottles covered with black polythene bags for chlorophyll-a concentration estimates. Furthermore, water samples (N = 10) were collected in 200 ml sterilized water bottles for microbiological analyses.

Surface sediments were collected at the sampling stations from 20 to 30 cm depths using an Ekman Grab (area: 0.04 m²) (Mudroch and Azcue, 1995). The sediment was put into interim storage in a bowl and immediately scooped into labelled polythene bags (bacteria and benthos, N=10 each) for further analyses.

The samples for nutrients and bacterial analyses were kept on ice cubes stored in ice-coolers to reduce biological activity. The sediment sample for macrobenthic analysis was preserved in 10% buffered formaldehyde and stained with Rose Bengal. All samples were then transported to the laboratory and kept in a refrigerator at 4°C for 30 min before analysis. The microbiological analyses were carried out within 24 h at the Environmental Biology Laboratory, Council for Scientific and Industrial Research (CSIR)-Water Research Institute (WRI), Accra, Ghana.

Determination of chemical parameters

The chemical parameters were determined according to procedures

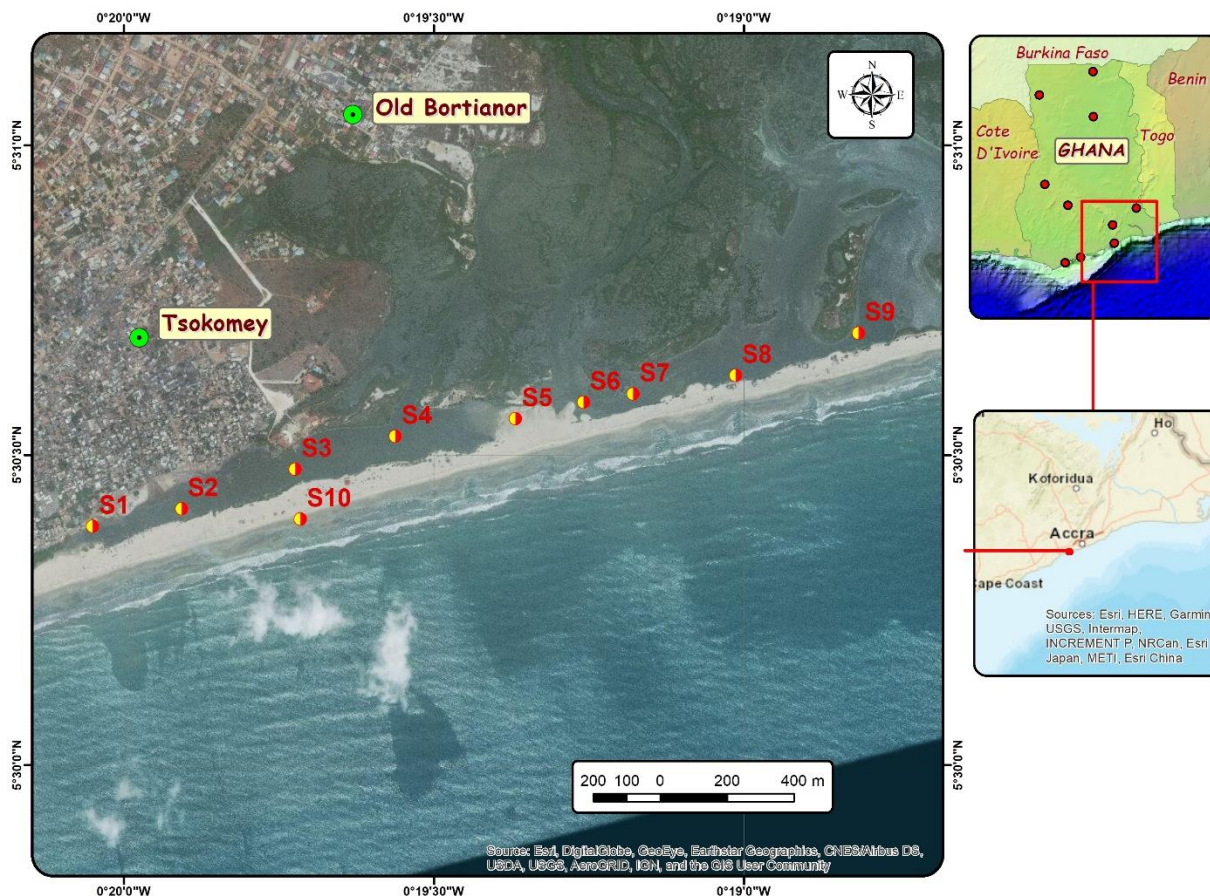


Figure 1. Map showing the ten sampling stations in the Densu Estuary, Ghana.

Table 1. Description of ten sampling stations at the Densu Estuary, Ghana.

Station	Site description of stations	Coordinates (Latitude N, Longitude W)
S1	Separated from the sea by sand, landfill site, Bortianor	5°30'23.1", 0°20'03.0"
S2	Fishing boat landing site, Bortianor	5°30'24.8", 0°19'54.4"
S3	Middle stream, river flow into estuarine, Bojo-Tsokomey	5°30'28.6", 0°19'43.4"
S4	Mixing of fresh and sea water	5°30'31.8", 0°19'33.7"
S5	Mixed fresh and sea water, wetland zone, Shore birds, crab farming	5°30'33.5", 0°19'22.1"
S6	Mixing zone, oysters farming, Faana village	5°30'35.1", 0°19'15.5"
S7	Mixing zone, Mangroves, Panbros village	5°30'35.9", 0°19'10.7"
S8	Tidal influence, mangrove rich zone	5°30'37.7", 0°19'00.8"
S9	Downstream, open to sea, intrusion of saline water	5°30'41.8", 0°18'48.9"
S10	Surf zone sea water	5°30'23.8", 0°19'42.9"

outlined in the Standard Methods for the Examination of Water and Wastewater (APHA, 1998, 2012). Nitrate (NO_3^-), phosphate (PO_4^{3-}) and sulfates (SO_4^{2-}) were measured using a HACH 2010 Spectrophotometer (Model DR/2010) with a precision of ± 0.10 v mg/L (HACH Company, Loveland, Colorado, USA) (www.hach.com; HACH, 2012). Total dissolved solids (TDS) are determined by filtering, weighing the sampled water and measuring it gravimetrically after drying it in an oven to a constant weight at

105°C (APHA 2012). To measure total suspended solids (TSS), 100 ml of the water sample was filtered through a pre-weighed filter that was dried in an oven at the temperature of 104°C to constant weight and repeated for 3 steps, then the total suspended solids is calculated (thus the TSS, mg/L is equal to average weight from step 3 in g minus average initial weight from step 1 in g multiple by 1000 mg/L divided by sample volume in L) (APHA, 2012).

Chlorophyll-a concentration was extracted from the water

Table 2. Average values of selected physicochemical parameters measured and computed water quality index for the Densu Estuary, Ghana.

Parameter	Average values	USEPA (2009) standards	Assigned Weight (AW)	Relative weight (RW)
pH	8.35	6.5-8.5	4	0.22
Alkalinity [mg/L]	3.66	100	2	0.11
Dissolved oxygen [mg/L]	10.48	5	4	0.22
Electrical conductivity [μScm^{-1}]	43850	2500	3	0.17
Nitrates [mg/L]	2.98	10	4	0.22
Phosphates [mg/L]	0.33	0.1-0.3	1	0.06
$\Sigma(\text{SI})$			18	1.00
			WQI	416.50 \pm 44.07
Classification			> 300-unsuitable water for drinking	

samples using 96% ethanol and measured with a UV/Vis spectrophotometer at 665 and 649 nm (APHA, 2012). Chlorophyll-*a* concentration was estimated as a proxy for phytoplankton concentration and thus as an indicator of the trophic state (Monbet, 1992; Hinga et al., 1995; Boyer et al., 2009). The trophic status of the ecosystem was determined based on the estimated chlorophyll-*a* concentrations and classified using the following scheme: <1.0 $\mu\text{g/L}$ = ultra-oligotrophic; 1.0 - 3.0 $\mu\text{g/L}$ = oligotrophic; > 3.0 - 8.0 $\mu\text{g/L}$ = mesotrophic; > 8.0 - 30.0 $\mu\text{g/L}$ = eutrophic; > 30.0 $\mu\text{g/L}$ = hypertrophic (da Silveira Fiori et al., 2013).

Water quality index

The Water Quality Index (WQI) is defined as a rating, reflecting the composite influence of different water quality parameters on the overall quality of water (Mophin-Kani and Murugesan, 2011; Tirkey et al., 2015; Fathi et al., 2016). It was first proposed in 1965 (Horton, 1965). The WQI was computed using recommended water quality standards (Sanchez et al., 2007; USEPA, 2009; Nyarko et al., 2015) and four steps followed. In the first step, each of the six environmental parameters (Table 2) has been assigned a weight (AW) according to its relative importance in the overall quality of water for drinking purposes. The maximum weight of 4 has been assigned to parameters such as pH, dissolved oxygen concentration and nitrate due to their major importance in water quality assessment (Ramakrishnaiah et al., 2009; Mophin-Kani and Murugesan, 2011; Nguyen and Sevando, 2019). Phosphate is given the weight of just 1 as it plays a minor role in the water quality assessment. Other parameters were electrical conductivity (assigned 3) and alkalinity (assigned 2) (Table 2). For the second step, the relative weight (RW) was computed using a weighted arithmetic index (Equation 1):

$$RW = \frac{AW_i}{\sum_{i=1}^n AW_i} \quad (1)$$

where RW is the relative weight, AW is the assigned weight of each parameter and *n* is the number of parameters.

In the third step, a quality rating scale (Q_i) for each parameter was assigned by dividing its measured value of the water quality parameter in each water sample by its respective standard according to the guidelines of USEPA (2009) and then multiplied by 100:

$$Q_i = \left[\frac{C_i}{S_i} \right] \times 100 \quad (2)$$

where Q_i is the quality rating, C_i is the measured value of the water quality parameter in each water sample in mg/L, and S_i is the WHO drinking water standard for each chemical parameter in mg/L according to the guidelines of USEPA (2009).

In the fourth step, the sub-indices (SI_i) were first determined for each chemical parameter (Equation 3),

$$SI_i = RW \times Q_i \quad (3)$$

where SI_i is the sub-index of the i^{th} parameter and Q_i is the rating based on the concentration of i^{th} parameter.

The overall WQI was then calculated by adding the sub-index values of each water sample as follows:

$$WQI = \sum_{i=1}^n SI_i \quad (4)$$

Computed WQI values were categorized based on the water quality classification scheme: < 50-excellent; 50-100, good water; 200-300, very poor water and > 300, unsuitable water (Sahu and Sikdar, 2008; Ramakrishnaiah et al., 2009; Lamptey et al., 2013; Duncan, 2018).

Biological analyses

Bacteriological examination of water and sediment samples was conducted using standard methods (Horan, 2003; Cabral, 2010; Odonkor and Ampofo, 2013). Total coliforms and faecal bacteria were determined by the membrane filtration method using M-Endo-Agar Les (Difco) at 37°C and on MFC Agar at 45°C, respectively (Cabral, 2010). In total 20 ml of each water sample were separately filtered through 0.45 μm pore size membrane filter paper, mounted on a filtration pump, whereas 5 g of each sediment sample was given into a sterile 50 ml tube. Thereafter, 45 ml of PBS was added to the sample vortexed for 30 s to homogenize it. The pH was slowly adjusted to 9.0 by adding drops of 0.1 N NaOH. The prepared sample was vigorously mixed with the help of a shaker for 30 min at room temperature. The sample was left to stand for 15 min and 1 ml of the supernatant diluted with 10 ml sterile distilled water before membrane filtration.

Determination of total coliforms and *Escherichia coli* were undertaken by aseptically placing filters on poured and solidified Cromocult Agar Media in Petri dishes and incubated at $37 \pm 0.5^\circ\text{C}$ for 18 to 24 h. Similarly, for the enumeration of *Enterococcus*

species, the filters were aseptically plated on Slanetz and Bartley medium and incubated at 45°C. Typical presumptive colonies were identified as total coliform (purple-blue colonies), *E. coli* (only blue colonies) and *Enterococcus* spp. (pinkish to red colonies); these were counted with the aid of a colony counter and expressed in CFU/100 ml and CFU/g for water and sediment samples, respectively.

For macrofauna analysis, the fixed sediment samples were washed with tap water through a 0.2 mm mesh sieve to remove the fixative. Thereafter, the samples were sorted and animal groups identified and quantified under a dissecting microscope. Their abundance was determined by counting their head, the identification followed taxonomical keys (Day, 1967a, b).

Statistical analysis

Physicochemical parameters and biological data that were normally distributed were subjected to a One-way analysis of variance (ANOVA) to test for spatial variation. A significance level of 5% was adopted. The physicochemical parameters were standardized, while the biological data were $\log(X+1)$ transformed.

Principal component analysis (PCA) was used to identify the relationship between the species composition and the effects of the physicochemical parameters (Šmilauer and Lepš, 2014). This allows separation of effects of space and environmental variables on the oribatid community structure (Šmilauer and Lepš, 2014). The PCA and Redundancy analysis (RDA) are both linear quantitative ordination methods, which are closely related to linear regression. However, PCA is an indirect gradient analysis, while RDA is a direct gradient analysis (Šmilauer and Lepš, 2014). The ordination scores can be used to model the distribution of taxa along physicochemical gradients and to estimate values of preferred environments, environmental tolerance and peak abundance (Patzkowsky and Holland, 2012). The PAST software was used to two-way constrained cluster analysis (Hammer et al., 2001). The Canoco software was employed for the multivariate statistical analyses (e.g., PCA, CA and RDA) (Šmilauer and Lepš, 2014). Descriptive statistics were calculated using PAST and Excel spreadsheets. Furthermore, the PRIMER 6 package was used to run cluster analyses (Clarke and Gorley, 2006) to identify groups of similar associations (e.g., taxa and environmental variables) and to display the relationships among them (Patzkowsky and Holland, 2012).

Pearson's correlation coefficient (r) was used to test the strength of linear associations between the biological data and physicochemical parameters (Khamis, 2008), using a statistical package for social sciences (SPSS 21.0). The correlation coefficient (r) was determined to estimate the degree of the relationships (Khamis, 2008; Yadav, 2018). The dimensionless quantity value of the coefficient of correlation (r) can range from -1 (perfect negative correlation) through 0 (no correlation) to +1 (perfect positive correlation) (Möller and Scharf, 1986; Nagelkerke, 1991; Yadav, 2018). Significance levels of 0.05 and 0.01% were adopted.

RESULTS

Physicochemical parameters

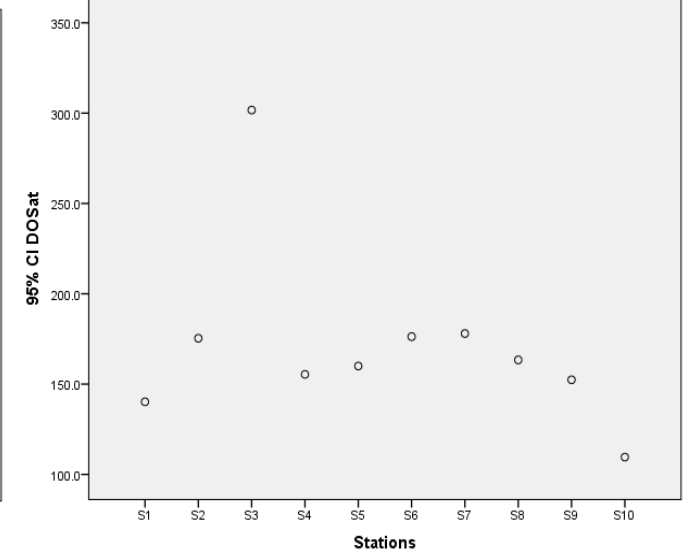
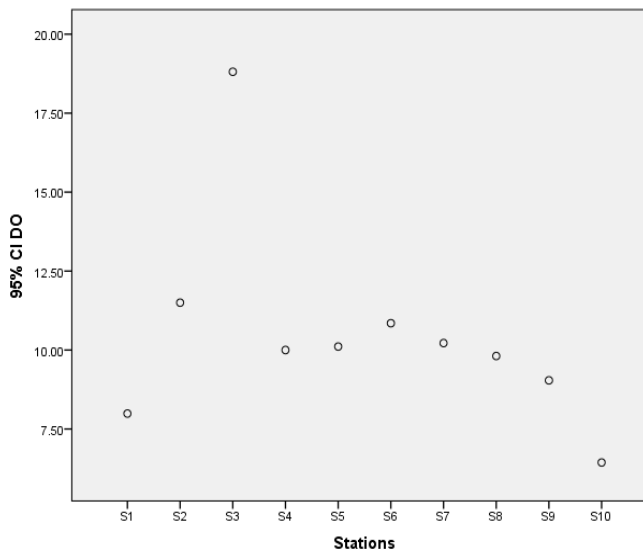
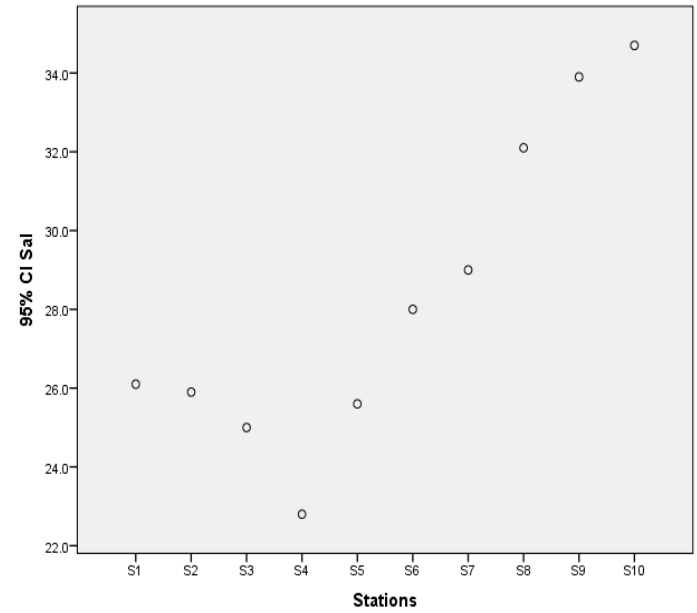
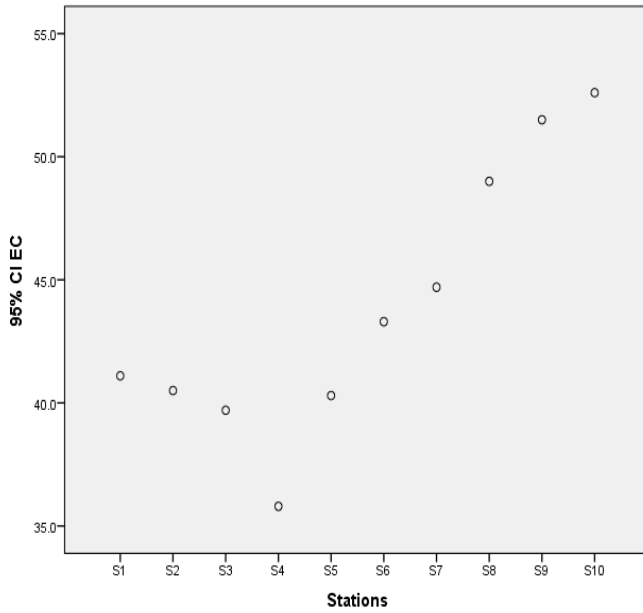
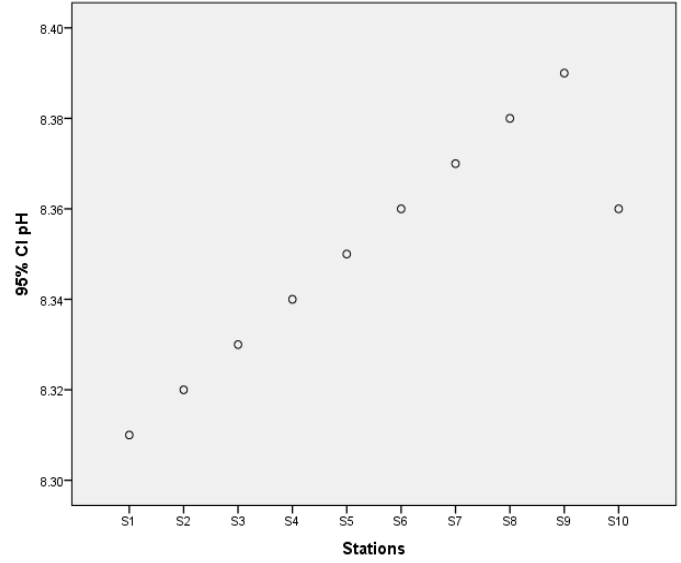
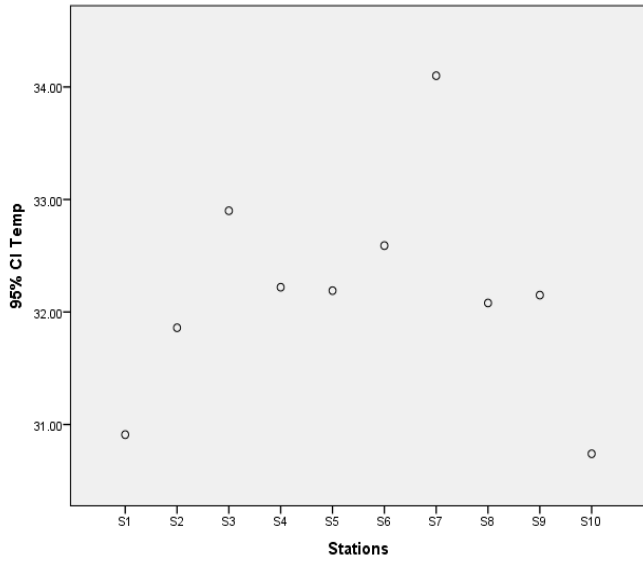
The spatial distribution of physicochemical and microbiological characteristics of the Densu Estuary is expressed in Figure 2, providing the 95% confidence interval. The mean values are summarized in Table 3. There was a significant variation for some physicochemical parameters (mainly dissolved oxygen

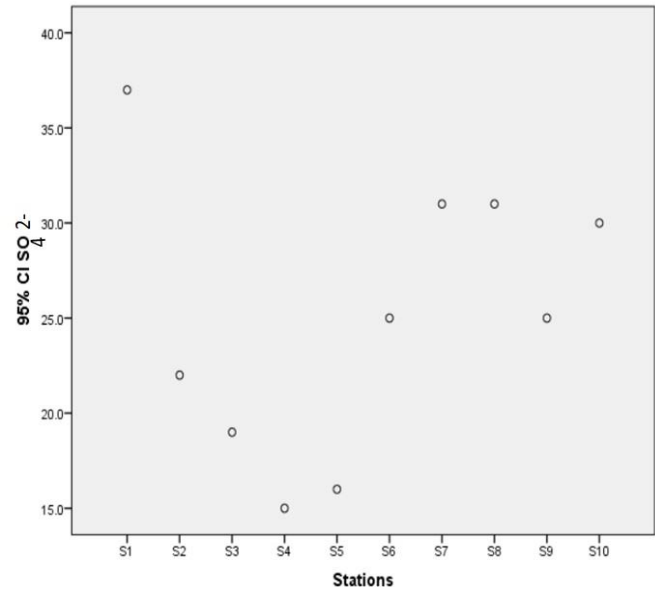
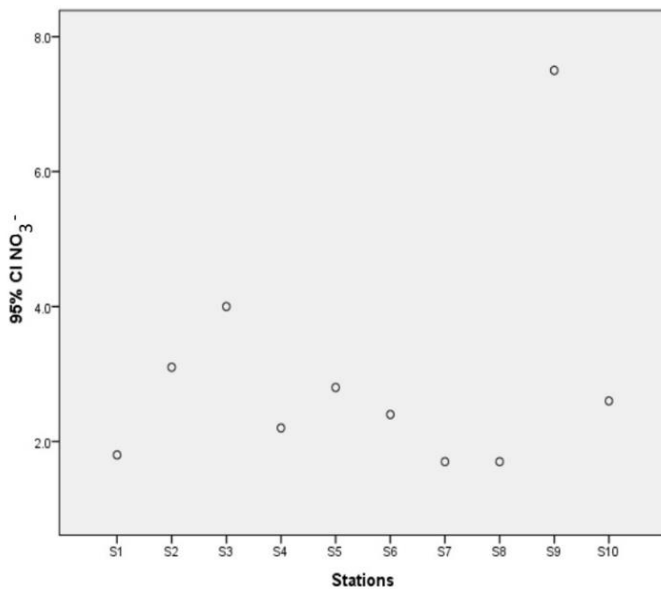
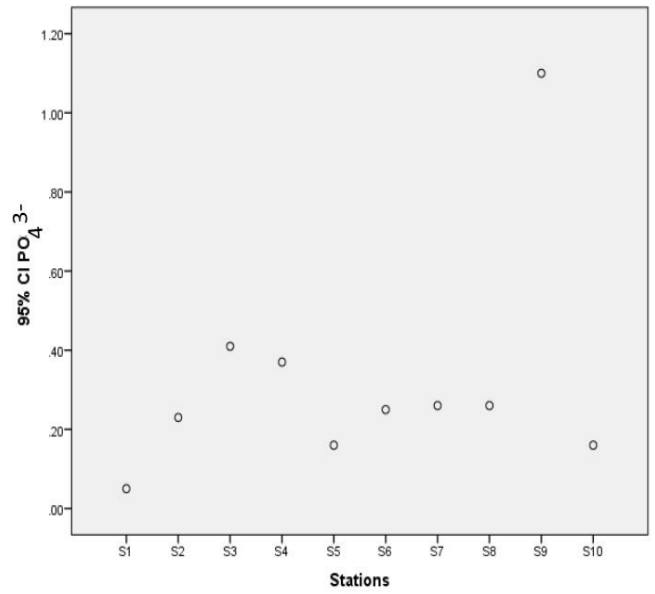
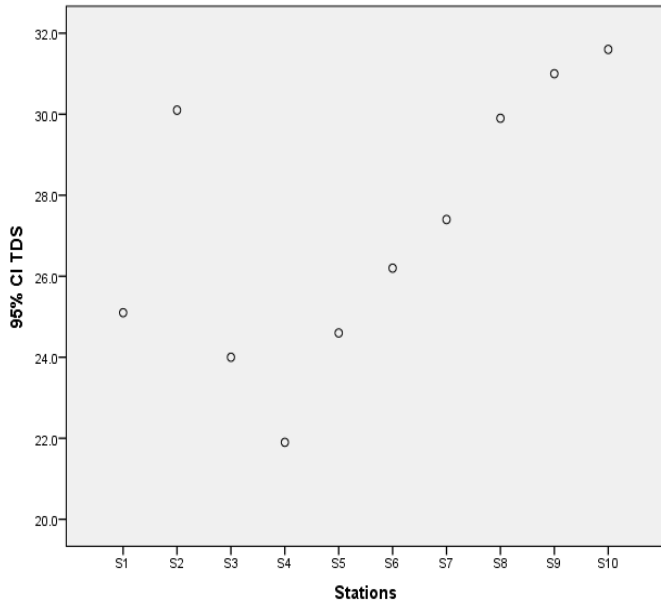
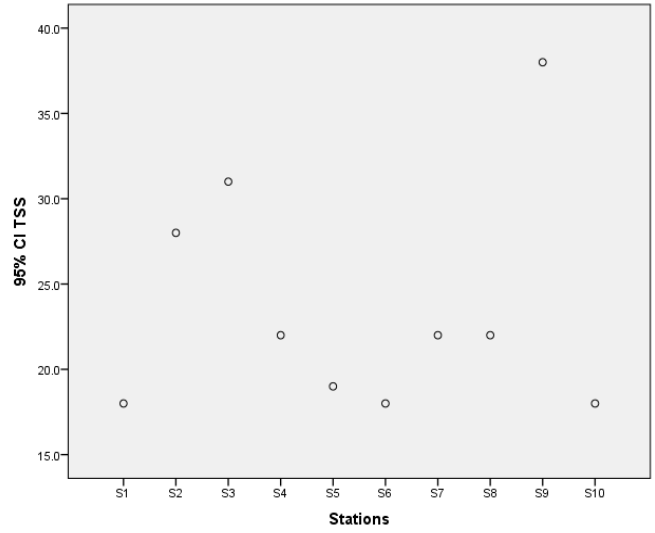
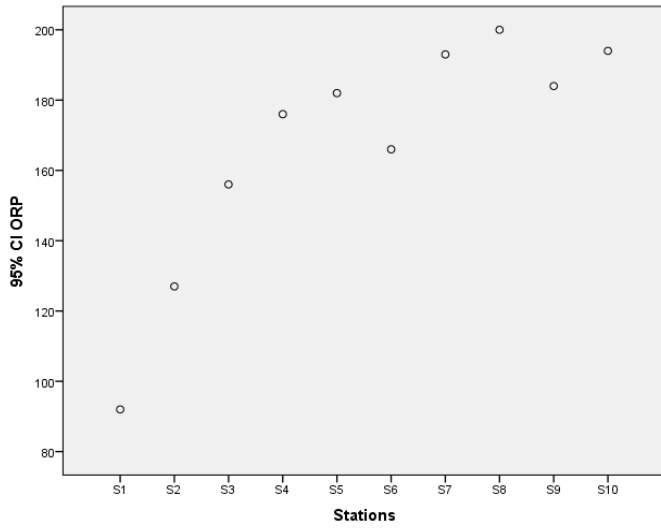
concentration and saturation, total dissolved solids, alkalinity, nitrate, phosphate and chlorophyll-*a* concentration) and microbiological organisms (total coliforms, *E. coli* and *Enterococcus* spp., in water and sediment) among the sampling stations (One-way ANOVA $F_{12, 117} = 3.50$; $p < 0.05$).

Surface water temperature ranged from 30.7 to 34.1°C. The lowest temperature was recorded at S1 and the highest at S7. S1 is located landwards, without any freshwater influence, separated from the sea by a sand bar and is characterized by shallow water depth, while S7 is characterized by an estuarine environment, more subject to marine water intrusions. The pH ranged from 8.31 to 8.39. The lowest pH was recorded at S9 and the highest at S1. S9 is influenced by near-shore oceanic waters with its typical pH. The electrical conductivity ranged from 35.8 to 52.6 mScm^{-1} , the salinity between 22.8 and 34.7 (PSU scale). Lowest values were recorded at S4 and highest at S10. S4 is characterized by a mixture of fresh and seawater, while S10 is surf zone, oceanic water hence high salinity.

The dissolved oxygen concentration ranged between 6.44 and 18.81 mg/L, and the water was in all cases oversaturated with oxygen. The highest dissolved oxygen concentration and saturation was recorded at S3. Redox potential ranged from 92 to 200 mV. The lowest redox potential was recorded at S1 and the highest at S8 (detritus zone). Total dissolved solids ranged from 21.9 to 31.6 mg/L. The lowest total dissolved solids were recorded at S4 (estuarine zone) and the highest at S10 (surf zone seawater). Total suspended solids ranged from 18 to 38 mg/L. The lowest concentration of total suspended solids was recorded at S1 and the highest at S9, which is influenced by the ocean and tidal influence, hence with loaded suspended materials from the near-shore environment.

Alkalinity ranged from 195.52 to 237.97 mg/L. The lowest alkalinity was recorded at S10 and the highest at S3 (more freshwater mixes with sea water). Phosphate concentrations ranged from 0.05 to 1.10 mg/L. The lowest phosphate was recorded at S1 and the highest at S9. Nitrates ranged from 1.7 to 7.5 mg/L. The lowest nitrates were recorded at S7 and S8 (intermediate zone) and the highest at S9. The liquid waste discharges directly into near-shore waters and swimming activities at the Densu beach may have contributed to an increase in nutrient load in seaward direction. Furthermore, a small village with cage cultures for crabs, fish farming and farming activities is located at the seaward direction. This may result in a higher nutrient load in downstream direction of the estuary. Sulfate ranged from 15 to 37 mg/L. The lowest sulfate concentration was recorded at S4 (estuarine zone) and the highest at S1 (landwards). Chlorophyll-*a* concentration ranged from 0.96 to 4.38 $\mu\text{g/L}$. The lowest concentration was recorded at S3 (mixing zone) and the highest at S1 (landwards). Areas, with intense freshwater discharge into the estuary system





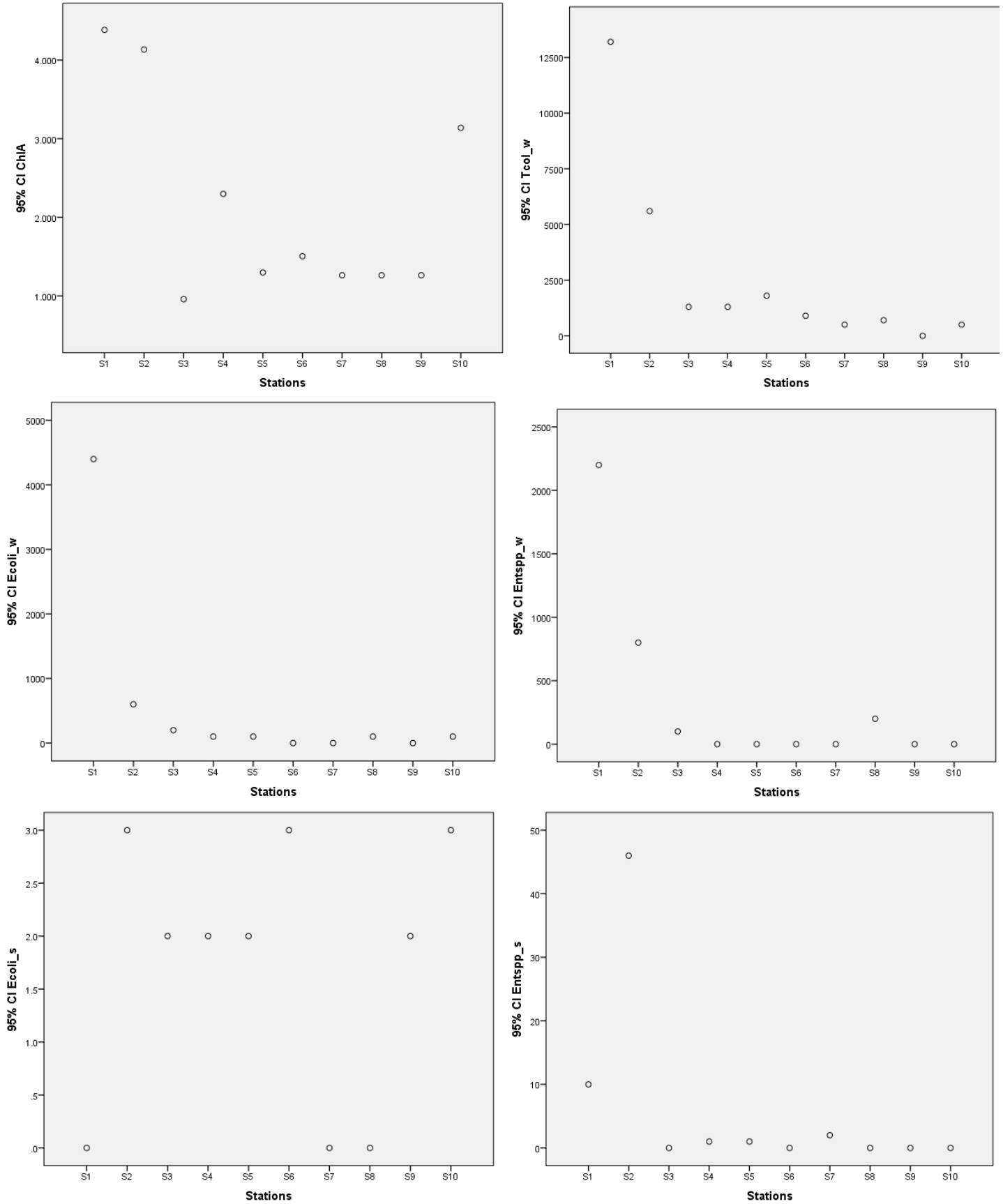


Figure 2. Spatial distribution of physicochemical and biological characteristics (95% Confident interval-CI) of the Densu Estuary, Ghana.

Table 3. Mean (\pm SD) of physicochemical and biological characteristics of the Densu Estuary, Ghana.

Parameter	Symbol [units]	Mean \pm standard deviation (SD)
Temperature	Temp [$^{\circ}$ C]	32.17 \pm 0.95
pH	pH	8.35 \pm 0.03
Electrical conductivity	EC [mS/cm]	43.85 \pm 5.54
Salinity	Sal	28.31 \pm 4.03
Dissolved oxygen concentration	DO [mg/L]	10.48 \pm 3.27
Dissolved oxygen saturation	DO Sat [%]	171.24 \pm 50.18
Total dissolved solids	TDS [g/L]	27.18 \pm 3.33
Total suspended solids	TSS [mg/L]	23.60 \pm 6.70
Alkalinity	Alk [mmol/L]	3.66 \pm 0.24
Phosphate	PO ₄ ³⁻ [mg/L]	0.33 \pm 0.29
Nitrate	NO ₃ ⁻ [mg/L]	2.98 \pm 1.74
Sulphate	SO ₄ ²⁻ [mg/L]	25.10 \pm 7.20
Chlorophyll-a	Chl-a [μ g/L]	2.25 \pm 1.32
<i>Escherichia coli</i> in water	<i>E. coli_w</i> [CFU/100 ml]	560.00 \pm 1360.72
<i>Enterococcus</i> spp. in water	<i>Ent. spp_w</i> [CFU/100 ml]	330.00 \pm 702.46
<i>Escherichia coli</i> in sediment	<i>E. coli_s</i> [CFU/1g]	1.67 \pm 1.32
<i>Enterococcus</i> spp. in sediment	<i>Ent. spp_s</i> [CFU/1g]	6.56 \pm 15.14
Polychaetes	POLY	27.5 \pm 9.24

(mixing zone), show high turbidity, leading to limited photosynthesis and hence low chlorophyll-a concentration at S3, whereas at S1 nutrient inputs from terrestrial land sources may facilitate increased primary production. The WQI ranged from 359.49 to 484.62, minimum values were recorded at S4 (estuarine zone) and maximum values at S9 (seaward zone).

Biological analyses

The abundance of bacteria (*E. coli* and *Enterococcus* spp.) significantly varied in the water of distinct stations (One-way ANOVA $F_{9, 10} = 8.52$; $p < 0.05$). However, the abundance of bacteria in the sediment showed no significant variation among the stations (One-way ANOVA $F_{9, 10} = 1.09$; $p > 0.05$). Bacterial (*E. coli* and *Enterococcus* spp.) loads in the water did not differ significantly ($p > 0.05$) from the counts in sediment ($p > 0.05$ both, at one tail and two tails). In water, total coliforms ranged from 0 to 13,200 CFU/100 ml; *E. coli* ranged from 0 to 4,400 CFU/100 ml and *Enterococcus* spp. ranged from 0 to 2,200 CFU/100 ml. In sediment, the total coliforms ranged from 136 to 558 CFU/1 g; *E. coli* ranged from 0 to 3 CFU/g and *Enterococci* spp. ranged from 0 to 46 CFU/g. High bacteria (total coliforms, *E. coli*, *Enterococci* spp.) counts from water and sediment samples were found at S1 and S2, closer to a landfill site and waste disposal, while low abundance was evident seawards (S9). *Escherichia coli* is the numerically dominant bacteria in water (Figure 3a), while *Enterococcus* spp. is more abundant in the sediment (Figure 3b).

Polychaetes were the most dominant living macrofauna. In total, 275 individuals of polychaetes were counted. The relative abundance of polychaetes ranged from 5.09 to 14.55%, mainly *Capitella* and *Nereis* species were found. Lowest abundance (14 individuals per 0.04 m²) was recorded at S1 and the highest abundance (40 individuals per 0.04 m²) at S8. S1 is a shallow area with coarse grains without much vegetation cover and high human impact, whereas station S8 is characterized by mangroves with rich detritus-debris, muddy soft bottom and possibly with high organic matter, favourable conditions for polychaetes.

Multivariate statistics

Cluster analyses

The cluster analyses revealed two main groups with similar physicochemical parameters (Figure 4a). There was a significant association between alkalinity, temperature and pH (Figure 4a). The dendrograms for the organisms, namely total coliforms, faecal bacteria (*E. coli* and *Enterococcus* spp.) and polychaetes showed two similar associations (Figure 4b), (i) total coliform in water and sediment, (ii) *E. coli* and *Enterococcus* spp. in water, and (iii) *E. coli*, *Enterococcus* spp. and polychaetes in sediment (Figure 4b). The combined biological data and physicochemical parameters (Figure 5a) were grouped into three distinct clusters, namely landwards (S1 and S2), mixing zone (S3-7) and seawards (S8-10) (Figure 5b).

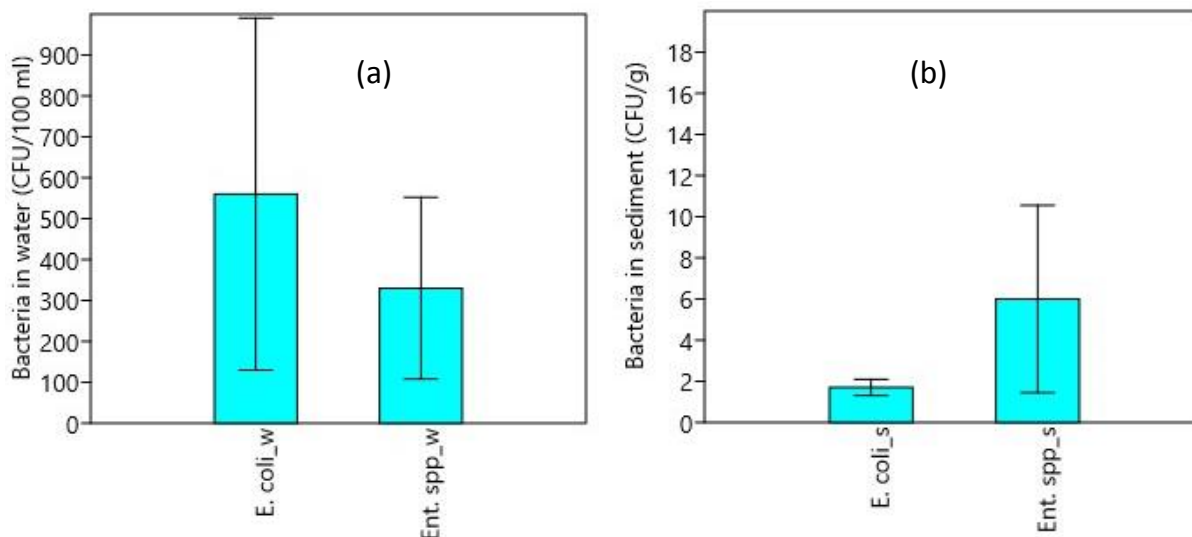


Figure 3. (a) Bacteria counts in water (CFU/100 ml) and (b) sediment (CFU/g). *Escherichia coli* is dominant in the water while *Enterococcus* spp. is more abundant in sediment. *E. coli_w* = *Escherichia coli* in water (CFU/100 ml), *Ent. spp_w* = *Enterococcus* spp. in water (CFU/100 ml), *E. coli_s* = *Escherichia coli* in sediment (CFU/g), *Ent. spp_s* = *Enterococcus* spp. in sediment (CFU/g).

Principal component analysis

The canonical analysis triplot diagram displays the spatial distribution of biological data and physicochemical parameters at the studied stations of the Densu Estuary (Figure 6). It shows the influence of physicochemical parameters on the spatial distribution of organisms at the ten stations. The first axis contributes 59.96% and the second axis 14.15% to the total variation (Figure 6). The long arrows (chlorophyll-*a*, pH, phosphate, nitrates, total dissolved solids and redox potential) show physicochemical parameters that significantly influence the spatial distribution of the species. The first axis is correlated with chlorophyll-*a*, alkalinity and temperature. The second axis reflects a gradient related to pH, phosphate, nitrates, total dissolved solids, redox potential, water depth, salinity, electrical conductivity, sulphate, total dissolved solids, dissolved oxygen concentration and saturation (Figure 6). The redundancy analysis (RDA) revealed that the first axis contributes 51.09% and the second axis 28.49% to the abundance of organisms at the ten stations (Figure 7). The pH is the primary environmental factor influencing the faecal bacteria and polychaete distribution in the Densu Estuary. The pH significantly ($p = 0.002$) explained 51.1% of the variation in the species abundance (Figure 7).

Pearson's correlation

The Pearson correlation coefficient (r) (Table 4) indicated that salinity significantly correlates positively with specific electrical conductivity ($r = 0.999$) and pH ($r = 0.735$). Specific electrical conductivity significantly correlates

positively with pH ($r = 0.720$). Furthermore, the redox potential significantly correlated positively with pH ($r = 0.850$). Total dissolved solids also correlated positively with two variables: specific electrical conductivity ($r = 0.863$) and salinity ($r = 0.864$). In contrast, chlorophyll-*a* significantly correlated negatively with three variables: temperature ($r = -0.691$), pH ($r = -0.675$) and dissolved oxygen saturation ($r = -0.725$). Alkalinity significantly correlated negatively with three parameters: specific electrical conductivity ($r = -0.891$), salinity ($r = -0.896$) and total dissolved solids ($r = -0.757$). The concentrations of phosphate and nitrate also correlated significantly ($r = 0.914$), as did the nutrients with total suspended solids (phosphate, $r = 0.862$, nitrates, $r = 0.870$). Sulfate significantly correlated positively with water depth ($r = 0.679$). The WQI significantly correlated positively with pH ($r = 0.727$), specific electrical conductivity ($r = 0.991$, strong positive linear relationship) and total dissolved solids ($r = 0.855$) and negatively with alkalinity ($r = -0.902$, strong negative linear relationship) (Table 4). However, a significant ($p < 0.005$) linear association exists between physicochemical variables only (Table 4) and among biological data only (Table 5).

The abundance of the organisms correlated significantly among each other. Total coliforms in sediment significantly correlated positively with total coliforms in water ($r = 0.641$, $p = 0.046$) and chlorophyll-*a* ($r = 0.815$, $p = 0.004$), and negatively with redox potential ($r = -0.656$, $p = 0.039$) and pH ($r = -0.832$, $p = 0.003$). *E. coli* in sediment significantly correlated positively with water depth ($r = 0.684$, $p = 0.029$). *Enterococcus* spp. in sediment significantly correlated positively with total coliforms in sediment ($r = 0.684$, $p = 0.029$) and

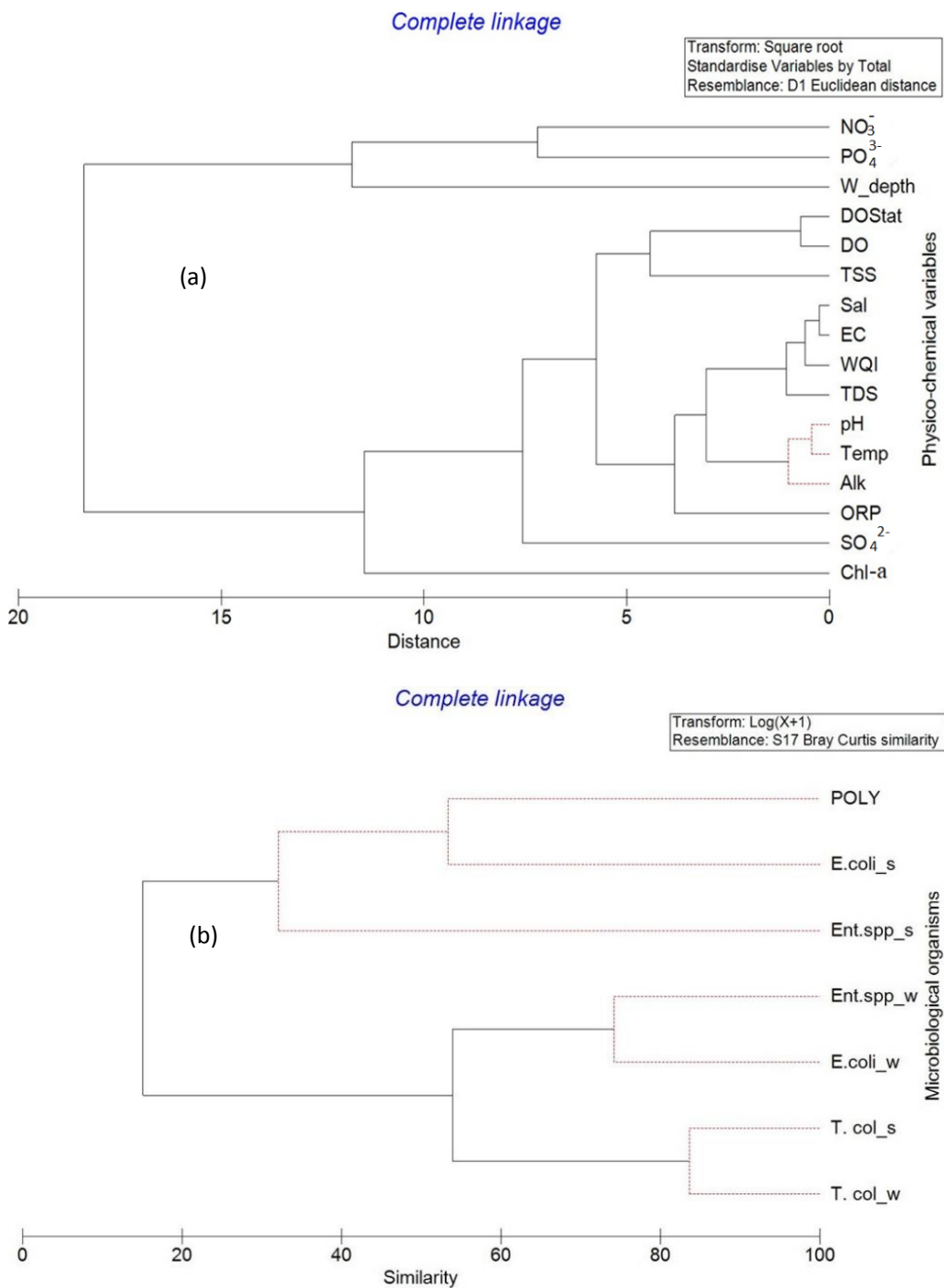


Figure 4. Hierarchical cluster of (a) physicochemical and (b) biological characteristics of the Densu Estuary. A significant similarity of associations exists between alkalinity, temperature and pH. A Significant similarity between organisms in the water and sediment. The thin red dotted lines indicate the significant structure of similarity (SIMPROF Test $p < 0.05$). The black thick lines indicate no significant structure.

chlorophyll-a ($r = 0.668$, $p = 0.035$). Polychaetes significantly correlated positively with temperature ($r = 0.639$, $p = 0.047$), pH ($r = 0.816$, $p = 0.004$), redox potential ($r = 0.778$, $p = 0.008$) and negatively with

chlorophyll-a ($r = -0.857$, $p = 0.002$), total coliforms in water ($r = -0.684$, $p = 0.029$), total coliforms in sediment ($r = -0.833$, $p = 0.003$), and *Enterococcus* spp. in water ($r = -0.643$, $p = 0.045$).

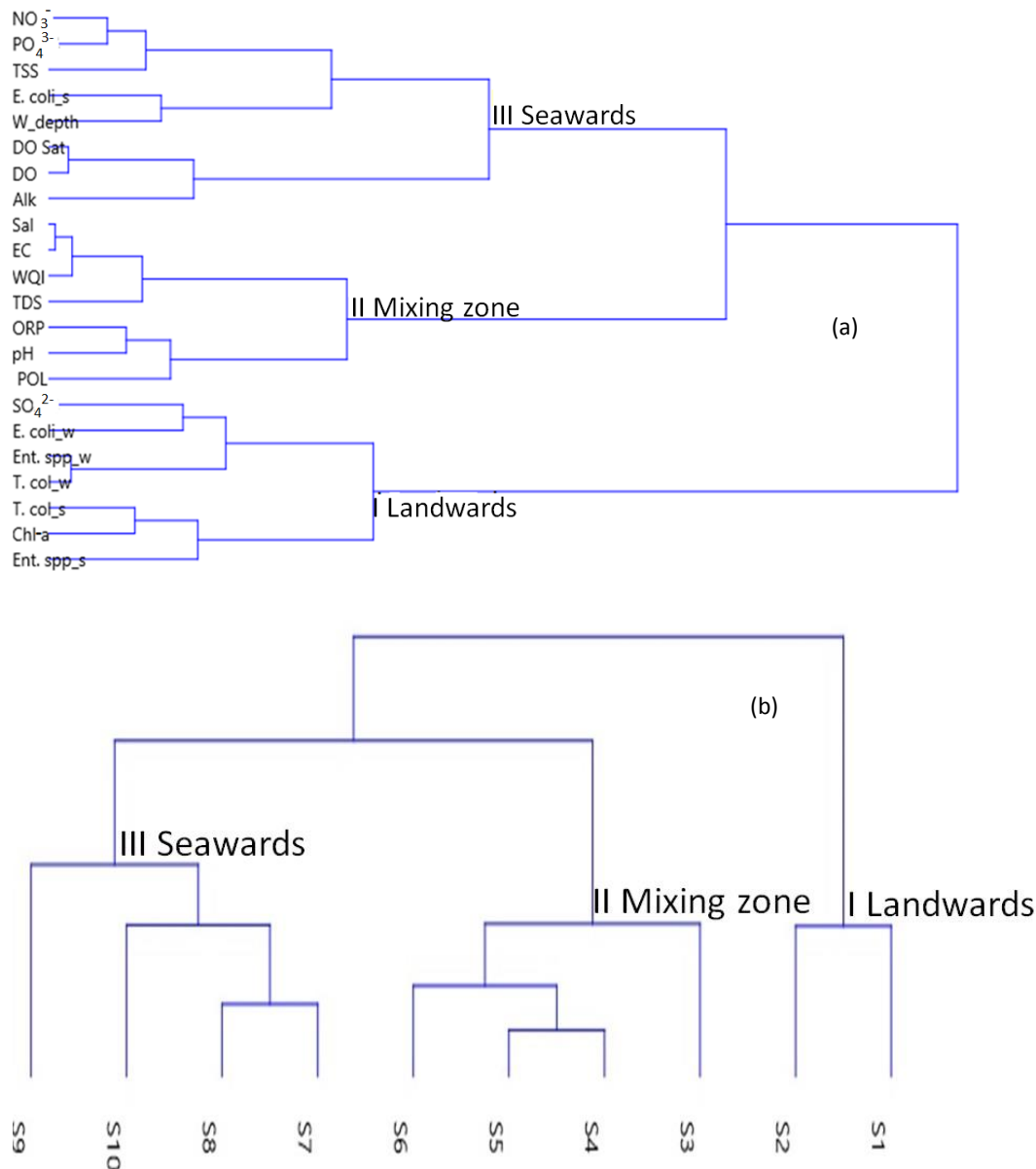


Figure 5. Cluster analysis (After Ward’s method two way-constrained) of combined physicochemical and microbiological data (a) with the corresponding cluster of stations (b). The species-physicochemical data were group into three distinct clusters; (i) landward sources of pollution; (ii) mixing zone–estuarine condition (a mixture of river water and seawater); (iii) seaward sources of contamination. The corresponding stations (three discernable clusters) are landwards (S1-2), mixing zone (S3-6) and seawards (S7-10).

DISCUSSION

Physicochemical parameters

Estuaries are highly variable environments and controlled by estuarine flushing times (Cloern and Jassby, 2010; Day Jr. et al., 2012). Some physicochemical parameters (Figure 2 and Table 3) varied among the stations, demonstrating the heterogeneous condition of the Densu Estuary. The physicochemical nature of this estuary can

be classified into three zones; the landward zone (without any freshwater input), the intermediate zone, (characterised by a mixture of fresh and oceanic water) and the end of the estuary (characterised by the intrusion of seawater).

The mean temperature ($32.17 \pm 0.95^{\circ}\text{C}$) (Table 3) recorded in April reflects the water temperature condition for coastal waters in the dry season (31 to 33°C) (Biney, 1982; Biney, 1993; Karikari and Ansa-Asare, 2006). The coastal waters of Ghana are situated in the tropical and

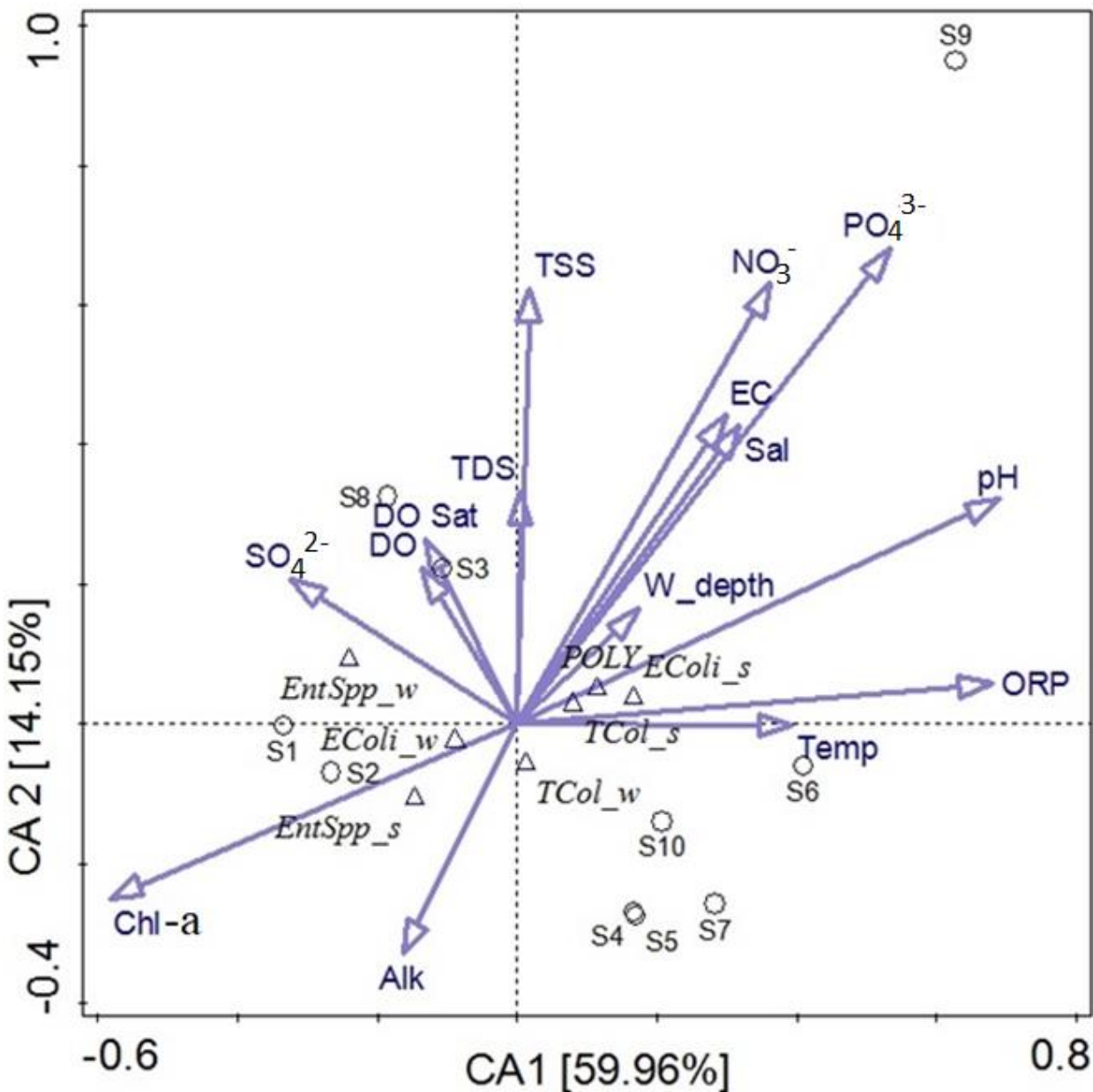


Figure 6. Canonical analysis (CA) of physicochemical (blue arrows) at the ten sampling stations (S1-10). The first and second axes contribute 74.11% of the total variation of the influence of physicochemical factors on the abundance of microbiological organisms among the stations. The orientations of these arrows indicate the correlation of these variables in CA ordination axes. The longer arrows indicate the most significant physicochemical variables on species distribution.

equatorial climate belt and annual mean temperatures range between 25 and 36°C with little variation throughout the year (Biney, 1982, 1993; Karikari and Ansa-Asare, 2006). The two climatic zones in the coastal areas of Ghana are both characterized by homogeneous temperatures between 23 and 32°C with a mean annual value of 27°C (Karikari and Ansa-Asare, 2006). Highest temperature (32°C) occurs in March-April and the lowest (23°C) in August (Dickson et al., 1988). A pH range from 7 to 9 is suitable for estuarine life (Anzecc, 2000). The pH

values for the Densu Estuary were between 8.31 and 8.39 and thus within the range for natural waters not acidified yet (Stumn and Morgan, 1981; Biney and Asmah, 2010; Lamptey et al., 2013). The pH may be modified by biological activity, photosynthesis, temperature, oxygen content, ocean acidification, cation and anion composition (Doney et al., 2015; Abdel-Halim and Aly-Eldeen, 2016; Apriani et al., 2018; Tanjung et al., 2019). Furthermore, increasing carbon dioxide in the atmosphere can cause acidification of coastal marine

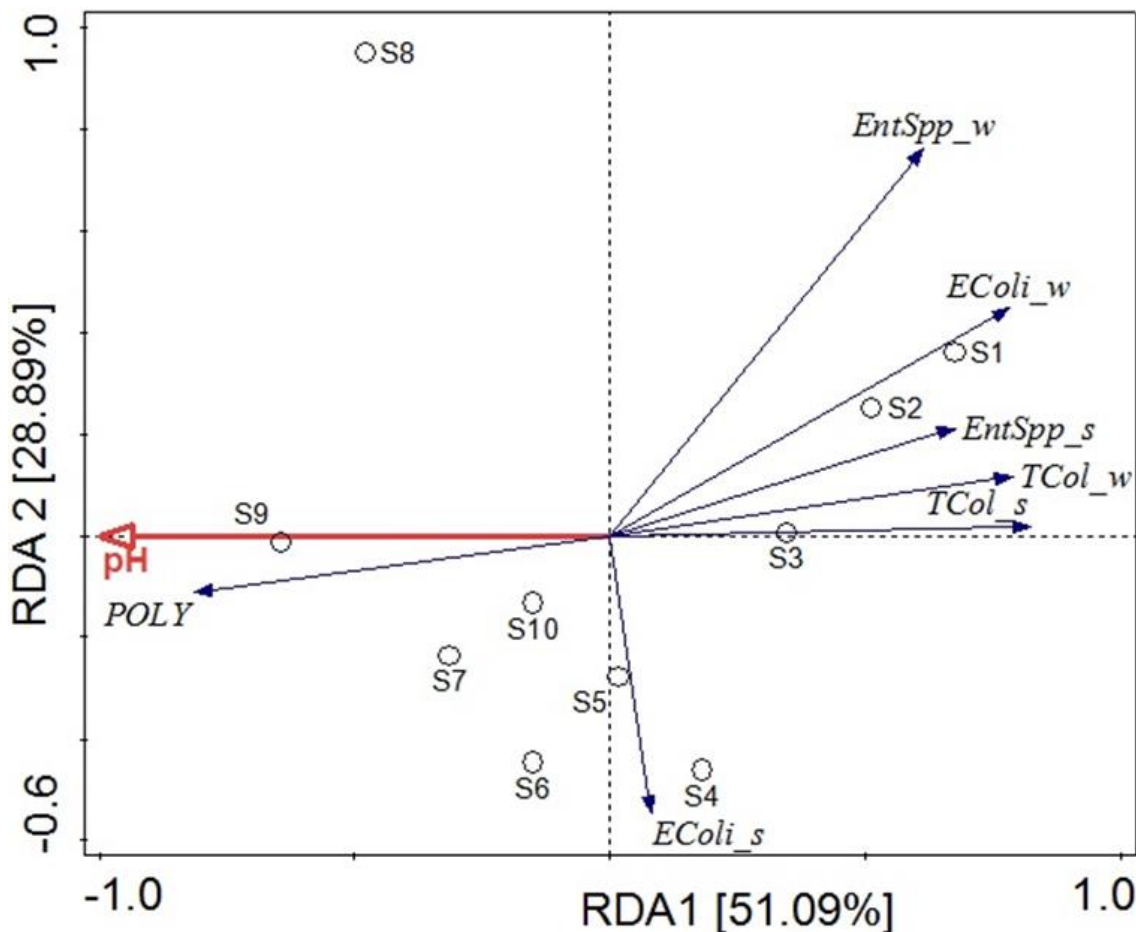


Figure 7. Redundancy analysis (RDA) diagram with best environmental variable (red arrow) selected by the forward selection procedure influencing the organisms (blue arrows) at the ten stations. The ordination diagram shows the first axis (horizontal) and the second (vertical) axis of distance-based constrained RDA. The first axis and second axis explained 79.58% of the total variation. The pH significantly ($p = 0.002$) explained 51.1% of the total variation in the faecal bacteria and polychaete distribution.

waters affecting its organisms (flora and fauna), function and ecosystem processes (Fabry et al., 2009; Doney et al., 2015; Curry, 2020).

The conductivity ranged from 35.8 to 52.5 mScm^{-1} , which is typical for estuarine waters (Biney and Asmah, 2010). Values for estuaries are typically from 20 to 40 mScm^{-1} , marine waters have much higher values (that is, 51.5 mScm^{-1}). Increased conductivity is directly related to increased concentrations of salinity and total dissolved solids. Thus, high conductivity levels are often associated with sewage discharge and leaching of inorganic contaminants (Harrison, 1999).

The salinity ranged from 22.8 to 34.7, which is categorized as polyhaline (18 - 30) at landward stations and mixoeuhaline (30 - 40) conditions at seaward stations (Vernice System, 1959). Salinity increases with increase specific electrical conductivity; this was also established for Songor Wetland (Klubi et al., 2019).

Salinity significantly ($r = 0.999$) correlated positively with conductivity, suggesting a strong linear association.

The mean dissolved oxygen concentration (6.44 - 18.81 mg/L) was above the natural background (7.0 mg/L) (Biney, 1993; Clark, 2000). Dissolved oxygen concentrations of unpolluted water bodies range from 8.0 to 10.0 mg/L at 25°C (Pearce et al., 1999). The low level of total dissolved solids at S4 could be due to a less turbulent environment, whereas the high total dissolved solids in marine oceanic waters due to accumulated solutes in suspension and tidal influence. The highest dissolved oxygen concentration and saturation were recorded at S3, which is influenced by freshwater inflow from the Densu River with high hydrodynamics condition.

The redox potential ranged from 92 to 200 mV, which is below the redox potential for natural waters (between 500 and 600 mV) (McLusky and Elliot, 2004, 2010). The alkalinity levels (195.52 - 237.97 mg/L) was also below

Table 4. Pearson correlation among physicochemical parameters measured at the Densu Estuary, Ghana.

Parameter	Temp	pH	EC	Sal	DO	DOSat	ORP	W_depth	TDS	TSS	Alk	PO ₄ ³⁻	NO ₃ ⁻	SO ₄ ²⁻	Chl-a	WQI
Temp	1															
pH	0.312	1														
EC	-0.226	0.720*	1													
Sal	-0.220	0.735*	0.999**	1												
DO	0.514	-0.278	-0.468	-0.486	1											
DOSat	0.549	-0.234	-0.409	-0.429	0.991**	1										
ORP	0.368	0.850**	0.483	0.501	-0.118	-0.108	1									
W_depth	-0.218	0.098	0.026	0.032	0.305	0.210	0.311	1								
TDS	-0.264	0.494	0.863**	0.864**	-0.413	-0.395	0.263	0.108	1							
TSS	0.232	0.219	0.161	0.156	0.425	0.423	0.041	0.353	0.260	1						
Alk	0.545	-0.552	-0.891**	-0.896**	0.625	0.597	-0.411	-0.179	-0.757*	-0.032	1					
PO ₄ ³⁻	0.203	0.544	0.350	0.356	0.107	0.119	0.296	0.295	0.266	0.862**	-0.240	1				
NO ₃ ⁻	0.000	0.339	0.339	0.333	0.156	0.154	0.102	0.382	0.317	0.870**	-0.229	0.914**	1			
SO ₄ ²⁻	-0.249	0.106	0.541	0.531	-0.475	-0.376	-0.204	-0.679*	0.468	-0.264	-0.460	-0.217	-0.252	1		
Chl-a	-0.691*	-0.675*	-0.142	-0.144	-0.407	-0.441	-0.725*	-0.204	0.139	-0.268	-0.082	-0.429	-0.264	.342	1	
WQI	-0.264	0.727*	0.989**	0.991**	-0.566	-0.512	0.467	-0.001	0.855**	0.151	-0.902**	0.382	0.366	.528	-0.099	1

*Correlation is significant at the 0.05 level (2-tailed). **Correlation is significant at the 0.01 level (2-tailed). Temp = Temperature (°C), EC = Electrical conductivity (mS/cm), Sal = Salinity, DO = Dissolved oxygen concentration (mg/L), DO Sat = saturation of dissolved oxygen (%), ORP = Redox potential (mV), TDS = Total dissolved solids (mg/L), TSS = Total suspended solids (g/L), Alk = Alkalinity (mg/L), PO₄³⁻ = Phosphate (mg/L), NO₃⁻ = Nitrates (mg/L), SO₄²⁻ = Sulphate (mg/L), Chl-a = Chlorophyll-a (µg/L) and WQI = Water quality index.

Table 5. Pearson correlation analysis between abundance of organisms found in water and sediment at the Densu Estuary, Ghana.

Correlation	T. col_w	E. coli_w	Ent. spp_w	T. col_s	E. coli_s	Ent. spp_s	POLY
T. col_w	1						
E. coli_w	0.962**	1					
Ent. spp_w	0.988**	0.971**	1				
T. col_s	0.641*	0.478	0.564	1			
E. coli_s	-0.308	-0.432	-0.380	0.256	1		
Ent. spp_s	0.456	0.217	0.429	0.684*	0.247	1	
POLY	-0.684*	-0.589	-0.643*	-0.833**	-0.360	-0.571	1

*Correlation is significant at the 0.05 level (2-tailed). **Correlation is significant at the 0.01 level (2-tailed). Bacteria in water (T. col_w = Total coliforms, E. coli_w = *Escherichia coli*, Ent. spp_w = *Enterococcus* spp.), Bacteria in sediment (T. col_s = Total coliforms, E. coli_s = *Escherichia coli*, Ent. spp_s = *Enterococcus* spp.) and POLY = Polychaetes.

the maximum contaminant levels of 500 mg/L suggested by the WHO, alkalinity ranging from

300 to 400 mg/L has been recommended for drinking water (WHO, 1999, 2011).

Nutrients (mainly phosphate and nutrients) are important chemical compounds in water quality

monitoring (Conley et al., 2009). In the Densu Estuary, the mean phosphate concentration ranged between 0.05 and 1.10 mg/L, which is higher than the typical value for coastal marine waters of 0.02 mg/L (Biney, 1993; Oduro, 2003; Ouffoué et al., 2013). In most natural waters, phosphate ranges from 0.005 to 0.020 mg/L (Chapman, 1992), in some pristine waters, the phosphate concentration may even be as low as 0.001 mg/L (Chapman, 1992). The phosphate concentration can be used to categorized ecosystem: (i), <0.02 mg/L = healthy ecosystem, (ii) 0.02 to 0.3 mg/L = fair ecosystem, and (iii) > 0.3 mg/L = poor ecosystem. Thus, the Densu Estuary is classified as a poor estuarine ecosystem.

The nitrate concentration ranged from 1.7 to 7.5 mg/L and are thus at four of the five stations (S2, S3, S5 and S10) higher than the recommended 0.25 mg/L for coastal waters. Large quantities of nitrate and phosphate lead to eutrophication with high primary productivity (algal blooms) (Conley, 2000; De Jonge et al., 2002; Saad and Younes, 2006; Cook et al., 2018). However, in turbid estuaries, the light may limit phytoplankton blooms (Ambasht and Ambasht, 2005; Bucci et al., 2012; Green et al., 2015). The trophic state (chlorophyll-*a* concentration ranged between 0.96 and 4.38 µg/L) is interpreted as ultra-oligotrophic (<1.0) to mesotrophic (3.0-8.0) condition. Chlorophyll-*a* concentration is an estimate of phytoplankton biomass (Tripathy et al., 2005) and thus a key component of food availability for benthic and filter-feeding animals (Fujii, 2007). A positive relationship was found between the chlorophyll-*a* concentration and the abundance of macrofaunal species (Lampthey and Armah, 2008; Musale and Desai, 2011).

The WQI ranged between 359.49 and 484.62 and was thus >300, which is categorized as unsuitable water for drinking and indicates a deteriorating ecosystem (Ramakrishnaiah et al., 2009; Lampthey et al., 2013; Nguyen and Sevando, 2019). However, a good water quality is necessary to sustain the living resources of the ecosystem (Nyarko et al., 2015; Duncan, 2018; Tanjung et al., 2019).

Biological indicators of environmental quality

The dominance organisms reflect the sediment quality, which is also reflection of the water quality status. High bacteria load (total coliforms, *E. coli* and *Enterococcus* spp.) (Figures 2 and 3 and Table 3) especially at S1 and S2 reflect high anthropogenic activities (e.g., landfill sites, domestic and animal waste discharges) in the landward direction of the estuary. Faecal bacteria enter surface waters by direct deposition of human and animal waste discharges and indirectly through land runoff and leach into the Densu Estuary. Microbial contamination of water and sediment is a growing concern for the ecosystem and human health (Odonkor and Ampofo, 2013; Walker et al., 2015). Faecal indicator organisms are often used

to detect and quantify aquatic pollution (Horan, 2003; Odonkor and Ampofo, 2013). The faecal bacteria (total coliforms, *E. coli* and *Enterococcus* spp.) are used to indicate pathogens of faecal origin in surface and coastal water bodies (Medema et al., 2003; Pandey et al., 2014). Faecal bacteria (*E. coli* and *Enterococcus* spp.) are characteristic intestinal bacteria of warm-blooded animals (Medema et al., 2003; Shuval, 2005). *Escherichia coli* (also known as faecal coliform) is the best bacterial indicator of faecal pollution (Stewart et al., 2008; Walker et al., 2015). Faecal enterococci are also used as complementary microbiological water quality indicator (Byamukama et al., 2000). The presence of coliform bacteria suggests a potential for waterborne related pathogens to be present (Shuval, 2003; Jain, 2013). The presence of faecal bacteria (*E. coli* and *Enterococci* spp.) indicates sources of human and animal pollution in the Densu Estuary.

The dominance of polychaetes (*Capitella* and *Nereis* spp.) also suggests environmental pollution in the Densu Estuary. Polychaete worms were the most dominant living macrofauna. These polychaete species are most abundant in organic matter enriched sediments (Saleh, 2012; Aqilah et al., 2016). *Capitella* spp. are sedentary deposit feeders (Levinton and Kelaher, 2004; Lampthey and Armah, 2008; Musco et al., 2009). Polychaetes may be used as sensitive indicators of anthropogenic disturbances, such as organic pollution (Cai et al., 2001; Elias et al., 2006; Metcalfe and Glasby, 2008). Several polychaetes are opportunistic species capable of reproducing after an increase in organic matter (Giangrande et al., 2005; Musale and Desai, 2011). In an estuary and mangrove environment, polychaetes provide food for shorebirds, for instance, the Bar-tailed Godwit *Limosa lapponica* feeds on *Nereis* spp. (McLusky and Elliot, 2010). The polychaetes, *Capitella* and *Nereis* spp. often dominate soft bottoms of polluted and organic enrichment waters (Alongi, 1990; McLusky and Elliot, 2004; Wada et al., 2008; Cai et al., 2013). Under anoxic conditions, most of the macrofaunal can become extinct (McLusky and Elliot, 2010). A small number of empty shells of molluscs and gastropods was observed.

Spatial similarity and variations of stations

The hierarchical clusters (Figures 4a-b and 5a-b) indicated spatial similarity among physicochemical factors only, biological data only and combined effects (Mac Nally, 1996). Cluster and Pearson's correlation analyses revealed a significant ($p < 0.05$) association of microbiological organisms in water and sediment (Figures 4a-b and 5a-b); (i) total coliforms in water and sediment, (ii) *E. coli* and *Enterococcus* spp. in water, and (iii) *E. coli*, *Enterococcus* spp. and polychaetes in sediment. There was a clear evidence of ecological interactions. Temperature, pH and alkalinity were significant factors in

the estuary system. Any change of these variables may change the condition of the estuary. The contamination of stations (S1 and S2) originates from land sources, apparently anthropogenically influenced (e.g., domestic and animal waste disposal). The mixing zone (S3-7) is characterized by catchments of the river mixing with marine water. The marine zone is located downstream of the estuary with the intrusion of saline, oceanic waters into the Densu Estuary (S8-10). This shows the interaction of water and sediment characteristics of eco-hydrochemical estuarine conditions. Principal component analyses (PCA), in harmony with the cluster analyses (CA) (Figures 5 to 7), indicated landward sources of major pollution, hydrodynamic condition of freshwater and seawater mixing and marine intrusion into the estuarine system. Thus, the Densu Estuary is characterized by distinct hydrochemical dynamic pathways as observed in Songor Wetland (Klubi et al., 2019).

There is a strong interaction of biotic and abiotic component of the ecosystem and among each other (Tables 4 and 5 and Figures 5 to 7), as expected (Borja et al., 2012). The state of water quality is reflected also in the sediment quality, an insight into the ecological integrity of the Densu Estuary. The integration of physico-chemical and biological assessment of coastal ecosystems pollution status is critical for the broader understanding of various pathways of environmental contamination and sustainable management of coastal waters (Ambasht and Ambasht, 2005; Ouffoué et al., 2013; Larbi et al., 2018).

Conclusion

The knowledge of ecological integrity of estuaries along the coast of Ghana is still scarce. Because of its fisheries resources the Densu Estuary is of high socio-economic importance for the coastal communities. The deforestation of the Densu Delta wetland (a Ramsar site) and poor sanitation in the vicinity will not only affect the regulation of the local hydrological cycles, loss of habitats and introduce flood-related risks, but also water-borne diseases. The environmental quality of the estuary was assessed using multiple ecological indicators. The study emphasized on physicochemical drivers of organisms in the Densu Estuary.

Significant variation ($p < 0.05$) of some physicochemical parameters occurred among the stations. There is a clear salinity gradient from 22.8 to 34.7. Nutrient (nitrate and phosphate) concentrations exceeded recommended levels for natural coastal waters, indicating a degraded ecosystem. Phosphate concentrations ranged from 0.05 to 1.10 mg/L. Nitrate ranged from 1.7 to 7.5 mg/L. Dissolved oxygen concentrations ranged from 6.44 to 18.81 mg/L. The computed WQI ranged from 359.49 to 484.62 and thus

indicated a deteriorating system.

The abundance of organisms significantly varied between the sampling stations. The presences of faecal bacteria (total coliforms, *E. coli* and *Enterococcus* spp.) suggest faecal contamination. The dominance of key macrofaunal (e.g., *Capitella* and *Nereis* spp.) suggests organic pollution. The results indicate an impacted environment of the Densu Estuary, which can impose ecosystem and human health risks, a cause for further investigation.

The cluster analyses helped to classify the stations into three major groups; landward zone, intermediate zone and seaward zone. The physicochemical parameters coupled with biological data were also grouped into three distinct clusters, mainly landward, mixed zone and marine sources. The significantly contaminated stations (S1 and S2), may be influenced by domestic and animal waste disposal, the intermediate zone (S3-7), characterized by mixing of freshwater and marine water and the seaward zone (S8-10) is characterized by seawater intrusions into the estuary. The PCA performed on physicochemical and biological data helped to identify natural and anthropogenic sources of the contamination. The first two axes explained 74.11% of the variation in the abundance data. The pH is the most influential ecological factor that explained the spatial distribution of faecal bacteria and polychaetes in the Densu Estuary.

The faecal bacteria (*E. coli* and *Enterococcus* spp.) showed significant ($p < 0.05$) positive correlation with chlorophyll-*a* concentration, but negatively correlated with redox potential and pH, whereas polychaetes displayed a significant positive correlation with temperature ($r = 0.64$), pH ($r = 0.82$) and redox potential ($r = 0.78$), but negative with chlorophyll-*a* concentration ($r = -0.86$).

The findings provide an ecological baseline for environmental monitoring and for effective policy formulation to control discharges of waste into coastal waters. The study contributes to an ecological perspective on the environmental quality of the Densu Estuary using multiple indicators to identify the different sources of environmental pollution.

CONFLICT OF INTERESTS

The authors have not declared any conflict of interests.

ACKNOWLEDGEMENTS

The authors thank all those who made this research possible, especially Prof. Peter Frenzel, Prof. Hartmut Stuetzel, Dr. Hanna Wielandt and Frau Sylvia Janning. Kwadwo Kyeremateng is deeply appreciated for designing Figure 1. The authors are also grateful to the Department of Marine and Fisheries Sciences for support during field and laboratory analyses; and Volkswagen

Foundation, Germany for funding the research to L.G.A (Grant no. 89371).

REFERENCES

- Abdel-Halim AM, Aly-Eldeen MA (2016). Characteristics of Mediterranean sea water in vicinity of Sidikerir region, west of Alexandria, Egypt. *The Egyptian Journal of Aquatic Research* 42:133-140.
- Aggrey-Fynn J, Galyuon I, Aheto DW, Okyere I (2011). Assessment of the environmental conditions and benthic macroinvertebrate communities in two coastal lagoons in Ghana. *Annals of Biological Research* 2:413-424.
- Aglanu LM, Appiah DO (2017). The Korle lagoon in distress: The stress of urban solid waste on water bodies in Accra, Ghana. *International Journal of Innovation and Applied Studies* 7:717.
- Alongi DM (1990). The ecology of tropical soft-bottom benthic ecosystems. *Oceanography and Marine Biology An Annual Review* 28:381-496.
- Ambasht RS, Ambasht PK (2005). *Environmental Pollution: An ecological approach*. 4th Edition. CBS Publishers, New Delhi. 323p.
- Anzecc (2000). *Australian and New Zealand Guidelines for Fresh and Marine Water Quality*. Volume 1, 314p.
- American Public Health Association (APHA) (1998). *Standard Methods for the Examination of Water and Wastewater*. 19th Edition. American Public Health Association, Washington, DC, United States. 874p.
- American Public Health Association (APHA) (2012). *Standard Methods for Examination of Water and Wastewater*. 22nd Edition. American Public Health Association, Washington, DC, United States, 1360p.
- Apriani M, Hadi W, Masduqi A (2018). Physicochemical properties of sea water and bittern in Indonesia: Quality improvement and potential resources utilization for marine environmental sustainability. *Journal of Ecological Engineering* 19:1-10.
- Aqilah N, Darif NAM, Shakila N, Samad NSA, Salleh S, Mohammad M, Nordin NAA, Javeed AMM, Jonik MGG, Zainudi MHM (2016). The abundance and spatial distribution of soft sediment communities in Tanjung Bungah, Malaysia: A preliminary study. *Tropical Life Sciences Research* 27:71-77.
- Armah AK (1993). Coastal wetlands of Ghana. *Coastal Zone* 93:313-322.
- Armah AK, Amalalo DS (1998). Coastal Zone Profile of Ghana. In: *Gulf of Guinea Large Marine Ecosystem Project*. Ministry of Environment, Science and Technology, Accra, Ghana, 111p.
- Biney CA (1982). Preliminary survey of the state of pollution of the coastal environment of Ghana. *Oceanologia Acta* 4:39-43.
- Biney CA (1993). Coastal zone management in Accra. In: *Reprinted for coastal lines of Western Africa*. Proceedings, 8th Symposium on Coastal and Oceans Management, New Orleans, pp. 115-128.
- Biney CA, Asmah R (2010). The effect of physico-chemical parameters on speciation of trace metals in sediments from inland and coastal waters of Ghana. *African Journal Aquatic Science* 25:299-305.
- Borja R, Basset A, Bricker S, Dauvin J, Elliot M, Harrison T, Marques J, Wiesberg S, West R (2012). Classifying ecological quality and integrity of estuaries. In E Wolanski and D McLusky (Eds). *Treatise on Estuarine and Coastal Science*. Academic Press, Waltham, pp. 125-162.
- Boyer JN, Kelbe CR, Ortnor PB, Rudnick DT (2009). Phytoplankton bloom status: Chlorophyll-a biomass as an indicator of water quality condition in the southern estuaries of Florida, USA. *Ecological Indicators* 9S:S56-S67.
- Bucci AF, Ciotti AM, Pollery RCG, de Carvalho RD, de Albuquerque HCD, Simões LTS (2012). Temporal variability of chlorophyll-a in the São Vicente Estuary. *Brazilian Journal of Oceanography* 60:485-499.
- Byamukama D, Kansime F, Mach RL, Farnleitner AHH (2000). Determination of *Escherichia coli* contamination with chromocult coliform agar showed a high level of discrimination efficiency for differing faecal pollution levels in tropical waters of Kampala, Uganda. *Applied Environmental Microbiology* 66:864-868.
- Cabral JPS (2010). Water microbiology. Bacterial pathogens and water. *International Journal of Environmental Research and Public Health* 7:3657-3703.
- Cai LZ, Hwang JS, Dahms HU, Fu SJ, Chen XW, Wu C (2013). Does high organic matter content affect Polychaete assemblages in a Shenzhen bay mudflat, China? *Journal of Marine Science and Technology* 21:274-284.
- Cai LZ, Lin J, Li H (2001). Macrofauna communities in an organic-rich mudflat at Shenzhen and Hong Kong, China. *Bulletin Marine Science* 69:1129-1138.
- Chapman D (1992). *Water Quality Assessment: A Guide to the Use of Biota, Sediment and Water in Environmental Monitoring*. 1st Edition. World Health Organization (WHO), Geneva, Switzerland. 585 p.
- Clark RB (2000). *Marine Pollution*. 4th Edition. Clarendon Press, Oxford, United Kingdom.
- Clarke KR, Gorley RN (2006). *PRIMER v6: User manual/tutorial*. PRIMER-E. 1992, Plymouth Marine Laboratory, Plymouth, UK.
- Cloern JE, Jassby AD (2010). Patterns and scales of phytoplankton variability in estuarine-coastal ecosystems. *Estuaries and Coasts* 33:230-241.
- Conley DJ (2000). Biogeochemical nutrient cycles and nutrient management strategies. *Hydrobiologia* 410:87-96.
- Conley DJ, Paerl HW, Howarth RW, Boesch DF, Seitzinger SP, Havens KE, Lancelot C, Likens GE (2009). Controlling eutrophication: nitrogen and phosphorus. *Science* 323:1014-1015.
- Cook PLM, Warry FY, Reich P, Nally RM, Woodland RJ (2018). Catchment land use predicts benthic vegetation in small estuaries. *Peer Journal* 6:e4378.
- Curry A (2020). Effects of Multiple Stressors on the Development and Performance of Decapod Crustaceans. In: *School of Ocean Sciences*. Bangor University, Bangor, Wales, United Kingdom, 202p.
- da Silveira Fiori C, de Castro Rodrigues AP, Santelli RE, Cordeiro RC, Carnevali RG, Araújo PC, Castilhos ZC, Bidone ED (2013). Ecological risk index for aquatic pollution control: A case study of coastal water bodies from the Rio de Janeiro State, southeastern Brazil. *Geochimica Brasiliensis* 27:24-36.
- Day JH (1967a). A Monograph on the Polychaeta of Southern Africa. Part 1, Errantia. Trustees of the British Museum, London, UK.
- Day JH (1967b). A Monograph on the Polychaeta of Southern Africa. Part II, Sedentaria. Trustees of the British Museum, London, UK.
- Day Jr. JW, John AB, Crump, BC, Kemp W, Yáñez-Arancibia A (2012). *Estuarine Ecology*. 2nd Edition. John Wiley-Blackwell & Sons, Inc.
- De Jonge VN, Elliot M, Orive E (2002). Causes, historical development, effects and future challenges of a common environmental problem: Eutrophication. *Hydrobiologia* 475/476:1-19.
- Debrah C (1999). Specialiation of heavy metals in waters and sediment from the Densu Basin. Department of Chemistry, University of Ghana, Legon-Accra, Ghana. 155 p.
- Dickson KB, Benneh G, Essah R (1988). *A New Geography of Ghana*. Longman Group Limited, Essex, London, UK.
- Doney SC, Balch VJ, Fabry VJ, Freely RA (2015). Ocean acidification: A critical emerging problem of the ocean sciences. *Oceanography* 22:16-25.
- Duncan AM (2018). Water pollution and water quality assessment of major transboundary rivers from Banat (Romania). *Journal of Chemistry*, pp. 1-8.
- Elias R, Rivero MS, Palacios JR, Vallarino EA (2006). Sewage-induced disturbance on polychaetes inhabiting intertidal mussel beds of *Brachidontes rodriguezii* off Mar del Plata (SW Atlantic, Argentina). *Scientia Marina* 70:187-196.
- Fabry VJ, Seibel BA, Feely RA, Orr JC (2009). Impacts of ocean acidification on marine fauna and ecosystem processes. *ICES Journal of Marine Science* 6:414-423.
- Fathi P, Ebrahimi E, Mirghafary M, Esmaili OA (2016). Water quality assessment in Choghakhor Wetland using water quality index (WQI). *Iran Journal of Fisheries Science* 15:508-523.
- Fiango JR, Osa S, Achel D (2009). Impact of anthropogenic activities on the Densu River in Ghana. *Water and Environmental Journal* 23:229-234.
- Fujii T (2007). Spatial patterns of benthic macrofauna in relation to environmental variables in an intertidal habitat in the Humber Estuary, UK: Developing a tool for estuarine shoreline management. *Estuarine Coastal Shelf Science* 75:101-119.
- Giangrande A, Licciano M, Musco L (2005). Polychaetes as

- environmental indicators revisited. *Marine Pollution Bulletin* 50:1153-1162.
- Greene CM, Blackhart K, Nohner J, Candelmo A, Nelson DM (2015). A national assessment of stressors to estuarine fish habitats in contiguous USA. *Estuaries and Coasts* 38:782-799.
- HACH (2012). *Water Analysis Handbook*. Hach Company, Loveland, Colorado, USA. pp 31-48, 65,1031-1039, 1129-1147, 1241-1359.
- Hagan GB, Ofosu FG, Hayford EK, Osae S, Oduro-Afriyie K (2011). Heavy metal contamination and physico-chemical assessment of the Densu River Basin in Ghana *Research Journal of Environmental and Earth Sciences* 3:385-392.
- Hammer Ø, Harper DAT, Ryan PD (2001). PAST: Palaeontological statistics software package for education and data analysis. *Palaeontologia Electronica* 4:9.
- Harrison RM (1999). *Understanding our Environment: An introduction to Environmental Chemistry and Pollution*. 3rd Edition. The Royal Society of Chemistry, Cambridge, Great Britain 326p.
- Hinga KR, Jeon H, Lewis NF (1995). *Marine Eutrophication Review Part 1: Quantifying the Effects of Nitrogen Enrichment on Phytoplankton in Coastal Ecosystems*. In: Part 2 Bibliography with abstracts. NOAA Coastal Ocean Program. Decision Analysis Series. NOAA Coast Ocean Office, Silver spring, MD, US Department of Commerce, United States of America. 36p.
- Horan NJ (2003). Faecal indicator organisms. In: Duncan M, Horan NJ (eds) *The Handbook of Water and Wastewater Microbiology*. Elsevier, Great Britain, pp. 105-112.
- Horton RK (1965). An index number system for rating water quality. *Journal of Water Pollution Control Federation* 37:300-306.
- Jain R (2013). Crucial need for water quality monitoring of biological contaminants. *Clean Technologies and Environmental Policy* 15:1-3.
- Karikari AY, Ansa-Asare OD (2006). Physico-chemical and microbial water quality assessment of Densu River of Ghana. *West African Journal of Applied Ecology* 10:87-100.
- Khamis H (2008). Measures of association: How to choose? *Journal of Diagnostic Medical Sonography* 24:155-162.
- Klubi E, Abril JM, Nyarko E, Delgado A (2018). Impact of gold-mining activity on trace elements enrichment in the West African estuaries: The case of Pra and Ankobra rivers with the Volta Estuary (Ghana) as the reference. *Journal of Geochemical Exploration* 190:229-244.
- Klubi E, Addo S, Akita LG (2019). Assessment of hydrological pathway and water quality of the Songor wetland, Ghana. *African Journal of Environmental Science and Technology* 13:511-523.
- Koranteng KA (1995). Ghana coastal wetlands management project, environmental baseline studies of Densu delta Ramsar site. Fisheries Report prepared for Ministry of Fisheries, Government of Ghana, Accra, Ghana.
- Lamprey AM, Ofori-Danson PK, Abbenney-Mickson S, Breuning-Madsen H, Abekoe MK (2013). The influence of land-use on water quality in a tropical coastal area: Case study of the Keta Lagoon Complex, Ghana, West Africa. *Open Journal of Modern Hydrology* 3:188-195.
- Lamprey E, Armah AK (2008). Factors affecting macrobenthic fauna in a tropical hypersaline coastal lagoon in Ghana, West Africa. *Estuaries and Coasts* 31:1006-1019.
- Larbi L, Nukpezah D, Mensah A, Addo KA (2018). An integrated assessment of ecological health status of coastal aquatic ecosystems of Ada in Ghana. *West African Journal of Applied Ecology* 26(1):89-107.
- Levinton J, Kelaher B (2004). Opposing organizing forces of deposit feeding marine communities. *Journal of Experimental Marine Biology and Ecology* 300:65-82.
- Mac Nally R (1996). Hierarchical partitioning as an interpretative tool in multivariate inference. *Australian Journal of Ecology*:224-228.
- Mahu E, Nyarko E, Hulme S, Coale KH (2015). Distribution and enrichment of trace metals in marine sediments from the Eastern equatorial Atlantic, off the coast of Ghana in the Gulf of Guinea. *Marine Pollution Bulletin* 98:301-307.
- Mahu E, Nyarko E, Hulme S, Swarzenski P, Asiedu DK, Coale KH (2016). Geochronology and historical deposition of trace metals in three tropical estuaries in the Gulf of Guinea. *Estuarine Coastal and Shelf Science* 177:31-40.
- McLusky DS, Elliot M (2004). *The Estuarine Ecosystem: Ecology, Threats and Management*. Oxford University Press, New York.
- McLusky DS, Elliot M (2010). *The Estuarine Ecosystem*, Oxford University Press, New York.
- Medema GJ, Payment P, Dufour A, Robertson W, Waite M, Hunter P, Kirby R, Anderson Y (2003). Safe drinking water: An ongoing challenge. In *assessing microbial safety of drinking water. Improving approaches and method*. WHO & OECD, IWA Publishing, London, UK, pp. 11-45.
- Metcalfe KN, Glasby CJ (2008). Diversity of Polychaeta (Annelida) and other worm taxa in mangrove habitats of Darwin Harbour, northern Australia. *Journal of Sea Research* 59:70-82.
- Möller WAA, Scharf BW (1986). The content of chlorophyll-a in the sediment of the volcanic maar lakes in the Eifel region (Germany) as an indicator for eutrophication. *Hydrobiologia* 143:327-329.
- Monbet Y (1992). Control of phytoplankton biomass in estuaries: A comparative analysis of microtidal and macrotidal estuaries. *Estuaries* 15:563-571.
- Monney I, Boakye R, Buamah R, Anyemedu FOK, Odai SN, Awuah E (2013). Urbanization and pollution of surface water resources in the two largest cities in Ghana. *International Journal of Environmental Monitoring and Analysis* 1:279-287.
- Mophin-Kani K, Murugesan AG (2011). Evaluation and classification of water quality of perennial River Tamirabarani through aggregation of water quality index. *International Journal of Environmental Protection* 1:24-33.
- Mudroch A, Azcue JM (eds) (1995). *Manual of Aquatic Sediment Sampling*. Taylor & Francis CRC Press. 240p.
- Musale AS, Desai DV (2011). Distribution and abundance of macrobenthic polychaetes along the South Indian coast. *Environmental Monitoring and Assessment* 178:423-436.
- Musco L, Terlizzi A, Licciano M, Giangrande A (2009). Taxonomic structure and the effectiveness of surrogates in environmental monitoring: A lesson from polychaetes. *Marine Ecological Progress Series* 383:199-210.
- Nagelkerke NJD (1991). A note on a general definition of the coefficient of determination. *Biometrika* 78:691-692.
- Nguyen NTT, Sevando M (2019). Assessing coastal water quality through an overall index. *Polish Journal of Environmental Studies* 28:2321-2330.
- Nyarko E, Lamprey AM, Owiredu-Amaning DA (2015). Application of water quality index for assessment of the nearshore coastal waters of Accra. *Journal of Pollution Research* 34:657-666.
- Odonkor ST, Ampofo JK (2013). *Escherichia coli* as an indicator of bacteriological quality of water: An overview. *Microbiology Research* 4:e2.
- Oduro L (2003). Gender and natural resources management of Weji lake and its environment. MPhil Thesis. University of Ghana, Legon-Accra, Ghana.
- Okyere I, Aheto DW, Aggrey-Fynn J (2011). Comparative ecological assessment of biodiversity of fish communities in three coastal wetland systems in Ghana. *European Journal of Experimental Biology* 1:178-188.
- Ouffoué KS, Salla M, Kicho DY, Soro D, DA.P. K, Tonzibo ZF (2013). Water Quality Assessment of the Coastal Tropical River'Sboubo (Côte d'Ivoire): Physico-Chemical and Biological Aspects. *Journal of Environment Pollution and Human Health* 1:9-15.
- Pandey PK, Kass PH, Soupier ML, Biswas S, Singh VP (2014). Contamination of water resources by pathogenic bacteria. *AMB Express* 4.
- Patzkowsky ME, Holland SM (2012). *Stratigraphic Paleobiology: Understanding the Distribution of Fossil Taxa in Time and Space*. University of Chicago Press, Chicago, United States of America. 259p.
- Pearce GR, Chaudhry MR, Ghulum S (eds) (1999). *A Simple Methodology Water Quality Monitoring*. Department for International Development Wallingford, 100p.
- Ramakrishnaiah CR, Sadashivaiah C, Ranganna G (2009). Assessment of water quality index for the groundwater in Tumkur Taluk, Karnataka State, India. *E-Journal of Chemistry* 6:523-530.
- Saad MAH, Younes WAN (2006). Role of phosphorus and nitrogenous species in water quality of a coastal Egyptian heavily polluted Mediterranean basin. *International Journal of Oceans and*

- Oceanography 1:1-19.
- Sahu P, Sikdar PK (2008). Hydrochemical framework of the aquifer in and around East Kolkata Wetlands, West Bengal. *India Environmental Geology* 55:823-835.
- Saleh AAT (2012). Effects of multiple-source of pollution on spatial distribution of polychaetes in Saudi Arabia. *Research Journal of Environmental Toxicology* 6:1-12.
- Sanchez E, Colmenarejo MF, Vicente J, Rubio A, Garcia MG, Travieso L, Borja R (2007). Use of the water quality index and dissolved oxygen deficit as simple indicators of watersheds pollution. *Ecological Indicators* 7:315-328.
- Shuval H (2003). Estimating the global burden of thalassogenic diseases: Human infectious diseases caused by wastewater pollution of the marine environment. *Journal of Water Health* 1:53-64.
- Shuval H (2005). Thalassogenic Infectious Diseases Caused by Wastewater Pollution of the Marine environment: An Estimate of the Worldwide Occurrence. In: Belkin S, Colwell RK (eds) *Oceans and Health: Pathogens in the Marine Environment*. Springer, Boston, MA, United States of America. pp. 373-389.
- Šmilauer P, Lepš J (2014). *Multivariate analysis of ecological data using CANOCO 5*. Cambridge University Press, Cambridge, U.K.
- Solley WB, Pierce RR, Perlman HA (1998). Estimated use of water in the United States in 1995. In: Circular. U.S. Geological Survey United States. U.S. Geological Survey Circular 1200.
- Stewart MR, Gast RJ, Fujioka RS, Solo-Gabriele HM, Meschke SJ, Amaral-Zettler LA, de Castillo E, Polz MF, Collier DR, Strom MS, Sinigalliano CD, Moeller PD, Holland AF (2008). The coastal environment and human health: Microbial indicators, pathogens, sentinels and reservoirs. *Environmental Health* S3 (7 Suppl. 2).
- Stumm W, Morgan JJ (1981). *Aquatic chemistry. An Introduction Emphasizing Chemical Equilibria in Natural Waters*. 2nd Edition. John Wiley and Sons Ltd. New York, 780p.
- Tanjung RHR, Hamuna B, Alianto (2019). Assessment of water quality and pollution index in coastal waters of Mimika, Indonesia. *Journal of Ecological Engineering* 20:87-94.
- Teley AH (2001). The impact of Waste disposal on the surface and groundwater environment: A case study of the Mallam landfill site, Accra. Department of Environmental Science. University of Ghana, Legon-Accra, Ghana.
- Tirkey P, Bhattacharya T, Chakraborty S (2015). Water quality indices-important tools for water quality assessment: A review. *International Journal of Advances in Chemistry* 1:15-30.
- Tripathy SC, Ray AK, Patra S, Sarma VV (2005). Water quality assessment of Gautami- Godavari mangroves estuarine ecosystem of Andhra Pradesh, India during Septemeber 2001. *Journal of Earth System Science* 114:185-190.
- Twilley RR, Chen RH, Hargis T (1992). Carbon sinks in mangrove forests and their implications to the carbon budget of tropical coastal ecosystems. *Water Air Soil Pollution* 64:265-288.
- USEPA (2009). The United States Environmental Protection Agency, National Primary Drinking Water Regulations.
- Vernice System (1959). The Venice System for the classification of marine waters according to salinity. In: Ancon D (ed) *The final resolution of the Symposium on the classification of brackwaters*. Symposium on the classification of brackish waters, Venice, Italy. *Arch Oceanography II* (Suppl. pp 243-248.
- Wada M, Zhang D, Do HK, Nishimura M, Tsutsumi H, Kogure K (2008). Co-inoculation of *Capitella* sp. with its synergistic bacteria enhances degradation of organic matter in organically enriched sediment below fish farms. *Marine Pollution Bulletin* 57:86-93.
- Walker JW, van Duivenboden R, Neal MW (2015). A tiered approach for the identification of faecal pollution sources on an Auckland urban beach. *New Zealand Journal of Marine Freshwater Research* 49:333-345.
- WHO (1999). *WHO Guidelines for Drinking Quality Water*. World Health Organisation, Geneva, Switzerland, pp. 160-220.
- WHO (2011). *Guidelines for Drinking Water Quality*. World Health Organisation, Geneva, Switzerland.
- WRI (2003). *Groundwater assessment: An element of integrated water resources management—The case study of Densu River Basin*. In. Council for Scientific and Industrial Research Institute (CSIR)-Water Research Institute (WRI), Accra, Ghana.
- Yadav S (2018). Correlation analysis in biological studies. *Journal of the Practice of Cardiovascular Sciences* 4:116-121.
- Yeleliere E, Cobbina SJ, Duwiewuah AB (2018). Review of Ghana's water resources: The quality and management with particular focus on freshwater resources. *Applied Water Science* 8:93.

Full Length Research Paper

Quantifying forest cover at Mount Kenya: Use of Sentinel-2 for a discrimination of tropical tree composites

Jonas Fierke*, Martin Kappas and Daniel Wyss

Cartography, GIS and Remote Sensing Section, Institute of Geography, University of Goettingen, Goldschmidt Street 5, 37077 Goettingen, Germany.

Received 4 March, 2020; Accepted 12 June, 2020

The aim of the present study is to test ESA's Sentinel-2 (S2) satellites (S2A and S2B) for an efficient quantification of land cover (LC) and forest compositions in a tropical environment southwest of Mount Kenya. Furthermore, outcome of the research is used to validate ESA's S2 prototype LC 20 m map of Africa that was produced in 2016. A decision tree that is based on significant altitudinal ranges was used to discriminate four natural tree compositions that occur within the investigation area. In addition, the classification process was supported by Google Earth images, and land use (LU) data that were provided by the local Kenyan Forest Service (KFS). Final classification products include four LC classes and five subclasses of forest (four natural forest subclasses plus one non-natural forest class). Results of the Jeffries-Matusita (JM) distance test show significant differences in spectral separability between all classes. Furthermore, the study identifies spectral signatures and significant wavelengths for a classification of all LC classes and forest subclasses where wavelengths of SWIR and the red-edge domain show highest importance for the discrimination of tree compositions. Finally, considerable differences can be seen between the utilized multi-temporal classification set (total of 39 bands from three acquisition dates) and ESA's S2 prototype LC 20 m map of Africa 2016. A visual comparison of ESA's prototype map within the investigation area indicates an overrepresentation of tree cover areas (as confirmed in previous studies) and also an underrepresentation of water.

Key words: Tropical tree composites, Mt. Kenya, Sentinel-2, ESA S2 LC 20 m map of Africa.

INTRODUCTION

Forests are subject to several policies of individual states and important agreements from the United Nations (UN) (FAO, 2017; IPCC, 2003; UN, 1992, 1997, 2015). The amount of people that directly profit from forests as a natural resource is vast (FAO, 2016b). This also applies

to the forests of Mount Kenya National Park, Lewa Wildlife Conservancy, and Ngare Ndare Reserve of the greater Mount Kenya ecoregion. Altogether, these forests shape an extensive ecosystem that represents habitat to numerous endemic species and provide water and other

*Corresponding author. E-mail: jonas.fierke@gmail.com.

Author(s) agree that this article remain permanently open access under the terms of the [Creative Commons Attribution License 4.0 International License](https://creativecommons.org/licenses/by/4.0/)

natural resources to people that live in the mountains and the adjacent foothills (Kenya Wildlife Service, 2010; Winiger and Brunner, 1986). Nevertheless, forests in general and also in Kenya are under massive pressure and in competition with other land-use (LU) systems to this day (McDowell et al., 2020; Barlow et al., 2016; Kenya Forest Service, 2010). Tropical forests are among the most threatened forests and often exposed to radical LU changes and impacts of climate change (Bastin et al., 2019; FAO, 2016a; Lambin et al., 2001). Agriculture is the primary economic activity in the bordering areas of the investigated forest reserve. The increase of agriculturally used areas is a major challenge for sustainable tropical forest management (Kenya Forest Service, 2010). In addition, wildfires, intensified by the effects of climate change, frequently occur within the reserve (Nyongesa, 2015). It is therefore of major concern to understand the structure of forests, to subsequently investigate their interactions with land-use and land cover (LULC) changes, as well as the effects of climate change to support sustainable management of tropical forest resources.

Satellite remote sensing (SRS) can bring important benefits for monitoring LULC changes regarding disturbances and changes within the forest ecosystem (DeFries et al., 1995; Hansen et al., 2013; Townshend, 1992). Quantifying forest cover changes on a large scale is a major challenge to this day. It requires high temporal and spatial accuracy to detect detailed changes within short time periods (Crowther et al., 2015). At the same time resources are limited and researchers need to find efficient solutions for forest monitoring (Wulder and Coops, 2014). Regional anomalies like persistent cloud cover in tropical environments make the process even more complex and limit the availability of up to date SRS data (Asner, 2001). However, techniques of SRS are continuously developing providing new possibilities for Earth observation.

In 2015, Sentinel-2A (S2A) was successfully launched by the European Space Agency (ESA) as part of the Copernicus program. Sentinel-2B (S2B) successfully followed in 2017. All of the data that is produced by the twin satellites is available for free to the scientific community and beyond. The Sentinel-2 (S2) Copernicus mission orbits the earth every five days using both satellites (S2A and S2B) that are equipped with 13 spectral bands at a bandwidth of the visible and near-infrared (VNIR) as well as the short-wavelength infrared (SWIR). The spatial resolution of the spectral bands ranges from 10 m (bands 2-4, and 8) to 20 m (bands 5-7, 8a, 11, and 12) and 60 m (bands 1, 9, and 10) (Fletcher, 2012). As already stated by other authors, strength of the S2 mission is the combination of systematic global coverage, high revisit frequency, multispectral information, wider field of view, and comparatively good spatial resolution (Sola et al., 2018). This enables researchers to see changes in land cover (LC) and forest

cover even at a small scale regarding the spatial and temporal resolution. Consequently, numerous studies with the objectives to test S2 products for their technical possibilities have arisen within the last years (Ganivet and Bloomberg, 2019).

Moreover, the Climate Change Initiative (CCI) of the ESA derived a LC classification prototype map of Africa at 20 m spatial resolution that was based on S2 observation data from December 2015 to December 2016 (Fabrizio et al., 2018). Only few studies have so far tested the potential of S2 to discriminate forest types, tree compositions, and tree species. These include but are not limited to: Immitzer et al. (2016) on the classification of tree species in Central Europe (Germany), Laurin et al. (2016) on forest types, dominant species and functional guilds in West Africa (Ghana), Puletti et al. (2017) on forest categories and types in Southern Europe (Italy), Karasiak et al. (2017) on tree species in Southern Europe (France), Persson, Lindberg and Reese (2018) on tree species in Northern Europe (Sweden), and Grabska et al. (2019) on forest types and tree species in Eastern Europe (Poland). However, most of the studies were conducted within a temperate environment. Consequently, more applied research within the tropical environment is needed. Driven by the motivation of the Karantina University and the Kenya Forest Service (KFS), this study aims to fill this research gap through combined use of LU data, Google Earth images, topographic data as well as historic field-based data to develop an efficient method for the creation of spectral signatures. Furthermore, the outcome of the present study will be used for a visual comparison with the existing LC product of ESA's S2 prototype LC 20m map of Africa 2016. The main objectives of the study are:

- i) Testing opportunities and challenges offered by S2 imagery for classification of tropical forest subclasses based on historical field acquisition and terrain information derived from Digital Elevation Models (DEM);
- ii) Visual comparison of S2 Prototype Land Cover 20 m Map of Africa 2016 and conducted classification within the investigation area;
- iii) Creating a detailed classification product for the investigation area that includes LC classes and forest compositions.

MATERIALS AND METHODS

Case study area

Mount Kenya, also known as Kirinyaga or Kinyaa in the language of Swahili, is the highest mountain massif in Kenya and the second highest in Africa with its highest peak of 5,199 MAMSL. It is located about 150 km north-northeast of the capital Nairobi right on the equator in the center of Kenya (Figure 1).

Part of the greater ecosystem is the Mount Kenya National Park/ Natural Forest in the center and the Lewa Wildlife Conservancy as well as the Ngare Ndare Forest Reserve in the north. Altogether, it

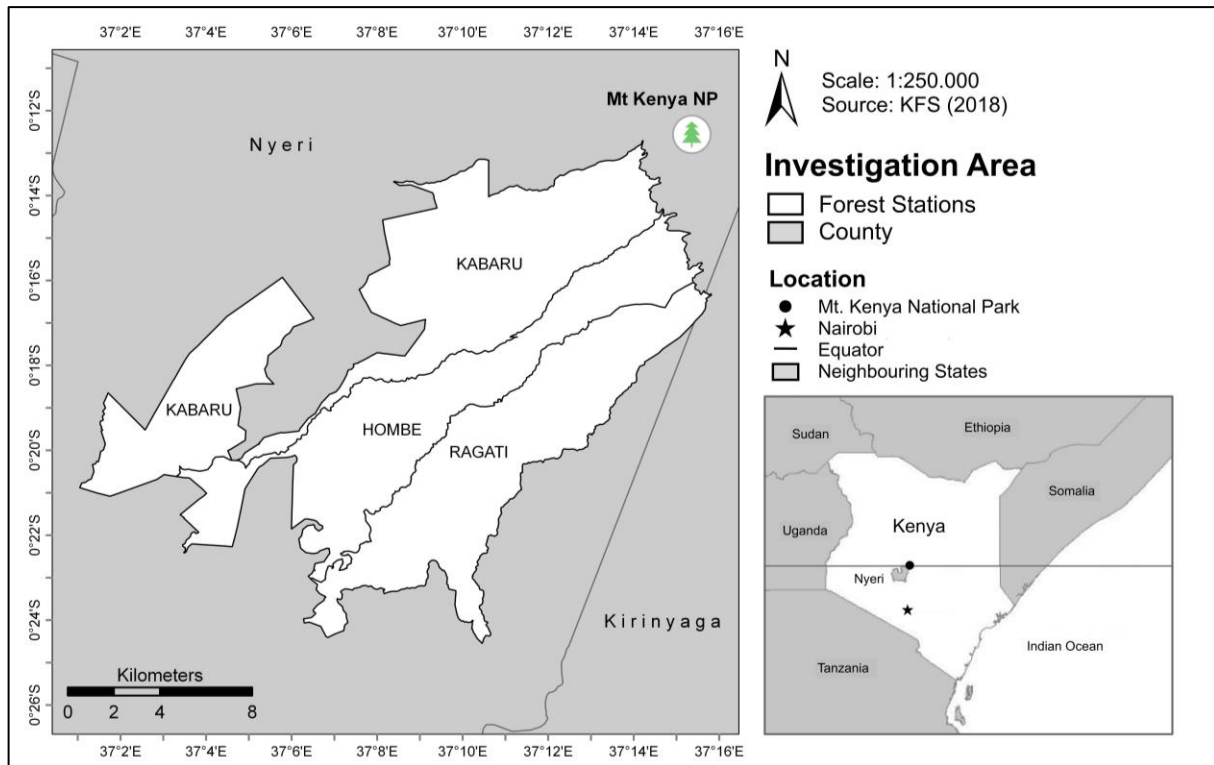


Figure 1. Geographical location and administrative borders of the investigation area (after Winiger and Brunner, 1986).

shapes an extensive ecosystem that provides habitat to numerous endemic species as well as water to people living in the mountains and the adjacent foothills (Kenya Wildlife Service, 2010). The investigation area is located in the southwest of the Mount Kenya area, bordering the northeastern National Park (Figure 1). Except for a very small part in the east that is attributed to Kirinyaga County, most of the investigation area is part of Nyeri County. Furthermore, it consists of three forest stations: Kabaru, Hombe and Ragati.

Field-based reference data

Based on an extensive recording of Mount Kenya's forests in 1992 to 1994, Bussmann and Beck (1995) accounted 41 tree associations with 47 sub-associations. Furthermore, 10 alliances, 5 orders and 4 classes were identified. Four of the ten alliances can be found in the investigation area southwest of the mountain spreading up to an altitude of 3,400 m (Table 1). Descriptions of the associations give detailed information about the ecological factors, locations, as well as character and differential species. According to Bussmann and Beck (1995), (1) *Ocotetea usambarensis* is the most common forest formation ranging from 1,970 m to 2,520 m altitude. Differential tree species of this formation is *Neoboutonia macrocalyx* Pax with a flowering time from September to December (Burrows et al., 2018). Another formation is (2) *Cassipourion malosanae* which is predominantly two-storey ranging from altitudes of 2,150 m to 2,650 m. Differential tree species of *Cassipourion malosanae* are Rhizophoraceae *Cassipoura malosana* with a flowering time from September to January and *Olea capensis* L. ssp. *Hochstetteri* with irregular flowering intervals of up to seven years (Burrows et al., 2018; Bussmann and Beck, 1995). Third formation is (3) *Podocarpus latifolius* – *Sinarundinarietum alpine* at

altitudes of 2,350 m to 3,050 m. A bamboo canopy overtopped with single trees of *Podocarpus latifolius* that in turn represents the differential tree species is characteristic for this forest type. The fourth formation that occurs in the investigation area is (4) *Haganietea abyssinicae*. At a range of 2,650 m to 3,350 m altitude, this subalpine forest forms the upper forest belt around Mount Kenya. Differential species is *H. abyssinicae* that is also known as Kosso tree (Bussmann and Beck, 1995).

Digital data applications

Digital data of the research include all data that was used through application of geographic information systems (GIS). Integral part of these data are Sentinel-2 satellite images, the S2 prototype LC 20 m map of Africa 2016, SRTM Digital Elevation Models (DEM), and a LU-map that was provided by the KFS.

Sentinel-2 data

The ESA mission uses twin satellites, equipped with a Multi Spectral Instrument (MSI) including 13 spectral bands at a bandwidth of the visible and near-infrared (VNIR) as well as the short wavelength infrared (SWIR) domain (Table 2) that orbit the Earth every five days. The satellites were launched in 2015 (S2A) and 2017 (S2B). Spatial resolution for the bands of the classical blue (490 nm), green (560 nm), red (665 nm) and near-infrared (842 nm) is 10 m. Four narrow bands in the vegetation red-edge spectral domain (705, 740, 783 and 865 nm) as well as two large SWIR bands (1610 nm and 2190 nm) are at 20 m spatial resolution. Finally, three bands at the spatial resolution of 60 m “[...] are mainly dedicated to atmospheric corrections and cloud screening (443 nm

Table 1. Phytosociological characteristics of forest alliances at Mount Kenya.

Tree composition	Altitudinal range	Vegetation structure	Differential species
<i>Ocotetea usambarensis</i>	1,970-2,520 m	(I) Lower species diversity than the forests of the lower altitude (II) One tree stratum with less dense shrub layer	<i>Neoboutonia macrocalyx</i> Pax
<i>Cassipourion malosanae</i>	2,150-2,650 m	Mainly two-storey	Upper canopy: (i) Rhizophoraceae <i>Cassipourea malosana</i> (ii) <i>Olea capensis</i> L. ssp. <i>Hochstetteri</i> Lower tree: <i>Lepidotrichilia volkensii</i>
<i>Podocarpus latifolius</i> - <i>Sinarundinarietum alpinae</i>	2,350-3,050 m	Bamboo canopy overtopped by single trees	Single trees: <i>Podocarpus latifolius</i>
<i>Haganietea abyssinicae</i>	2,650-3,350 m	(I) Upper forest belt around whole Mount Kenya (II) Often very thick mossy cushions especially on the more or less horizontal stems and branches	<i>Hagenia abyssinica</i>

Source: Adopted from Bussmann and Beck (1995).

Table 2. Sentinel-2 images of the years 2018 and 2019 (till April only) with indication of cloud cover (CC) in % (ESA, 2019).

Year/Month	Jan	Feb	Mar	Apr	May	Jun	Jul	Aug	Sep	Oct	Nov	Dec
CC in 2018 (%)	<4	<4	=4-10	>10	=4-10	>10	>10	<4	<4	=4-10	>10	>10
CC in 2019 (%)	<4	<4	>10	>10	N/A	N/A	N/A	N/A	N/A	N/A	N/A	N/A

more aerosol retrieval, 945 nm for water vapor retrieval and 1275 nm for cirrus cloud detection)" (Fletcher, 2012: 12).

Sentinel-2 prototype land covers 20 m of the map of Africa

The CCI Land Cover consortium provides global and continental LC maps as result of the CCI Land Cover project. As part of the project, the prototype of a high-resolution LC map at 20 m of Africa was successfully developed (S2 prototype LC 20m map of Africa 2016). Data basis of the map are one year of S2A observations from December 2015 to December 2016. Whereas an official validation of the map has not yet been done, a user evaluation of Lesiv et al. (2017) estimates an overall accuracy of approximately 65% regarding the prototype. The evaluation was done using two independent datasets. Furthermore, the user evaluation highlights an overestimation of individual classes including Tree cover areas (Fabrizio et al., 2018). Figure 2 shows a cutout of the investigation area of the aforementioned S2 prototype LC 20m map of Africa 2016. As can be seen in the map, LC classes that mainly appear within the investigation area are Tree cover areas; Shrub cover areas; Grassland; Cropland; and Bare areas.

The shuttle radar topography mission (SRTM)

SRTM provides digital elevation data of the Earth's surface between 60° north latitude and 56° south latitude. Spatial resolution

of the free available product is close to 30 m, which makes it one of the highest-resolution models of the Earth Data for the SRTM were acquired by the Space Shuttle Endeavour (STS-99) in February 2000 (Farr et al., 2007). The elevation of the investigated area ranges from 1,752 m above sea level in the west to 3,259 m above sea level in the northeast. The elevation model derived from SRTM data was used to determine the height limits (Altitudinal Belts) of the forest type distribution.

Land use map of the kenya forest service

Based on Sentinel and Google Earth data of 2018, a LU map of the forest stations Ragati, Hombe and Kabaruu was produced by the Kenya Forest Service (KFS) in 2018. The classification of the map includes Air Strips, Shrublands, Swamps, Tea zone, PELIS, Forest Plantation (including indigenous species as well as Cypress, Pines, and Eucalypts (Mbugua, 2000), Grassland, and Natural Forest Zones that all appear within the investigation area.

Approach

Figure 3 illustrates the overall scheme of the research showing underlying steps of data preprocessing and classification. Before starting with the pre-processing, a status-quo analysis using present LC and LU maps of the investigation area was done. After selecting and downloading satellite products at Level-1C, images

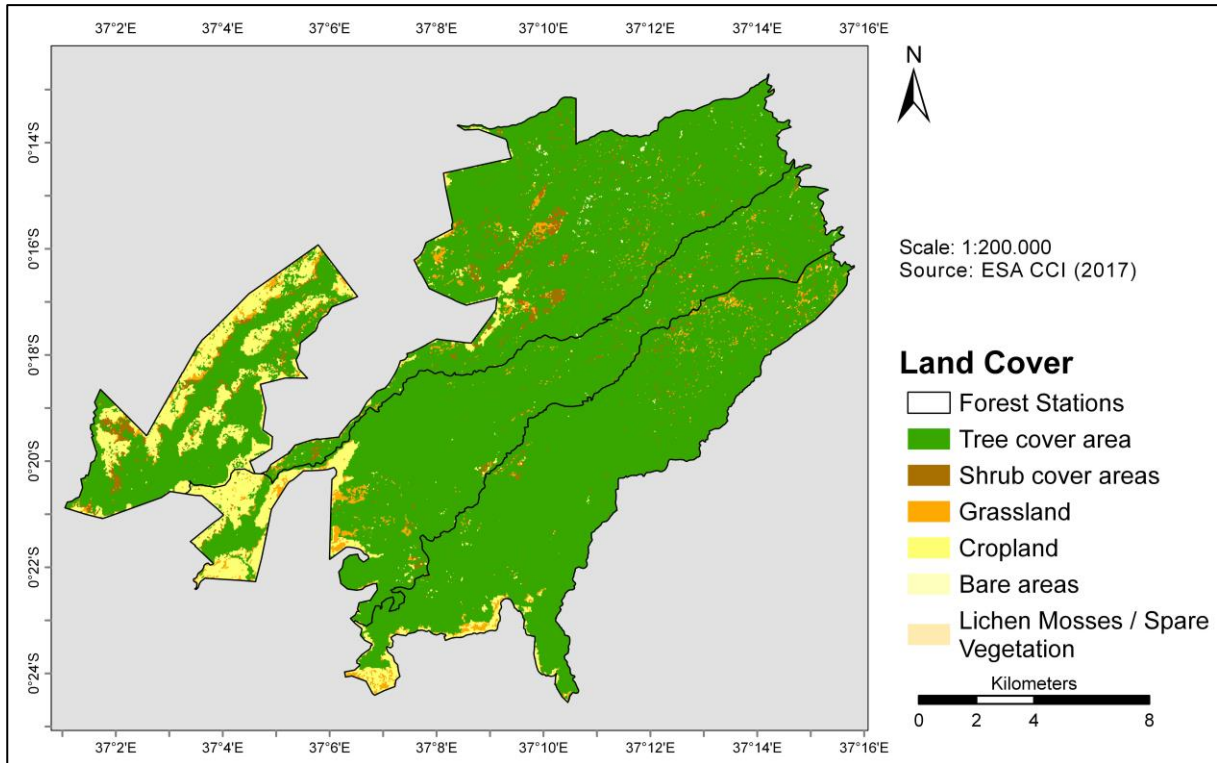


Figure 2. Cutout of the investigation area of S2 prototype LC 20 m map of Africa 2016 adopted from (ESA Climate Change Initiative - Land Cover project 2017, 2016).

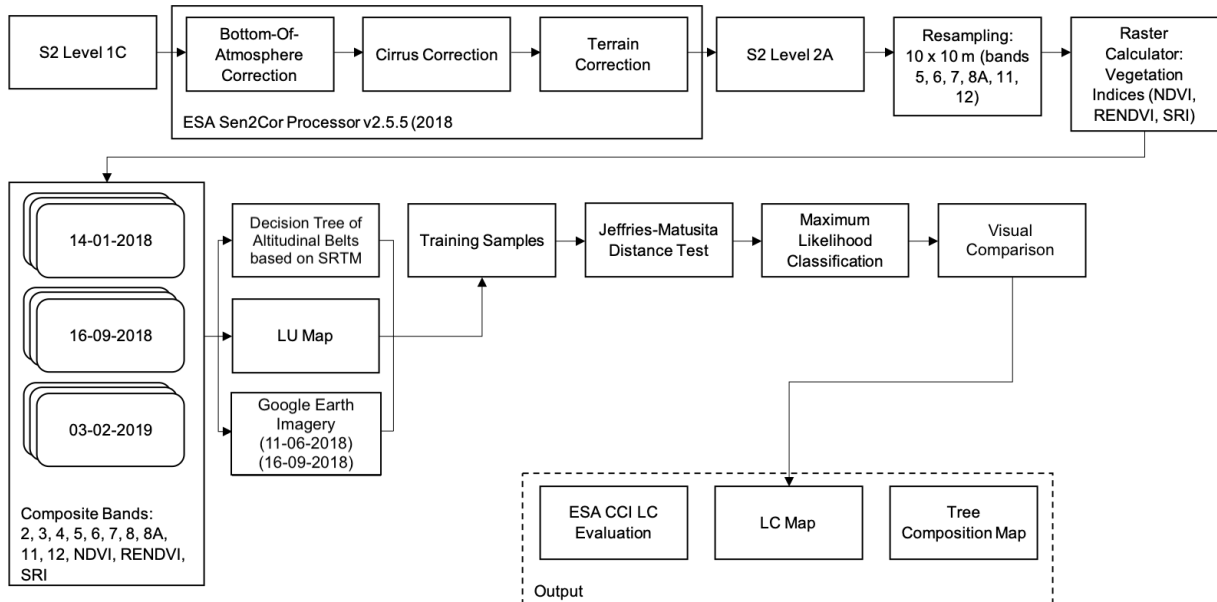


Figure 3. Overall scheme of methods and research structure.

had to be pre-processed before starting the classification process. This step of pre-processing involved steps of data correction, data resampling, and calculation of several Vegetation Indices (VIs) that were needed for the classification process at a later stage.

Furthermore, image composites of spectral bands and VIs were processed. Representative training samples were created based on the available LU map, and visual interpretation of Google Earth images and tested on their spectral separability using the

Jeffries-Matusita (JM) distance test. Finally, a Maximum Likelihood Classification and visual comparison was performed.

High quality and preferably cloud free imagery are a pre-requisite for further image processing and analysis. Table 1 shows most suitable S2 imagery for the years 2018 and 2019 (until April) via the Copernicus Open Access Hub (OAH) portal of the ESA. Persistent cloud cover is characteristic for the study area, nevertheless a total of six images with a cloud cover less than 4% could be acquired.

Due to their suitable distribution of cloud cover, three acquisition dates (14th January, 2018, 16th September, 2018 and 3rd of February, 2019) were chosen for further pre-processing including image correction, spatial resampling and the calculation of Vegetation Indices (VIs). The second step of the overall process and first partial step of the image pre-processing was an upgrade of Level-1C images to Level-2C. This was performed with the support of ESA's Sen2Cor Processor v2.5.5 (ESA, 2018). The process of the upgrade for all three images included atmospheric correction, cirrus correction, and terrain correction, respectively. The spectral bands of S2 satellite images come with different spatial resolutions ranging from 10 m to 60 m. To get a suitable overall resolution for canopy applications as well as in order to exploit the potential of the visible R, G, B and the NIR bands at 10 m, all 20-m bands were resampled to a spatial resolution of 10 m (Puletti et al., 2017). The process was performed, using the nearest neighbor function of the Resampling tool in ArcGIS 10.7 which is primarily used for discrete data, such as LC classifications, since it does not change the digital values of the pixels (Patil et al., 2012). Bands at a spatial resolution of 60 m were not used for further processing since they are mainly designed for atmospheric corrections (Fletcher, 2012). After resampling all bands from a resolution of 20 m to a resolution of 10 m, resampled spectral bands as well as original bands with a resolution of 10 m were used to calculate several VIs (Table 2).

The last step of data pre-processing involved the creation of the following five image composites using the resampled bands (2, 3, 4, 5, 6, 7, 8, 8A, 11, 12) as well as the computed VIs (NDVI, RENDVI, SRI):

- (i) Band 2, 3, 4, 5, 6, 7, 8, 8A, 11, 12
- (ii) Band 2, 3, 4, 5, 6, 7, 8, 8A, 11, 12, NDVI
- (iii) Band 2, 3, 4, 5, 6, 7, 8, 8A, 11, 12, RENDVI
- (iv) Band 2, 3, 4, 5, 6, 7, 8, 8A, 11, 12, SRI
- (v) Band 2, 3, 4, 5, 6, 7, 8, 8A, 11, 12, NDVI, RENDVI, SRI.

At the same time, cloud cover within the image composites was removed to prevent interferences during the classification process. The first step of the classification process was the determination of natural-forest subclasses using the reference data of Bussmann and Beck (1995). Unique altitudinal belts regarding the occurrence of different tree alliances were derived from the reference data. The altitudinal belts for indigenous forest are from 1,970 to 2,150 m altitude for *Ocotetea usambarensis*, 2,520 m to 2,650 m altitude for *Cassipourion malosanae*, 2,651 to 3,050 m altitude for *Podocarpus latifolius* - *Sinarundinarietum alpinae*, and 3,051 m to 3,350 m altitude for *Haganietea abyssinicae* (Figure 4). The derived decision tree for the four different subclasses of Natural Forest is shown in Figure 5.

With reference to the decision tree, class "A" is represented by *Ocotetea usambarensis*, class "B" by *C. malosanae*, class "C" by *Podocarpus latifolius* - *Sinarundinarietum alpinae*, and class "D" by *Haganietea abyssinicae*. The decision tree starts with a general query whether a pixel is defined as Natural Forest (four subclasses) or non-natural forest (Forest Plantation). This decision can be determined by the LU-map described by KFS. If the forest is declared as Natural Forest, the next question is whether a pixel is above or below an altitude of 3,050 m. If the pixel of Natural Forest is above 3,050 m altitude, it is declared as class "D". If not, the next question is whether the Natural Forest is above or below 2,150 m altitude. Below 2,150 m altitude and different from class "D", Natural Forest is defined as class "A". Above 2,150 m altitude, the next

question is whether the pixel is above or below 2,520 m altitude. If the pixel is below 2,520 m altitude, it is not possible to define the Natural Forest as a specific class. These pixels cannot be used within training sample since they are located in a transition zone of two or more forest subclasses. If the pixel is above 2,520 m altitude, the next question is whether it is above or below 2,650 m altitude. If it is above 2,650 m altitude and different from class "D", it is defined as class "C". If it is below 2,650 m altitude and different from class "A" and class "C", it is defined as class "B". Finally, information of the four subclasses of Natural Forest with reference to their unique altitudinal appearance was used to create four shapefiles of the areas that are potentially covered by the same classes. In addition, shape files of all subclasses were collated to the LU class of Natural Forest and intersected if not coextensive to each other.

The third step within the classification process involved the selection of training samples for all classes. For this purpose, 23 high resolution satellite image subsets (1 m spatial resolution) from Google Earth were imported into ArcGIS 10.7. The locations of the individual images can be seen in Figure 6. The acquisition date of the image subsets (*Image Copyright 2019 CNES / Airbus*) was June 6th, 2018 and September 16th, 2018 which partially coincide with the acquisition date of the second S2 image used within the study.

Figure 7 shows four examples of image subsets *that were used for the classification process*. (A) Classes of Water and Forest Plantation. (B) Natural-forest subclass of *Ocotetea usambarensis*. (C) Classes of Grassland and Forest Plantation (D) Class of Grassland and the natural-forest subclass of *Ocotetea usambarensis* (Google, 2019).

Based on the decision tree (Figure 5), Google Earth images (Figure 7), and the LU map by the KFS multiple training samples for a total of nine LC classes were defined, using the Training Sample Manager in ArcGIS Pro 2.2.4 (ESRI, 2019). As can be seen in Table 3, a total amount of 9067 pixels are separated into the classes of Water (585), Bare Land (941), Forest Plantation (2702), Tea (154), *Ocotetea usambarensis* (1629), *Podocarpus latifolius* - *Sinarundinarietum alpinae* (982), *H. abyssinicae* (136), *C. malosanae* (1377), and Grassland (561).

To analyze the quality of training samples of LC classes and forest subclasses, spectral distances were calculated for all classes by using the JM distance test. The test measures the average distance between two spectral class density functions and is defined by Wacker and Landgrebe (1972) as:

$$J_{ij} = \int_x \{ \sqrt{p(x|\omega_i)} - \sqrt{p(x|\omega_j)} \}^2 dx$$

Moreover, for normally distributed classes the formula is defined as:

$$J_{ij} = 2(1 - e^B)$$

Where:

$$B = \frac{1}{8}(m_i - m_j)^t \left\{ \frac{\Sigma_i + \Sigma_j}{2} \right\}^{-1} (m_i - m_j) + \frac{1}{2} \ln \left\{ \frac{|\Sigma_i + \Sigma_j|/2|}{|\Sigma_i|^{1/2}|\Sigma_j|^{1/2}} \right\}$$

Where m_i is the first spectral signature vector, m_j is the second spectral signature vector, Σ_i is the covariance matrix of m_i , and Σ_j is the covariance matrix of m_j . Results of the test close to 0 imply identical signatures whether values close to 2 imply completely different signatures (Richards and Jia, 2006). Spectral distances were computed for all three days using band composites of 10 bands (2, 3, 4, 5, 6, 7, 8, 8A, 11, 12), 10 bands (similar to step one) plus NDVI, 10 bands (similar to step one) plus RENDVI, 10 bands (similar to step one) plus SRI, and 10 bands (similar to step one)

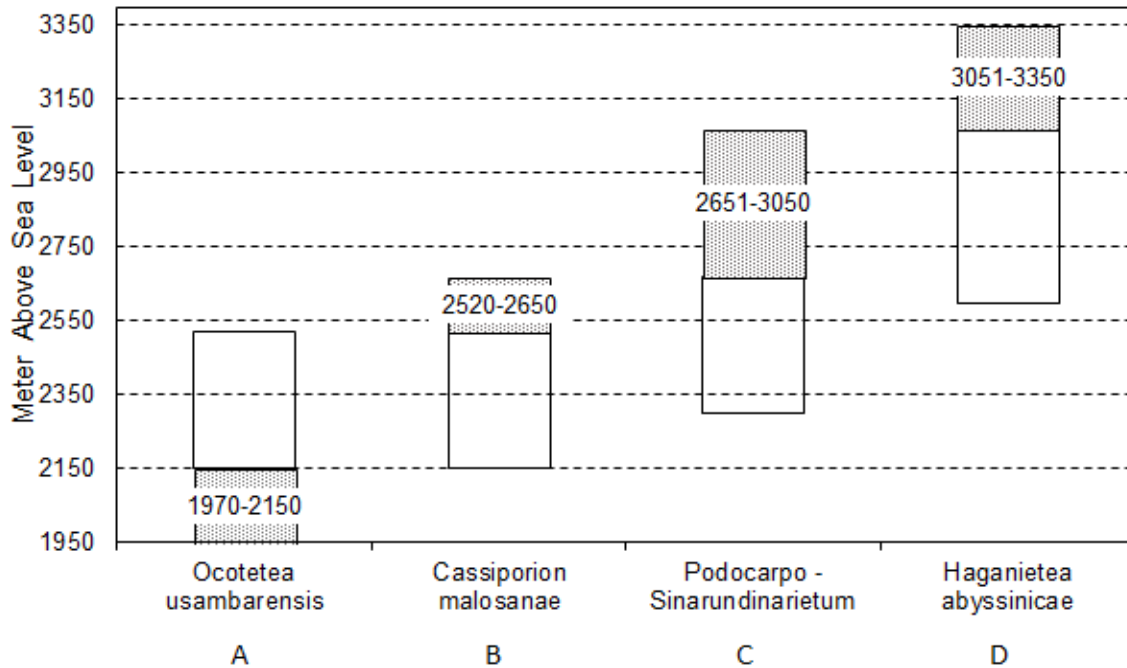


Figure 4. Differential altitudes of natural-forest subclasses based on reference data of Bussmann and Beck (1995).

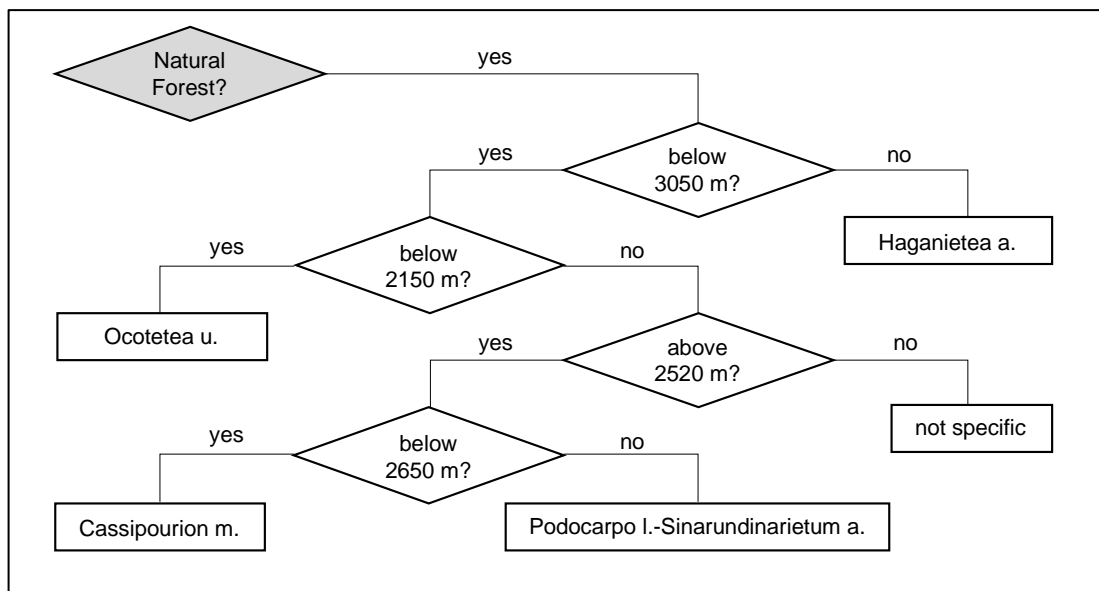


Figure 5. Decision-Tree for the differentiation of natural-forest subclasses. Class “A” is represented by *Ocotetea usambarensis*, class “B” by *Cassipourion malosanae*, class “C” by *Podocarpo latifolii – Sinarundinarietum alpinae*, and class “D” by *Haganietea abyssinicae*

plus NDVI, RENDVI, and SRI for each day.

The next step of the classification process was the performance of a Maximum Likelihood Classification. For this purpose, all training samples (Table 3) were used to produce classified satellite images for each acquisition date. In addition, a multi-temporal classification combining all three products was computed. Based on

the results of spectral separability, the following layer stacks were used for Maximum Likelihood Classifications:

- (1) 14-01-2018 (band 2, 3, 4, 5, 6, 7, 8, 8A, 11, 12, NDVI, RENDVI, SRI)
- (2) 16-09-2018 (band 2, 3, 4, 5, 6, 7, 8, 8A, 11, 12, NDVI, RENDVI,

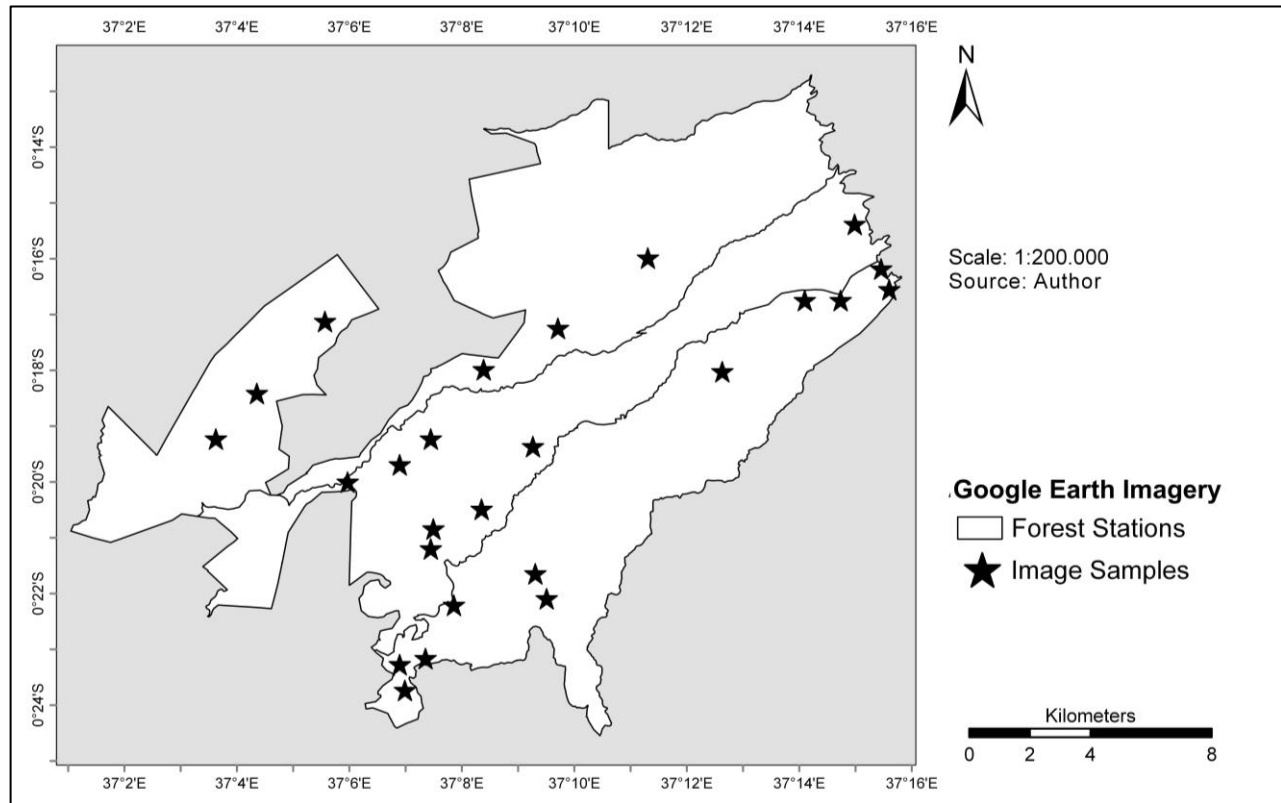


Figure 6. Location of 23 high resolution Google Earth image subsets that were used for the classification process.

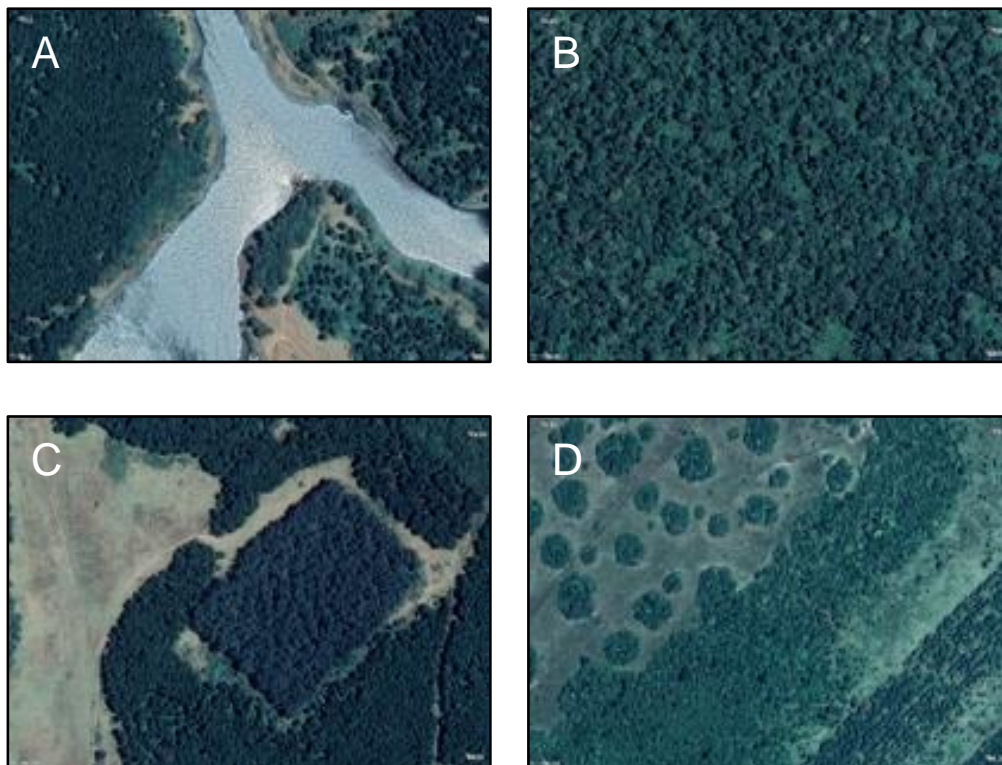











Figure 7. Examples of Google Earth images that were used for the classification process.

Table 3. Calculated formulas of vegetation indices adapted from (Puletti et al., 2017).

Vegetation index	Formula
NDVI	$\frac{(\text{Band 8} - \text{Band 4})}{(\text{Band 8} + \text{Band 4})}$
RENDVI	$\frac{(\text{Band 6} - \text{Band 5})}{(\text{Band 6} + \text{Band 5})}$
SRI	$\frac{\text{Band 8}}{\text{Band 4}}$

Table 4. Class ID, class names, class colors, and amount of training area pixels that were used for the classification process.

Class ID	Class name	Class color	Training pixels
1	Water		585
2	Bare land		941
3	Forest plantation		2702
4	Tea		154
5	<i>Ocotetea usambarensis</i>		1629
6	<i>Podocarpus latifolius</i> - <i>Sinarundinaria alpina</i>		982
7	<i>Hageniopsis abyssinica</i>		136
8	<i>Cassipourea malosana</i>		1377
9	Grassland		561
	Total		9067

SRI).

(3) 03-02-2019 (band 2, 3, 4, 5, 6, 7, 8, 8A, 11, 12, NDVI, RENDVI, SRI).

(4) Multi-temporal (14-01-2018 + 16-09-2018 + 03-02-2019).

RESULTS

Spectral distances

Table 4 shows the calculated spectral distances between all tree subclasses that include *Ocotetea usambarensis*, *C. malosanae*, *Podocarpus latifolius* – *Sinarundinaria alpina*, *Hageniopsis abyssinica*, and Forest Plantation for the band composite of 10 bands and three Vis. Most class pairs show equal separability values for the three different dates, but some considerable differences are apparent. The lowest overall value is shown for the class pair *C. malosanae* versus *Ocotetea usambarensis* on September 16th, 2018 with a spectral distance of 1.65 (JM). In contrast, all other comparisons show excellent values at the same day. Similar values can be seen on February 3rd, 2019 where spectral distance between *C. malosanae* versus *Ocotetea usambarensis* is slightly higher (1.81 [JM]) but still below 1.9 (JM). In addition, a difference between the two aforementioned dates is shown for the class pair *Hageniopsis abyssinica* versus

C. malosanae. On September 16th, 2018, the comparison shows an excellent value of 2.00 (JM). On February 3rd, 2019, the comparison shows a good value of 1.90 (JM). Best overall values are identified on January 14th, 2018 with a lowest value of 1.90 (JM) for the class pair *Ocotetea usambarensis* versus Forest Plantation. However, all other spectral distances of January 14th are above 1.90 (JM), which makes it a good day for separation of all the Natural Forest subclasses and the Forest Plantation class.

Spectral signatures

Spectral signatures and profiles were computed for all three S2 acquisition dates. Furthermore, class reflection characteristics were analyzed using box plot statistics of all bands and VIs for each date. In the following, the spectral signatures of one acquisition date (January 14th, 2018) are described.

Figure 8 shows a spectral profile of mean reflection values on January 14th, 2018. The graph shows that all classes except from Grassland show highest amplitudes between band 5 and band 11 with the highest point at band 8A. Grassland shows the highest amplitude at band 11. Band 8 and band 8A seem most feasible for the

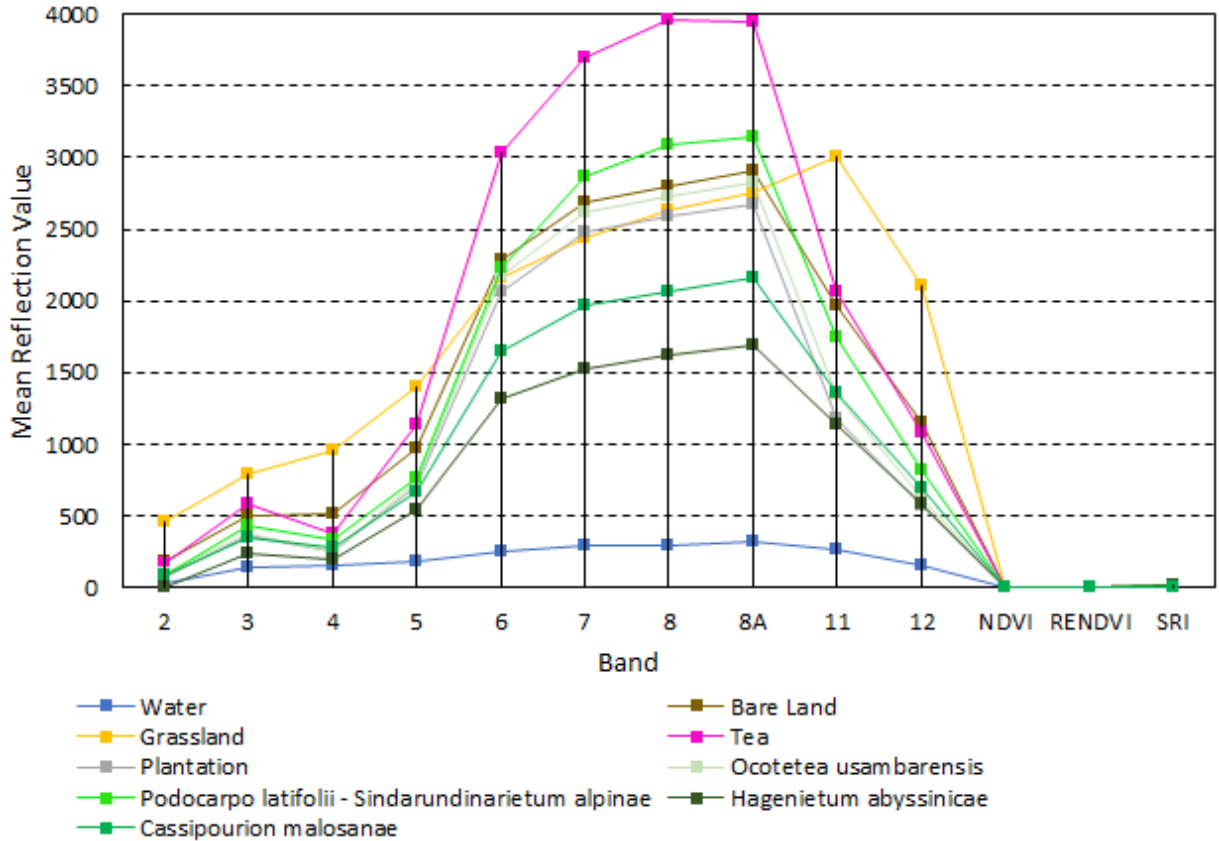


Figure 8. Spectral profile of 13 bands composite on January 14th, 2018.

differentiation of LC classes since mean value lines of the classes are further apart in comparison to other bands. With reference to the mean reflection of all classes, values of Water stand out in almost all spectral bands (Figure 8). Mean values for water are by far the lowest compared to all other classes. For all non-water classes (mostly vegetated except from Bare Land) the significance of red-edge is apparent. This is especially shown comparing the class Tea to classes of Grassland and Bare Land where mean values at bands 6 (3035.8 and 2155.01/2291.89), 7 (3699.98 and 2442.22/2680.53), and 8 (3965.68 and 2629.5/2803.66) differ considerably. Values of Grassland (2629.5) and Bare Land (2803.66) are similar in the NIR spectrum (band 8) with highest differences in the SWIR at Band 11 (3007.94/1971.43) and 12 (2100.06/1154.84). Clear differences can be seen in all three VIs (NDVI, RENDVI, SRI) for Water (0.3/0.15/1.27), Grassland (0.47/0.22/2.29), Tea (0.8/[0.44]/11.95), and Bare Land (0.68/[0.4]/0.55). Only RENDVI shows similar values when comparing the class of Tea (0.44) and with the class Bare Land (0.4).

Although, mean reflection values of all forest subclasses (Figure 8) are lot denser compared to those of non-forest classes, major differences appear within the red-edge region. Lowest difference of mean values is

measured between *Ocotetea usambarensis* and Forest Plantation. For all red-edge bands, the difference between these two classes is below 160 reflection units. On the contrary, highest separability can be determined between *Podocarpus latifolius - Sinarundinarietum alpinum* and *Hagenietyea abyssinicae* with up to nearly 1500 reflection units in the NIR (band 8) and red-edge (band 8A). Red-edge values of Grassland and Bare Land are quite close to the values of *Ocotetea usambarensis* and Forest Plantation. Considering the VIs, some forest subclasses show same values. This accounts for *Ocotetea usambarensis* (0.82) and Forest Plantation (0.82) at the NDVI, *Ocotetea usambarensis* (4.9), *Podocarpus latifolius - Sinarundinarietum alpinum* (4.9), and Forest Plantation (4.9) at the RENDVI, as well as *C. malosanae* (0.42) and *Hagenietyea abyssinicae* (0.42) at the RENDVI.

A detailed visualization of all ten spectral bands on 14 January, 2018 is shown in Figure 9. Figure 10 shows band reflection statistics of the three VIs. With reference to Grassland, it is possible to discriminate the class from all others within bands 2, 3, 4, 5, 11, 12, and the NDVI. At bands 6, 7, 8, 8A and the RENDVI as well as the SRI, the interquartile range of Grassland overlaps completely or partially with other classes. Almost the same applies for

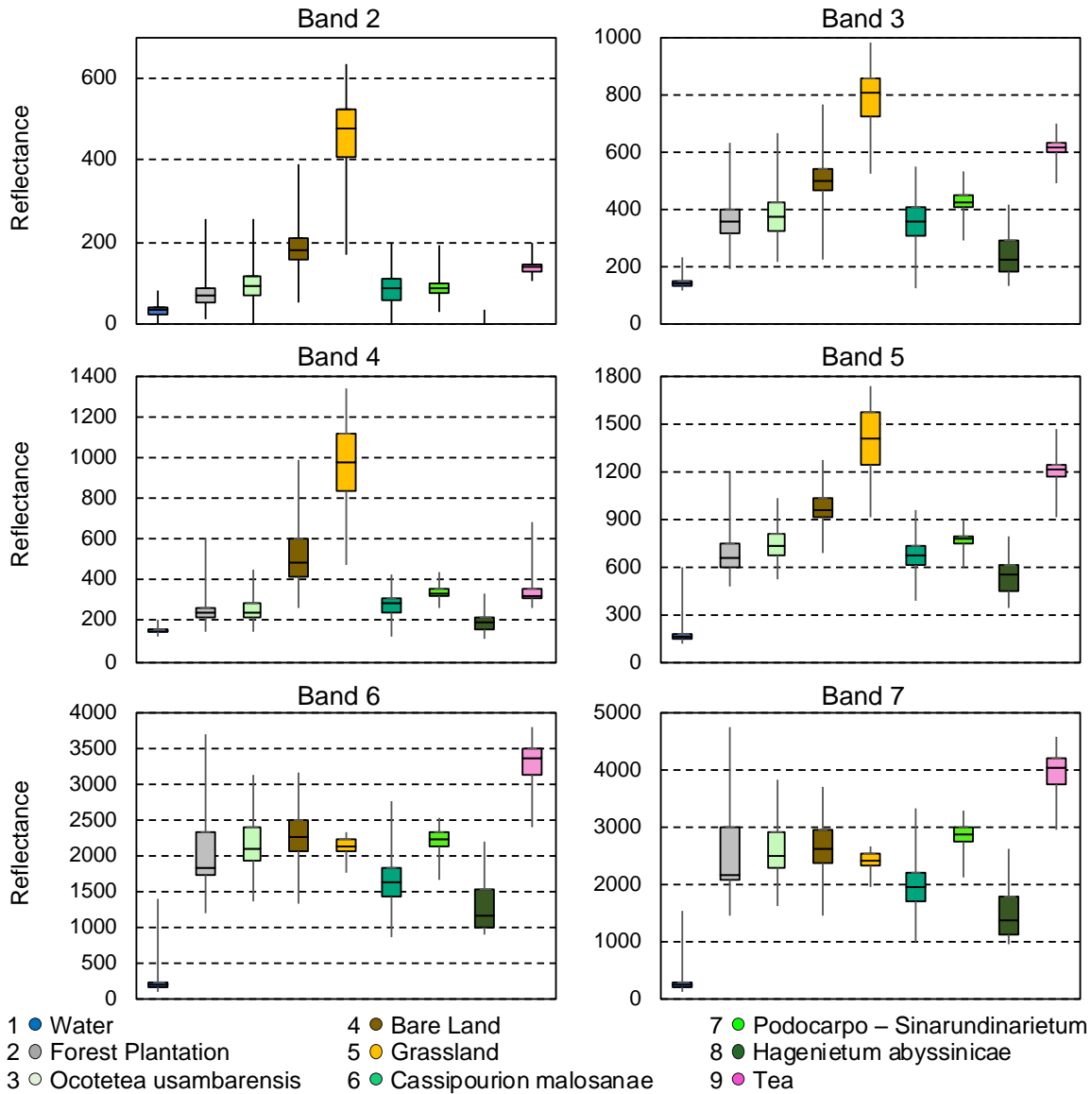


Figure 9. Band reflection statistics of bands 2, 3, 4, 5, 6, 7 on January 14th, 2018.

the class of Bare Land. The only difference in comparison to Grassland is that the interquartile range overlaps with *Hagenietea abyssinicae* at the NDVI. Furthermore, Tea can be discriminated from other classes at bands 3, 5, 6, 7, 8, and 8A. At all other bands as well as the VIs, the interquartile range of Tea overlaps with the interquartile range of other classes. The Water class can be separated at almost every spectral band and VI. Only exception is given by the RENDVI where the interquartile range of Water overlaps with Grassland. Consequently, all four non-forest classes can be separated quite well on January 14th, 2018.

A discrimination of forest subclasses is much more

complex which is also confirmed by the results of spectral distances. Probably the clearest discrimination of forest subclasses is identified for *Hagenietea abyssinicae*. Especially at bands 2 and 3 the difference of *Hagenietea abyssinicae* to all other classes is very high. At bands 4, 5, 6, 7, 8, and 8A the interquartile range overlaps with other classes to a very small extent. Furthermore, a total overlap with other classes is seen at bands 11, 12 and at all VIs. For the forest subclass *Podocarpus latifolii* – *Sinarundinarietum alpinae* most effective discrimination can be seen at bands 3, 8, and 8A where the interquartile range overlaps just slightly with other classes. According to the box plots of bands 6, 7, 8, and 8A, *C. malosanae*

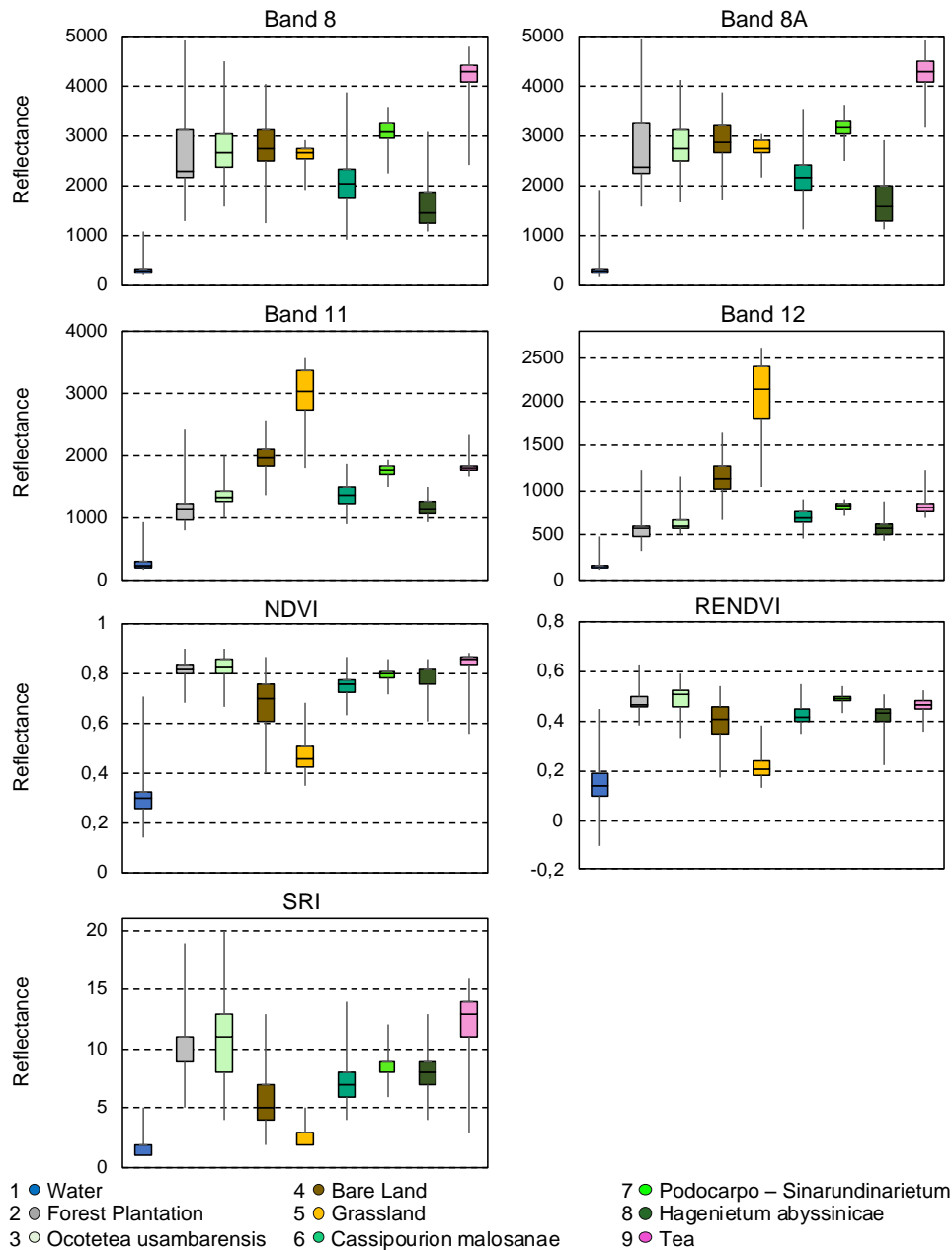


Figure 10. Band reflection statistics of bands 8, 8A, 11, and 12, as well as NDVI, RENDVI and SRI on January 14th, 2018.

can be differentiated best in the spectral region of red-edge and NIR. The forest subclasses of *Ocotetea usambarensis* and Forest Plantation and most difficult to separate. Except for band 11, the interquartile range of both classes overlaps within all other bands. This result is congruent with results of spectral distances, where comparisons between *Ocotetea usambarensis* and Forest Plantation show the lowest values on January 14th, 2018.

Land cover classification

Table 5 lists area statistics of all LC classes on January 14th, 2018, September 16th, 2018, and February 3rd, 2019 combined to a multi-temporal composite. The composite classification map (Figure 11) is illustrated below. Forest subclasses cover a total area of 189 km² (76%), whereas non-forest classes cover an area of 60 km² (24%).

Figure 11 shows several spatial characteristics of the

Table 5. Spectral distances of five forest subclasses at three different dates.

Composite bands	Class pairs	Level of Separability (JM)		
		14/01/18	16/09/18	03/02/19
10 Bands +NDVI +RENDVI +SRI	<i>Haganietea abyssinicae</i> vs. <i>Podocarpus latifolius</i> – <i>Sinarundinarietum alpinae</i>	2.00	2.00	2.00
	<i>Haganietea abyssinicae</i> vs. <i>Cassipourion malosanae</i>	1.93	2.00	1.90
	<i>Haganietea abyssinicae</i> vs. <i>Ocotetea usambarensis</i>	2.00	2.00	2.00
	<i>Haganietea abyssinicae</i> vs. forest plantation	2.00	2.00	2.00
	<i>Podocarpus latifolius</i> - <i>Sinarundinarietum alpinae</i> vs. <i>Cassipourion malosanae</i>	2.00	2.00	2.00
	<i>Podocarpus latifolius</i> - <i>Sinarundinarietum alpinae</i> vs. <i>Ocotetea usambarensis</i>	2.00	2.00	2.00
	<i>Podocarpus latifolius</i> - <i>Sinarundinarietum alpinae</i> vs. Forest Plantation	2.00	2.00	2.00
	<i>Cassipourion malosanae</i> vs. <i>Ocotetea usambarensis</i>	1.94	1.65	1.81
	<i>Cassipourion malosanae</i> vs. forest plantation	1.97	2.00	2.00
	<i>Ocotetea usambarensis</i> vs. forest plantation	1.90	2.00	1.98

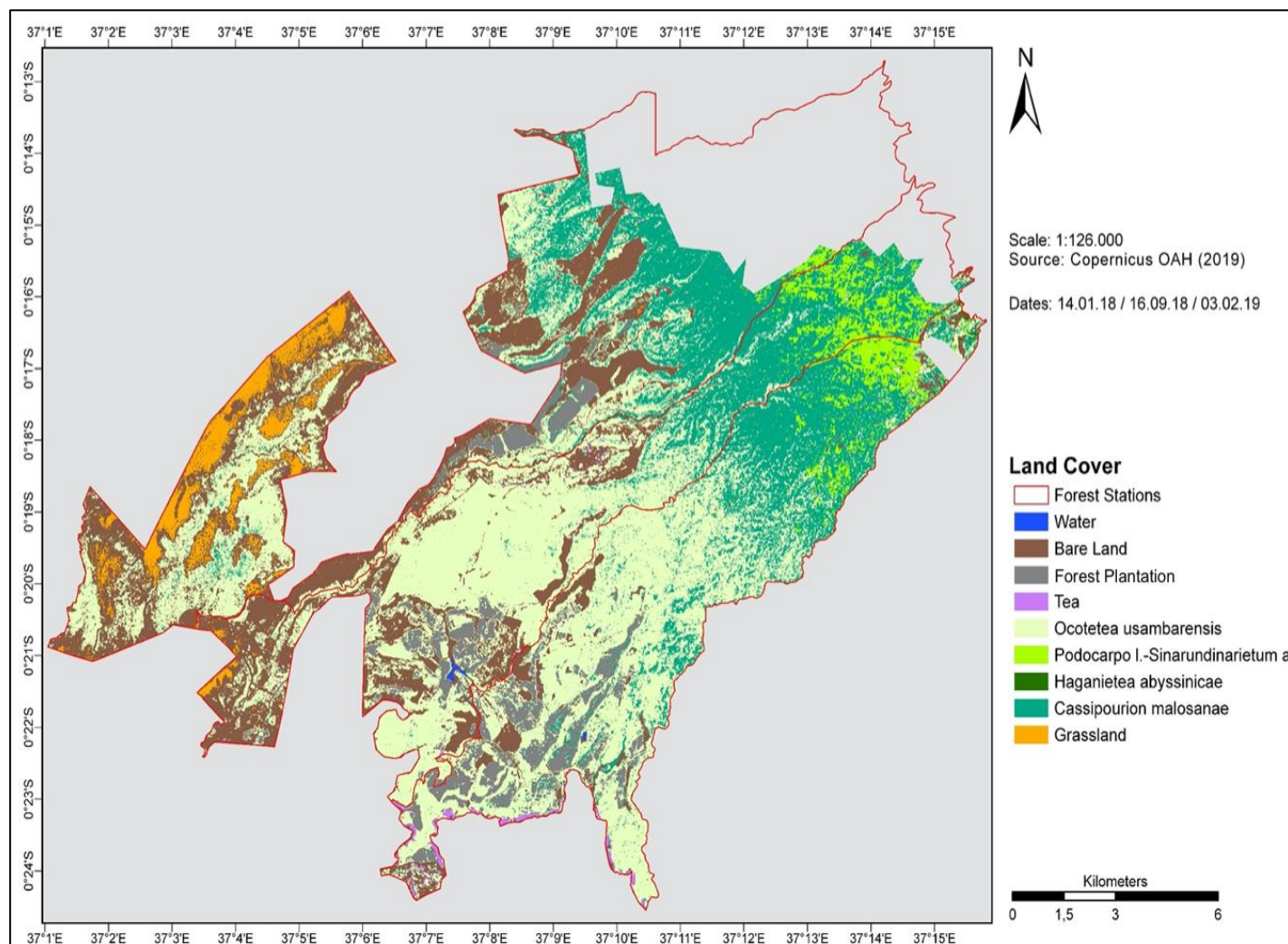


Figure 11. Multi-temporal Maximum Likelihood Classification on January 14th, 2018, September 16th, 2018, and February 3rd, 2019.

nine LC classes for multiple dates that for the most part coincide with characteristics of single-dates. (1) Small

water bodies are visible east and west of the southern center, similar to all other dates. (2) Bare Land is located

in the western and central areas of the investigation area including small expansions in the northeastern parts. (3) Forest Plantation covers large parts of southern central areas with further coherent areas in the central north (similar to all other dates). (4) Small areas of Tea are visible in the southern investigation area. (5) *Ocotetea usambarensis* covers large parts of the southern center, representing the largest class with an extent of more than 40%. (6) *Podocarpus latifolius* - *Sinarundinaria alpinae* is visible in high altitudes in the northeast (similar to all other dates). (7) Small areas of *Haganietea abyssinicae* appear within the highest altitudes in the northeast. (8) *C. malosanae* covers large parts of the central east and north with some additional coverage in the west and (9) Grassland covers the western edge of the investigation area.

Visual comparison

Figure 12 shows a side by side display of multi-temporal classification, Google imagery and ESA's S2 prototype samples. Furthermore, Table 6 shows a legend of Figure 12 including class names as well as class colors of visible LC classes within the samples.

Image subset "F" in row 1 shows a significant water body surrounded by different LC. This can be verified by the multi-temporal sample "A" of row 1 that clearly shows the class of Water, Bare Land, Forest Plantation, *Ocotetea usambarensis*, and some individual pixels of *C. malosanae*, and Tea. On the contrary, no water is determined at sample "K" of row 1 of the S2 prototype. Instead, areas of Shrub cover areas and Grassland are surrounded by Tree cover areas. Image subset "G" of row 2 shows sparsely vegetated areas with several small islands of trees and shrubs surrounded by areas of trees and shrubs. This is partially verified by multitemporal sample "B" of row 2 that shows several small islands of Bare Land surrounded by Grassland, and *Ocotetea usambarensis*. In addition, individual pixels of *C. malosanae* appear. Sample "L" of ESA's S2 prototype shows a large area of Cropland surrounded by Tree cover areas and small areas of Shrub cover areas and Grassland. No islands can be identified within the sample of ESA's S2 prototype. At first glance, Google Earth image "H" of row 3 shows different forest types. This is confirmed by the multi-temporal sample "C" of row 3 that shows forest subclasses of *C. malosanae*, *P. latifolius* – *S. alpinae*, and *Ocotetea usambarensis* as well as a small area of Bare Land on the bottom right. Sample "N" of row 3 of ESA's S2 prototype exclusively shows Tree cover areas with a small number of Shrub cover areas. Image subset "I" of row 4 shows two different types of forests with fields of tea in the bottom left. In addition, several paths/streets cross the image. This is mainly verified by multi-temporal sample "D" of row 4 that shows classes of Forest Plantation, *O. usambarensis*, *C. malosanae*, and

Tea. Moreover, aforementioned paths/streets are represented by small areas of Bare Land within the classified image. Sample "N" of row 4 of ESA's S2 prototype shows mostly Tree cover areas with a small area of Cropland in the bottom left. Finally, image subset "J" of row 5 shows non-vegetated areas separated by large areas of tree cover that indicate human impact. Multi-temporal sample "E" of row 5 is partially correspondent to this. The classification is characterized by large areas of Forest Plantation and Bare Land but includes a differentiation between Forest Plantation and *Ocotetea usambarensis* as well as some pixels of Tea. Hence, a differentiation of trees is shown in the multi-temporal classification but not in the Google Earth image. Sample "O" of ESA's S2 prototype shows predominantly Tree covered areas with an individual spot of Shrub. In conclusion, the most significant difference between the multi-temporal classification and ESA's S2 prototype is the appearance of water (row 1), the differentiation of details within the LC (row 1 to 5), and the discrimination of forest subclasses (row 1, 3, 4, and 5). Moreover, the overrepresentation of Cropland as well as Tree cover areas (Figures 2 and 11) can be confirmed as stated by Fabrizio et al. (2018).

DISCUSSION

The present study demonstrates the potential of multi-temporal S2 images combined with historic reference data, topographic data, high resolution imagery, and LU data for LC classification and discrimination of tree compositions in a tropical environment, which is characterized by decreasing forest area and an increase of agricultural activity (Barlow et al., 2016; FAO, 2016a). The study also supports the envisaged shift to freely available SRS programs (Wulder and Coops, 2014; Wulder et al., 2018) providing opportunities to scientists and policy-makers with limited resources and barriers of access due to the lack of high-performance technology and permission rights, which are not always available to the global community (Pettorelli et al., 2014; Shukla and Kot, 2016; Wulder and Coops, 2014; Wulder et al., 2018).

The major outcome of the study is a multi-temporal Maximum Likelihood Classification that shows LC classes and tree compositions based on the analysis of spectral signatures using three single-day images for the area of interest. The new product can help to support the improvement of Kenya's national forest monitoring and remote sensing capacities (Romijn et al., 2015; FAO, 2016b) and complements existing regional forest monitoring studies conducted by Song et al. (2013) and Nyongesa (2015). The study shows the high potential of ESA S2 products for the classification of tropical tree composites. The high temporal and spatial resolution of the ESA S2 products is a necessary requirement to identify, map and monitor detailed changes in forest

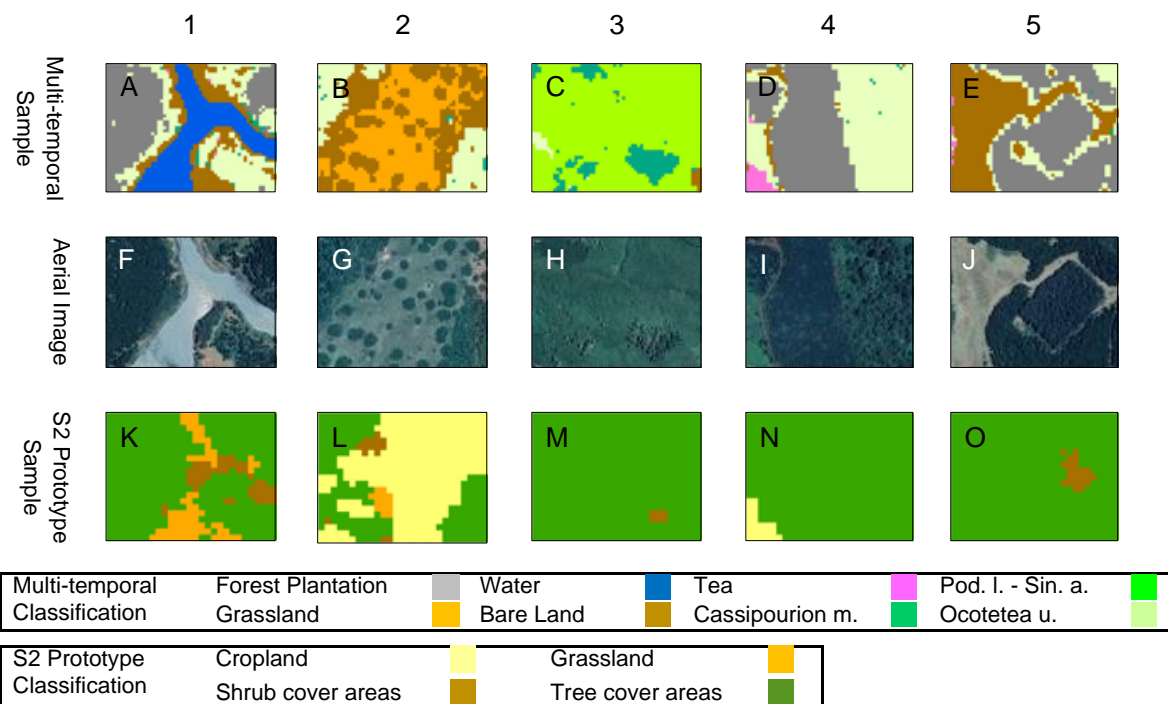


Figure 12. Side by side display of multi-temporal classification (A, B, C, D, E), high resolution satellite imagery (Google) - (F, G, H, I, J), and ESA's S2 prototype (K, L, M, N, O).

Table 6. Areas of LC classes in km² and % of multi-temporal dates.

LC CLASS	Area (km ²)	Area (%)
<i>Ocotetea usambarensis</i>	72.11	29.08
<i>Cassipourion malosanae</i>	69.95	28.20
Bare land	49.44	19.93
Forest plantation	25.02	10.09
<i>Podocarpus latifolius</i> – <i>Sinarundinarietum alpinae</i>	15.27	6.16
Grassland	10.14	4.09
<i>Hagenietum abyssinicae</i>	5.30	2.14
Tea	0.68	0.27
Water	0.11	0.04
Total	248.01	100.00

structure (Gao et al., 2006). This can be confirmed through the successful analysis of spectral LC class separability. The results of the performed JM distance test show that the best separability for discrimination of LC classes and tree compositions is given on January 14th, 2018 using a band composite of 10 spectral bands and three VIs (total of 13 layers). Spectral differences on this day show scores of 1.90 (JM) and above, including six class pairs with scores of 2.00 (JM). According to Jin et al. (2016) and Richards and Jia (2006), these results can be considered as well separable. However, the intersection of individual forest classes can be a reason

for the relatively low separability between class pairs of *C. malosanae* and *H. abyssinicae* (1.93 JM), *C. malosanae* and *O. usambarensis* (1.94 JM), as well as *O. usambarensis* and Forest Plantation (1.90 JM) within the present research.

ESAs' existing S2 prototype LC 20 m map of Africa from 2016 shows a total of five LC classes and one tree cover class within the investigation area. The present study shows that mapping of nine LC classes including five forest subclasses of tree compositions is possible. In combination with regional climate data, the classification results can help to further explore climate-related

phenomena such as climate-induced tree mortality on a regional scale. Since forests of all climate zones are threatened by climate change, including East African montane forests in Kenya (Bastin et al., 2019; Kogo et al., 2019), detailed regional studies as presented by the authors are highly relevant for the community of environmental monitoring (Allen et al., 2010). However, due to the high variety of species within the investigation area and the spatial resolution of 10 m of partially resampled S2 images, classification at species level can be too demanding for similar applications on a regional scale. This specific problem was realized in a previous study of Immitzer et al. (2016) for temperate regions and should be even more relevant for tropical environments with a high level of biodiversity (Ganivet and Bloomberg, 2019; Laurin et al., 2016). Consequently, Fassnacht et al. (2016) suggest a focus on broader forest types instead of single trees when using S2 data. Part of the present study is forest compositions that consist of different species that appear in alliances (Bussmann and Beck, 1995). A similar approach was applied by Laurin et al. (2016) using S2 for a discrimination of functional guilds in a tropical environment. Both methods should provide an efficient alternative for monitoring functional changes (Laurin et al., 2016) without the claim to discriminate single trees at species level.

Conclusion

The opportunities of S2 imagery for the classification of tropical forest subclasses through additional integration of historical field acquisitions (in situ data) and terrain information were successfully tested. However, as suggested by previous authors and confirmed within the present study, multi-temporal classifications should be favored to reduce the bias potential due to irregular flowering times in tropical regions (Immitzer et al., 2016; Mickelson et al., 1998; Wolter et al., 1995).

Visual comparison of the classification product, ESA's S2 prototype LC 20 m map of Africa 2016, and high-resolution Google Earth imagery from September 16th, 2018 show considerable differences between the classified products. The overestimation of *Tree cover areas* by ESA's LC classification as mentioned by Lesiv et al. (2017) can be confirmed in the present research. Whereas *Tree cover areas* of ESA's LC product cover approximately 85% of the investigation area; a combination of all forest subclasses within the present research shows forest coverage of slightly below 75% (Intended areas for *Natural Forests* as well as *Forest Plantation* in the KFS LU map cover an area larger than 90%). Another aspect is the non-identification of notable water bodies within ESA's S2 prototype. Two large water bodies can be identified in the high-resolution Google Earth images which are also contained in the classification of the present study. Since ESA's product is

based on imagery acquired between 2015 and 2016 and the Google Earth image was taken on September 16th, 2018, differences in LC are possible. However, radical changes of large water bodies are unlikely. Moreover, these water bodies do not appear within the LU map of 2018 by the KFS either. One reason could be a better spatial resolution of the present classification product. Due to a resampling of initial S2 data at 20 m to a spatial resolution of 10 m, classification of the present study is considerably more precise than ESA's S2 prototype with a remaining resolution of 20 m. This is most obvious in areas with small-scale appearances such as streets/tracks and human created *Plantations* with clear structures.

The spatial distribution of specific tree compositions is largely dependent on altitude. This was considered during the classification using reference data from Bussmann and Beck (1995) and DEM integration. However, some deviations and outliers can be recognized. A considerable number of pixels classified as *Ocotetea usambarensis* (total of 212,705) range below altitudes of 1,970 m and above 2,520 m. For *C. malosanae*, most of 185,867 divergent pixels are above a defined range of 2,150 m to 2,650 m altitude. *P. latifolia* – *S. alpinae*, and *H. abyssinicae* show the lowest deviations where a very low number of classified pixels (5,155 and 50) range between 2,350 and 3,050 m as well as 2,650 m and 3,350 m altitude, respectively. High deviations for *O. usambarensis* and *C. malosanae* need to be tested through use of current ground truth data. Furthermore, forest subclasses need to be extended for secondary forest or shrubs if necessary.

CONFLICT OF INTERESTS

The authors have not declared any conflict of interests.

REFERENCES

- Allen CD, Macalady AK, Chenchouni H, Bachelet D, McDowell N, Vennetier M, Kitzenberger T, Rigling A, Breshears AK, Hogg EH, Gonzalez P, Fensham R, Zhang Z, Castro J, Demidova N, Lim J, Allard G, Running SW, Semerci A, Cobb N (2010). A global overview of drought and heat-induced tree mortality reveals emerging climate change risks for forests. *Forest Ecology and Management* 259(4):660-684.
- Asner GP (2001). Cloud cover in Landsat observations of the Brazilian Amazon. *International Journal of Remote Sensing* 22(18):3855-3862.
- Barlow J, Lennox GD, Ferreira J, Berenguer E, Lees AC, Mac Nally R, Thomson JR, de Barros Ferraz SF, Louzada J, Oliveira VH, Parry L (2016). Anthropogenic disturbance in tropical forests can double biodiversity loss from deforestation. *Nature* 535(7610):144-147.
- Bastin J-F, Finegold Y, Garcia C, Mollicone D, Rezende M, Routh D, Zohner CM, Crowther TW (2019). The global tree restoration potential. *Science* 365(6448): 76-79
- Burrows J, Burrows S, Lötter M (2018). *Trees and Shrubs Mozambique*. Cape Town: Print Matters Heritage.
- Bussmann RW, Beck E (1995). The forests of Mt Kenya (Kenya): A phytosociological synopsis. *Phytocoenologia* 25(4):467-560.
- Crowther TW, Glick HB, Covey KR, Bettigole C, Maynard DS, Thomas

- SM, Smith JR, Hintler G, Duguid MC, Amatulli G, Tuanmu MN, Jetz W, Salas C, Stam C, Piotto D, Tavani R, Green S, Bruce G, Williams SJ, Wiser SK, Huber MO, Hengeveld M, Nabuurs GJ, Tikhonova E, Borchardt P, Li CF, Powrie LW, Fischer M, Hemp A, Homeier J, Cho P, Vibrans AC, Umunay PM, Piao SL, Rowe CW, Ashton MS, Crane PR, Bradford MA (2015). Mapping tree density at a global scale *Nature* 525(7568):201-205.
- DeFries RS, Field CB, Fung I, Justice CO, Los S, Matson PA, Matthews E, Mooney HA, Potter CS, Prentice K, Sellers PJ, Townshend JRG, Tucker CJ, Ustin SL, Vitousek PM (1995). Mapping the land surface for global atmosphere-biosphere models: Toward continuous distributions of vegetation's functional properties. *Journal of Geophysical Research* 100(D10):20867.
- Environmental System Research Institute, ESRI (2019). ArcGIS Desktop Pro 224: ESRI
- ESA (2018). Sen2Cor Processor v255.
- ESA (2019). Copernicus Open Access Hub: Sentinel-2 Level-1c.
- ESA Climate Change Initiative - Land Cover project 2017 (2016). S2 Prototype Land Cover 20 m Map of Africa 2016 Contains modified Copernicus data (2015/2016): European Space Agency.
- Fabrizio R, Fabrizio P, Arino O (2018). 'S2 prototype LC map at 20m of Africa 2016': Users Feedback Compendium [6th February 2018].
- FAO (2016a). Forests and agriculture: Land-use challenges and opportunities State of the world's forests: Volume 2016 Rome: FAO.
- FAO (2016b). How are the world's forests changing? (Second edition) Global forest resources assessment: Volume 2015 Rome.
- FAO (2017). Voluntary guidelines on national forest monitoring. Rome: FAO.
- Farr TG, Rosen PA, Caro E, Crippen R, Duren R, Hensley S, Kobrick M, Paller M, Rodriguez E, Roth L, Seal D, Schaaffner S, Shimada J, Umland J, Werner M, Oskin M, Burbank D, Alsdorf D (2007). The Shuttle Radar Topography Mission *Reviews of Geophysics* 45(2):1485.
- Fassnacht FE, Latifi H, Stereńczak K, Modzelewska A, Lefsky M, Waser LT, Straub C, Ghosh A (2016). Review of studies on tree species classification from remotely sensed data. *Remote Sensing of Environment* 186:64-87.
- Fletcher K (2012). Esa's optical high-resolution mission for GMES operational services (ESA SP No ESA-SP-1322/2). Noordwijk.
- Gao F, Masek J, Schwaller M, Hall Forest G (2006). On the blending of the Landsat and MODIS surface reflectance: Predicting daily Landsat surface reflectance. *IEEE Transactions on Geoscience and Remote Sensing* 44(8):2207-2218
- Ganivet E, Bloomberg M (2019). Towards rapid assessments of tree species diversity and structure in fragmented tropical forests: A review of perspectives offered by remotely-sensed and field-based data. *Forest Ecology and Management* 432:40-53.
- Google LLC (2019). Google earth v 73.
- Grabska E, Hostert P, Pflugmacher D, Ostapowicz K (2019). Forest Stand Species Mapping Using the Sentinel-2 Time Series. *Remote Sensing* 11(10):1197.
- Hansen MC, Potapov PV, Moore R, Hancher M, Turubanova SA, Tyukavina A, Thau D, Stehman SV, Goetz SJ, Loveland TR, Kommareddy A, Egrov A, Chini L, Justice CO, Townshend JRG (2013). High-resolution global maps of 21st-century forest cover change. *Science* (New York NY) 342(6160):850-853.
- Immitzer M, Vuolo F, Atzberger C (2016). First Experience with Sentinel-2 Data for Crop and Tree Species Classifications in Central Europe. *Remote Sensing* 8(3):166.
- IPCC (2003). Good practice guidance for land use land-use change and forestry /The Intergovernmental Panel on Climate Change Ed By Jim Penman Hayama Kanagawa
- Jin C, Xiao X, Dong J, Qin Y, Wang Z (2016). Mapping paddy rice distribution using multi-temporal Landsat imagery in the Sanjiang Plain northeast China *Frontiers of Earth Science* 10(1):49-62.
- Karasiak N, Sheeren D, Fauvel M, Willm J, Dejoux J-F, Monteil C (2017). Mapping tree species of forests in southwest France using Sentinel-2 image time series In 2017 9th International Workshop on the Analysis of Multitemporal Remote Sensing Images (MultiTemp): June 27-29, 2017 Bruges Belgium (pp 1-4) Piscataway NJ: IEEE.
- Kenya Forest Service (2010). Mt Kenya Forest Reserve Management Plan: 2010-2019 Nairobi.
- Kenya Wildlife Service (2010). Mt Kenya Ecosystem: Management Plan 2010-2020.
- Kogo BK, Kumar L, Koech R (2019). Forest cover dynamics and underlying driving forces affecting ecosystem services in western Kenya *Remote Sensing Applications. Society and Environment* 14:75-83.
- Lambin EF, Turner BL, Geist HJ, Agbola SB, Angelsen A, Bruce JW, Coomes OT, Dirzo R, Fischer G, Folke C, George PS, Homewood K, Imbernon J, Leemans R, Li X, Moran EF, Mortimore M, Ramakrishnan PS, Richards JF, Skånes H, Steffen W, Stone GD, Svedin U, Veldkamp TA, Vogel C, Xu J (2001). The causes of land-use and land-cover change: Moving beyond the myths. *Global Environmental Change* 11(4):261-269.
- Laurin G, Puletti N, Hawthorne W, Liesenberg V, Corona P, Papale D, Chen Q, Valentini R (2016). Discrimination of tropical forest types dominant species and mapping of functional guilds by hyperspectral and simulated multispectral Sentinel-2 data. *Remote Sensing of Environment* 176:163-176.
- Lesiv M, Fritz S, McCallum I, Tsendbazar N, Herold M, Pekel JF, Buchhorn M, Smets B, van de Kerchove R (2017). Evaluation of ESA CCI prototype land cover map at 20 m IIASA Working Paper.
- Mbugua D (2000). FOSA Country Report - Kenya: Forest Outlook studies in Africa.
- McDowell N, Allen C, Anderson-Teixeira K, Aukema B, Bond-Lamberty B, Chini L, Clark J, Dietze M, Grossiord C, Hanbury-Brown A, Hurr G, Jackson R, Johnson D, Kueppers L, Lichstein J, Ogle K, Poulter B, Pugh T, Seidl R, Turner M, Uriarte M, Walker A, Xu C (2020). Pervasive Shifts in Forest Dynamics in a Changing World.
- Mickelson J, Civco D, Silander J (1998). Delineating forest canopy species in the northeastern United States using multi-temporal TM imagery. *Photogrammetric Engineering and Remote Sensing* 64:9.
- Nyongesa KW (2015). Fire management if Forests and National Parks of Kenya: Case studies at Kakamega Mt Elgon and Mt Kenya Forest and National Park In *Forestry 1st ed*; Ivan G Ed; OmniScriptum Publishers: Saarbrücken Germany.
- Patil BM, Desai GC, Umrikar B (Eds) (2012). Proceedings of the 6th National Conference on Computing for Nation Development (23rd - 24th February 2012) INDIACOM-2012 New Delhi: Bharati Vidyapeeth's Institute of Computer Applications and Management .
- Pettorelli N, Laurance WF, O'Brien TG, Wegmann M, Nagendra H, Turner W (2014). Satellite remote sensing for applied ecologists: Opportunities and challenges. *Journal of Applied Ecology* 51(4):839-848.
- Puletti N, Chianucci F, Castaldi C (2017). Use of Sentinel-2 for forest classification in Mediterranean environments. *Annals of Silvicultural Research* 42(1)
- Richards JA, Jia X (2006). *Remote Sensing Digital Image Analysis: An Introduction* (4th Edition) Berlin Heidelberg: Springer-Verlag Berlin Heidelberg.
- Romijn E, Lantican CB, Herold M, Lindquist E, Ochieng R, Wijaya A, Murdiyarto D, Verchot L (2015). Assessing change in national forest monitoring capacities of 99 tropical countries. *Forest Ecology and Management* 352:109-123.
- Sola I, García-Martín A, Sandonis-Pozo L, Álvarez-Mozos J, Pérez-Cabello F, González-Audicana M, Montorio Llovería R (2018). Assessment of atmospheric correction methods for Sentinel-2 images in Mediterranean landscapes. *International Journal of Applied Earth Observation and Geoinformation* 73 63-76.
- Shukla A, Kot R (2016). An Overview of Hyperspectral Remote Sensing and its applications in various Disciplines IRA. *International Journal of Applied Sciences* (ISSN 2455-4499) 5(2):85.
- Song Y, Njoroge JB, Morimoto Y (2013). Drought impact assessment from monitoring the seasonality of vegetation condition using long-term time-series satellite images: A case study of Mt Kenya region *Environmental Monitoring and Assessment* 185(5):4117-4124.
- Townshend JRG (1992). Land cover. *International Journal of Remote Sensing* 13(6-7):1319-1328.
- United Nations (UN) (1992). Convention on Biological Diversity: 1760 UNTS 69 Rio de Janeiro.
- United Nations (UN) (1997). Kyoto Protocol to the United Nations Framework Convention on Climate Change Kyoto.
- United Nations (UN) (2015). Transforming our world: The 2030

- Agenda for Sustainable Development: A/RES/70/1 New York.
- Wacker A, Landgrebe D (1972). Minimum distance classification in remote sensing LARS Technical Reports
- Winiger M, Brunner R (Eds) (1986). Geographica Bernensia A African studies series: Vol 1 Mount Kenya area: Contributions to ecology and socio-economy Berne: Institute of Geography, University of Bern.
- Wolter PT, Mladenoff DJ, Host GE, Crow TR (1995). Improved forest classification in the northern Lake States using multi-temporal Landsat imagery Photogrammetric Engineering and Remote Sensing (USA).
- Wulder MA, Coops NC (2014). Satellites: Make Earth observations open access Nature 513(7516): 30-31.
- Wulder MA, Coops NC, Roy DP, White JC, Hermosilla T (2018). Land cover 2.0. International Journal of Remote Sensing 39(12):4254-4284.

Related Journals:

